

People's Democratic Republic of Algeria
Ministry of Higher Education and Scientific Research
University of Ahmed Draia, Adrar
Faculty of Science and Technology
Department of Technology Science



A dissertation submitted for the fulfillment of

Master's Degree

In Electrical Engineering

OPTION: Electrical Control

**Control of a Z–source inverter integrated
in a photovoltaic system**

Presented by:

MAHDJOUBI Soumya

HALA Amina

Supervised by:

Mr. OULED ALI Omar

Academic Year: 2019/2020

République Algérienne Démocratique et Populaire
Ministère de l'Enseignement Supérieur et de la Recherche Scientifique
Université Ahmed Draia- Adrar
Faculté des Sciences et de La Technologie
Département des Sciences de La Technologie



Mémoire De Fin d'étude en vue de l'obtention du

Diplôme Master En Electrotechnique

OPTION : Commande Electrique

**Commande d'un onduleur Z-source intégré
dans un système Photovoltaïque**

Présenté par :

MAHDJOUBI Soumya

HALA Amina

Encadré par

Mr. OULAD ALI Omar

Année Universitaire : 2019 / 2020

Abstract:

The aim of this work is to study of Z-source inverter connected with PV generator, to improve the performance of the classic inverter. This system is used to feed an induction motor. Moreover, this inverter makes sure the both function of a booster chopper and an inverter in one stage. In addition, a modified space vector pulse-width modulation (SVPWM) control method has been used to control the Z-source inverter by insertion of shoot-through state with the Z-source network together to achieve the best efficiency and reduce the Total Harmonic Distortion (THD). The MPPT technique is used to obtain optimal power performance of the photovoltaic generator (GPV). The MPPT technique allowed obtaining the optimal power performance of the photovoltaic generator (GPV). The simulations results have been obtained by numerical MATLAB/Simulink Software to validate the propose study.

Keywords: Z-source inverter, photovoltaic generator (GPV), Shoot through State, PWM Control, MPPT technique.

Résumé:

Ce travail visé à étudier le cas d'un onduleur à Z-source en mode de connecter avec un générateur photovoltaïque pour le but d'améliorer les performances des convertisseurs classiques à deux étages, ce système est alimenté un moteur asynchrone. Cet onduleur assure la fonction d'un hacheur survolteur et d'un onduleur dans un seul étage. D'autre part, une méthode de contrôle de modulation de largeur d'impulsion vectorielle modifiée (SVPWM) a été utilisée pour commander avec l'onduleur Z-source par l'insertion de l'état court-circuit, pour obtenir le meilleur rendement et une réduction de taux des Distorsions Harmonique Totale (THD). La technique MPPT est utilisée pour obtenir un fonctionnement optimal en puissance du générateur Les simulations sont effectuées par l'environnement Matlab/Simulink pour vérifier l'étude proposée.

Mots clés : Z-Source, Générateur photovoltaïque (GPV), court-circuit, technique MPPT, Modulation large impulsion (MLI).

ملخص:

العمل المقدم في هذه المذكرة يتضمن دراسة مموج ذو مصدر ممانع (Z-Source) متصل بمولد كهروضوئي من اجل تحسين خصائص المموج وتغذية محرك غير تزامني. المموج المدروس يؤمن وظيفة المقطع الرافع (hacheur survolteur) للتوتر والمموج في ان واحد. لتحكم في هذا المموج تم اختيار طريقة تحكم لتعديل عرض النبضة (SVPWM) المعدلة مع اظهار حالة قصر الدارة (court-circuit) لتحسين جودة المموج وتقليل نسبة التشوه التوافقي الكلي (THD). بالإضافة لاستعمال تقنية تتبع الطاقة العظمى (MPPT) للحصول على المردود الأمثل للمولد الكهروضوئي. تم إجراء عمليات المحاكاة للمموج باستعمال برنامج Simulink / Matlab.

الكلمات المفتاحية: المموج Z-Source ، المولد الكهروضوئي، حالة الدارة القصيرة، طرق التحكم (SVPWM)، تقنية تتبع الطاقة العظمى (MPPT).

Dedicate

To my grandmother's soul, "El-Hadjah Karmiya", who pushed us to learn and always supported us with her prayers, May Allah will not tempt us after her or deprive us of her reward".

To my grandmother, "El-Hadjah Fatna", may God prolong her life and not deprive us of her prayers.

To my dear mother, the source of my strength, thank you from all of my depths for your encouragement.

To my dear father, thank you for always being there, and for all your advices, without you I would not have reached what I am now .

To my dear sisters, and brothers, thanks for your patience.

To "Mohammed Nadjib".

To my uncle "Embarek", for his continuous support and guidance.

To our teachers for their guidance, to all my friends and colleagues.

Sincere thanks to my colleague in this work, Soumya,

Thanks to everyone who contributed from near or far to the completion of this work.

Amina

Dedicate

Specially dedicated to...

My parents for their endless love, support and encouragement;

My dear grandmother, may Allah bless you;

My brothers, sister and my family who made this achievement possible;

My dear sister and best friend "Hadjer", that supports me morally and helps me for the duration of the work.

My colleague in this work, Amina;

My instructors who have helped me in difficult times,

Without forgetting who advised me and contributed in a direct or indirect way from near or far to the completion of this work.

Thank you.

Soumya

ACKNOWLEDGMENTS

Firstly, we thank Allah Almighty who gave us the strength and the will to be able to finish this master thesis.

This work would not have been successful without the contribution and encouragement of many people. We would like to express our sincere thanks as well as our deep gratitude to all those who have contributed directly or indirectly to the achievement of this modest work.

We would first like to thank:

Mr.OULEDALI. OMAR, Assistant Professor at the University of Adrar for accepting the direction of this thesis. We express our gratitude to him for his experience, his support and for sharing his knowledge.

Our gratitude also go to:

Mr. BOUTADARA Abdelkader, **Dr. NECAIBIYYA Ammar** Electronic System Team Leader at URER/MS Adrar, **Dr. YAICHI Mohammed** Pumping Team Leader at URER/MS Adrar.

We would also like to thank our colleges of 2019/2020 promotion and all of our teachers who have contributed to our training.

Table of Contents

Abstract
List of table IV
List of figure..... V
List of abbreviations VIII
General Introduction1

CHAPTER I

I.1 Introduction:.....5
I.2 Renewable energies:5
 I.2.1 The different types of renewable energy:5
 I.2.2.1 Solar energy:.....5
 I.2.2.2 Wind energy:7
 I.2.2.3 Geothermal energy:7
 I.2.2.4 Hydropower:.....8
 I.2.2.5 Marine energy:9
 I.2.2.6 Bioenergy:9
I.3 Photovoltaic solar energy:10
 I.3.1 Solar radiation:10
 I.3.1.1 Radiation components:10
 I.3.2 Principle of the photoelectric conversion:11
 I.3.3 Photovoltaic cell:12
 I.3.3.1 Historical Development:12
 I.3.3.2 Photovoltaic Cells Technologies:13
 I.3.3.3 Photovoltaic module:15
I.4 Photovoltaic systems:16
 I.4.1 Stand-alone systems:16
 I.4.2 Grid-connected systems:17
 I.4.3 Hybrid Systems:17
I.5 General information on Z-source converters:18
 I.5.1 Converter:18
 I.5.2 Solar Inverter:18
 I.5.3 Types of inverters:19
 I.5.4 Z-source Inverter:19
 I.5.5 Z-source inverter topologies:20
I.6 Conclusion:22

CHAPTER II

II.1 Introduction:.....24
PART 1: Modeling Of Photovoltaic Panels.....24
II.2 Basic Functioning Of the Solar Cell:24
 II.2.1 Photovoltaic Modules Interconnection:24
II.3 Mathematical model for a PV module:25
II.4 Reference Model:.....27
PART 2: Converter DC/DC and MPPT control:27
II.5 Optimization of the performance of the GPV:27
 II.5.1 DC-DC converter (chopper):28

II.5.1.1	Boost converter (step-up converter):.....	28
II.5.1.2	Buck converter (step-down converter):	30
II.5.1.3	Buck-Boost converter (step-to-step converter):	30
II.5.2	The MPPT Control Technique:.....	31
II.5.2.1	Definition:	31
II.5.2.2	Converter For the continuation of the maximum power point:	31
II.5.2.3	Principle of finding the maximum power point:	32
II.5.2.4	MPPT research methods:.....	32
II.5.2.5	Perturb and observe (P&O) method:.....	32
II.6	Simulation Model:	33
II.6.1	Simulink model PV cell:	33
II.6.2	Simulink model of Step-up DC/DC Converter:	34
II.6.3	Simulink Block diagram of P&O MPPT:.....	35
II.6.4	Simulink Block of PV model with P&O MPPT:	35
II.7	Simulation Results:.....	35
II.7.1	Solar cell simulation results:.....	35
II.7.1.1	Effect of Variation of Solar Irradiation:	36
II.7.1.2	Effect of Variation of Temperature:	38
II.7.2	Simulation Results of MPPT and the Converter Model:	39
II.7.3	Analyze and discuss:.....	40
II.8	Conclusion:	41

CHAPTER III

III. 1	Introduction	44
III. 2	Inverter:	44
III. 3	Traditional voltage source inverter (VSI):.....	44
III. 4	Z-Source converter (ZSC):	46
III.4.1	Comparison between CSI, VSI and ZSI:.....	47
III. 5	Z-Source inverter:	47
III.5.1	Topology of a three phase inverter with Z-Source structure:	48
III.5.2	Configurations of a three-phase inverter with Z-Source structure:	49
III.5.3	Operating principle and circuit analysis of Z-source network:.....	50
III.5.3.1	Shoot-Through State:	51
III.5.3.2	Active States (Non shoot-Through State):	52
III.5.4	Calculation of the Elevation Factor β :	52
III. 6	Control strategies for Z-source inverter:	53
III.6.1	Sinusoidal Pulse Width Modulation (SPWM):	54
III.6.2	Space Vector Pulse Width Modulation (SVPWM) Control:	57
III.6.2.1	Modified Space Vector PWM (MSVPWM):	57
III.6.2.2	Rotating Transformation:	58
III.6.2.3	Principle of SVPWM:	59
III.7	Simulation Model:	64
III.7.5	Simulink model of hardware circuit:	64
III.7.6	Model building of Z-source inverter:.....	65
III.7.7	Simulink model of SPWM signal generator:.....	65
III.7.8	Simulink model of SVPWM signal generator:	66
III.8	Simulation Results:.....	67
III.8.1	The simulation results of SPWM control:	67

III.8.2 The simulation results of SVPWM control:	69
III.8.3 The three-phase inverter with SPWM control simulation results:	71
III.8.4 The three-phase ZSI with SPWM control simulation results:.....	74
III.8.5 The three-phase ZSI with SVPWM control simulation results:.....	78
III.8.6 Interpretation of results:	79
III. 9 Conclusion:	80

CHAPTER IV

IV. 1 Introduction:.....	82
IV. 2 Asynchronous Motor:	82
IV.2.1 Definition:.....	82
IV.2.2 Types of Induction Motors:	82
IV.2.3 Parts of Induction Motor:	82
IV. 3 Operating Principle of Induction Motors:	83
IV. 4 Synchronous Speed and the Slip:.....	83
IV. 5 Advantages of Induction Motor:.....	84
IV. 6 SVPWM Controlled ZSI Drive for Speed Control of three- Phase Induction Motor: 84	84
IV. 7 Simulation Model:	85
IV.7.1 Simulink Model of MAS connected with three phase VS:	85
IV.7.2 Simulink Model of MAS connected with three phase ZSI:	85
IV. 8 Simulation Results:.....	86
IV.8.1 The asynchronous machine simulation result:.....	86
IV.8.2 ZSI fed induction motor drives simulation result:.....	87
IV. 9 Conclusion:	87
General conclusion:.....	89
Bibliography	XII
ANNEX.....	XVII

List of table**CHAPTER I**

Table I.1: Classification of Solar panels according to the crystalline structure.	14
--	----

CHAPTER II

Table II.1: Electrical characteristics of the SOLKAR 36 W PV module [PNR 11].	27
--	----

CHAPTER III

Table III.1: Comparisons of CSI, VSI and Impedance Source Inverter (ZSI) [ZPH 12].	47
Table III.2: Switching states of three-phase Z-source inverter [LPC 04].	49
Table III.3: The states used with the Z-source command [BEF 16].	50
Table III.4: Space Vectors, Switching States, and On State Switches.	60
Table III.5: The corresponding relationship between N and sector	61
Table III.6: Parameters used for simulation.	66

List of figure

CHAPTER I

Figure I.1: Solar energy resources [GSH 17].	5
Figure I.2: Solar energy types.	6
Figure I.3: Wind Turbines [GSH 17].	7
Figure I.4: Modern Wind Turbines [GSH 17].	7
Figure I.5: Geothermal energy resources [GSH 17].	8
Figure I.6: Hydropower resources [GSH 17].	8
Figure I.7: Tidal Turbines Technology for generation of water power [GSH 17].	9
Figure I.8: Solar radiation types [BYA 17].	11
Figure I.9: The pyranometers [URERMS 2020].	11
Figure I.10: Photoelectric conversion.	12
Figure I.11: Photovoltaic cell.	12
Figure I.12: Classification of PV technologies with their current market share in percentage.	13
Figure I.13: Organic solar cells.	15
Figure I.14: PV array.	15
Figure I.15: Stand-alone system.	16
Figure I.16: Grid-connected systems.	17
Figure I.17: Hybrid system (Solar/wind).	17
Figure I.18: Schematic diagrams of a Voltage and Current Source Inverter [SHS 18].	19
Figure I.19: Schematic diagram of a Z-source Inverter [BKP 17].	20
Figure I.20: Bidirectional-Z source inverter [BKP 17].	21
Figure I.21: The transformer-based ZSI topology [EHA 16].	21
Figure I.22: Quasi Z-source inverter [AUS 13].	22

CHAPTER II

Figure II.1: Connection of Modules in Series.	25
Figure II.2: Connection of Modules in Parallel.	25
Figure II.3: Connection of Modules in Series and Parallel.	25
Figure II.4: PV modeled as diode circuit.	26
Figure II.5: Circuit diagram of a Boost converter.	28
Figure II.6: ON state of the IGBT switch.	29
Figure II.7: OFF state of the IGBT switch.	29
Figure II.8: Circuit diagram of a Buck converter.	30
Figure II.9: Circuit diagram of a Buck-Boost chopper.	30
Figure II.10: PV system with DC-DC Boost converter.	31
Figure II.11: P&O algorithm.	33
Figure II.12: External view of PV module in Simulink window.	34
Figure II.13: Model of Boost Converter.	34
Figure II.14: Simulink Block diagram of P&O MPPT.	35
Figure II.15: MPPT System used for simulation.	35
Figure II.16: I-V characteristics of a solar cell.	36
Figure II.17: P-V characteristics of a solar cell.	36
Figure II.18: Input – Time varying irradiation.	36

Figure II.19: Input - Constant temperature – 25°C.	37
Figure II.20: Output – I-V characteristics with varying irradiation.	37
Figure II.21: Output – P-V characteristics with varying irradiation.	37
Figure II.22: Input – Time varying temperature.	38
Figure II.23: Input – Constant irradiation at 1000 W/m ²	38
Figure II.24: Output – I-V characteristics with varying temperature.	39
Figure II.25: Output – P-V characteristics with varying temperature.	39
Figure II.26: Input current (the output current of PV) and output current of Boost converter.	39
Figure II.27: Input voltage (the output voltage of PV) and output voltage of Boost converter.	40
Figure II.29: Input power (the output power of PV) and output power of Boost converter.	40

CHAPTER III

Figure III.1: General block diagram of DC-AC converter.	44
Figure III.2: Voltage Source Inverter.	45
Figure III.3: Traditional two-stage DC/AC power conversion.	45
Figure III.4: Single stage DC/AC power conversion.	46
Figure III.5: General structure of the Z-source converter.	46
Figure III.6: General structure of a Z-source inverter.	47
Figure III.7: Topology of a three phase inverter with Z-Source structure.	48
Figure III.8: Equivalent circuit of the Z-source inverter viewed from the dc link.	50
Figure III.9: Equivalent circuit shoot-through zero state of the ZSI viewed from the dc link.	51
Figure III.10: Equivalent circuit non shoot-through switching states of the ZSI viewed from the dc link.	52
Figure III.11: SPWM signal produce: reference voltage and carrier wave vs. output voltage.	54
Figure III.12: Simple Boost PWM Control.	55
Figure III.13: Maximum Boost PWM Control.	55
Figure III.14: Maximum Constant Boost PWM Control [SHM 04].	56
Figure III.15: Maximum Constant Boost PWM Control with third-harmonic injection [PMZ 05].	57
Figure III.16: The relationship of abc reference frame and stationary dq reference frame.	58
Figure III.17: Park transformation from three-phase to rotating dq0 coordinate system.	59
Figure III.18: Voltage vector through conventional SVPWM of VSI.	61
Figure III.19: Switching patterns and placement of ST states in all sectors by SVPWM.	62
Figure III.20: PWM switching patterns at sector I.	63
Figure III.21: Simulink model of three-phase full bridge inverter system.	64
Figure III.22: Simulink model of the LC filter.	64
Figure III.23: Simulink model of three-phase full bridge Z-Source inverter system.	65
Figure III.24: Three-phase Pulse Width Modulation (PWM).	65
Figure III.25: SVPWM signal generator.	66
Figure III.26: Three-phase sinusoidal signals (Va, Vb and Vc) and output waveforms.	67
Figure III.27: Pulse Width Modulation (PWM) Control.	67
Figure III.28: SPWM signal produce: reference voltage and carrier wave vs. output voltage (upper and lower switches).	68
Figure III.29: FFT Analysis of output reference voltage Va of three- phase inverter with MI=0.8.	69
Figure III.30: Three-phase sinusoidal signal generator and output waveform.	69
Figure III.31: FFT Analysis of output sinusoidal signal generator.	69

Figure III.32: Clarke transformation block and output waveform.....	70
Figure III.33: Reference angel sector block.....	70
Figure III.34: Space vector modulation signal generator and the output waveform.....	70
Figure III.35: PWM signal generator.....	71
Figure III.36: Output voltage of three- phase inverter at 300 V.....	71
Figure III.37: Three Phase Voltage (Line to Neutral voltage) of three phase inverter across Load for MI= 0.8.....	71
Figure III.38: Three Phase Current waveform of three phase inverter across Load for MI= 0.8.....	72
Figure III.39: FFT Analysis of output Voltage (Va) of three phase inverter with MI= 0.8.....	72
Figure III.40: FFT Analysis of output current (Ia) of three phase inverter with MI= 0.8.....	72
Figure III.41: Three Phase Voltage (Line to Neutral voltage) of three phase inverter across Load for MI=0.8 after filtering.....	73
Figure III.42: Three Phase Current waveform of three phase inverter across Load for MI=0.8 after Filtering.....	73
Figure III.43: FFT Analysis of output Voltage (Va) of three phase inverter after filtering.....	73
Figure III.44: FFT Analysis of output Current (Ia) of three phase inverter after filtering.....	74
Figure III.45: Voltage across Impedance Network of three- phase ZSI for MI= 0.8.....	74
Figure III.46: Output voltage of three- phase Z-Source Inverter.....	74
Figure III.47: Three Phase Voltage (Line to Neutral voltage) of three- phase ZSI across Load for M=0.8.....	75
Figure III.48: Three Phase Current waveform of three- phase ZSI across Load for M=0.8.....	75
Figure III.49: FFT Analysis of Output Voltage (Va) of three- phase ZSI with MI= 0.8.....	76
Figure III.50: FFT Analysis of Output Current (Ia) of three- phase ZSI with MI= 0.8.....	76
Figure III.51: Three Phase Voltage (Line to Neutral voltage) of three- phase ZSI across Load for MI=0.8 after Filtering.....	76
Figure III.52: Three Phase Current waveform of three- phase ZSI across Load for MI=0.8 after Filtering.....	77
Figure III.53: FFT Analysis of Output Voltage (Va) of three- phase ZSI with MI= 0.8.....	77
Figure III.54: FFT Analysis of Output Current (Ia) of three- phase ZSI with MI= 0.8.....	77
Figure III.55: Output voltage of three- phase Z-Source Inverter.....	78
Figure III.56: Three Phase Voltage (Line to Neutral voltage) of three- phase ZSI across Load for M=0.8.....	78
Figure III.57: Three Phase current waveform of three- phase ZSI across Load for M= 0.8.....	78

CHAPTER IV

Figure IV.1: Induction Motor Parts.....	83
Figure IV.2: Project block diagram.....	84
Figure IV.3: Model of the asynchronous machine connected with three phase voltage source.....	85
Figure IV.4: Model of the asynchronous machine connected with three phase ZSI controlled by SPWM.....	85
Figure IV.5: Output waveforms of parameter of IM powered by three phase voltage source.....	86
Figure IV.6: Output waveforms of parameter of IM powered by three phase ZSI.....	87

List of abbreviations

<u>Acronym</u>	<u>Meaning</u>
RES	Renewable Energy Sources
PV	Photovoltaic
ZSI	Z-Source Inverter
CSP	Concentrated Solar Power
DC	Direct Current
AC	Alternating Current
SI	Silicon
OSC	Organic solar cells
CdTe	Cadmium Telluride
CIGS	Copper Indium Gallium Selenide
CSI	Current Source Inverter
VSI	Voltage Source Inverter
OC	Open Circuit
SC	Short Circuit
ST	Shoot-Through
PWM	Pulse Width Modulation
MPPT	Maximum Power Point Tracking
P&O	Perturb And Observe
STC	Standard Test Condition
SVPM	Space Vector Modulation
IGBT	Insulated Gate Bipolar Transistor
THD	Total Harmonic Distortion

ZSC	Z-Source Converter
SPWM	Sinusoidal Pulse Width Modulation
SBC	Simple Boost Control
MBC	Maximum Boost Control
MCBC	Maximum Constant Boost Control
EMI	Electromagnetic Interference
SVPWM	Space Vector Pulse Width Modulation
MSVPWM	Modified Space Vector PWM
EmF	Electrometric Force
IM	Induction Motor

LIST OF ABBREVIATIONS

<u>Symbol</u>	<u>Signification</u>	<u>Unit</u>
h	Planck's Constant	(Js)
V_{pv}	Output Voltage Of A PV Module	(V)
I_{ph}	Module Photo-Current (Current Source)	(A)
I_d	Diode Current	(A)
I_{RS}	Module Reverse Saturation Current	(A)
R_s	Series Resistance	(Ω)
R_p	Parallel Resistances	(Ω)
I_s	Saturation Current	(A)
I	The Current Output Of PV Module	(A)
N_s	The Number Of Cells Connected In Series	/
N_p	The Number Of Cells Connected In Parallel	/
G	The PV Module Illumination	(W/m^2)
K	Boltzman Constant	(J/K)
A	Ideality Factor	/
T	The Module Operating Temperature	(K)
T_r	The Reference Temperature	(K)
q	The Reference Temperature	(C)
K_i	The Short-Circuit Current Temperature Co-Efficient	(A / $^{\circ}C$)
E_g	The Band Gap For Silicon	(eV)
V_{in}	Input Voltage	(V)
D	The Converter Duty Cycle	/
V_{out}	Output Voltage	(V)
f	The Switching Frequency Of The Converter	(Hz)

LIST OF ABBREVIATIONS

V_a, V_b and V_c	Line To Neutral Voltage	(V)
V_{dc}	DC Source Voltage Of Three Phase Inverter	(V)
C1 and C2	Two Capacitors Of Z-Source Inverter	(H)
L1 and L2	Two Inductors Of Z-Source Inverter	(F)
S1, S2, S3	The Ups Switch States	/
M	The Modulation Index	/
T_s	Total Switching Time Period	(Sec)
T_0	The Zero/Null State Time Periods	(Sec)
D_0	The Shoot Through Duty Ratio	/
β	Boosting Factor	/
G	Voltage Gain	/
V_p and V_n	The Upper And Lower Envelope Curves	/
U_m	The Peak Value Of Three-Phase Sinusoidal Voltage	/
ω	The Radian Frequency	(rad/sec)
A, b, c	Indices Corresponding To The Three Phases A, B, C	/
d, q	Axes Corresponding To The Frame Of Reference Linked To The Rotating Field.	/
α, β	Axes Corresponding To The Fixed Reference Frame Relative To The Stator	/
N_{sync}	The Synchronous Speed Of Stator	(rpm)
P	The Number Of Poles	/
N_r	The Speed Of The Rotor	(rpm)
S	The Slip	/
E_r	Rotor Induction Electrometric Force.	(N)
I_r	Rotor Induction Current	(A)

GENERAL INTRODUCTION

General Introduction

Overview:

Nowadays, the power electronics has evolved and becomes very important in our life, is a technology that deals with the conversion and the control of electrical power with high-efficiency switching mode electronic devices for a wide range of applications, this includes a DC and AC power supplies.

Power electronics has found an important place in modern technology a core of power and energy control. In recent years, the energy has increased at a rapid pace. As the rate of electricity consumption at a user end is growing more rapidly than the growth of the energy generation hence there is a need for more generation for whole of world.

Contribution of renewable energy in total electricity generation is eagerly welcomed by all nations, renewable generation facilities are growing at the fastest rate due to increase a global public awareness, dependent on fossil fuel (increasing cost). All of the hazardous consequences coming from fossil fuels can eliminate by using the renewable energy sources (RES).

Among the renewable energy sources (RES), the solar energy is promising and the photovoltaic (PV) system provides the most direct method to convert the solar energy into the electrical energy without any an environmental pollution. It uses modules or photovoltaic panels, composed of solar cells or photocells which carry out this energy. Photovoltaic conversion is based on photon absorption in a semiconductor material that provides loads electrical, therefore current, in an external circuit.

The integration of these renewable energies into the grid poses technical problems, knowing these energies are intermittent: The nature variable of these sources requires adaptation stages that allow the optimal use adapted with the different applications and ensure a transfer quality of the energy produced. So the static converters and their control have become unavoidable in current electrical energy conversion devices.

This work precisely on the study of the possibility of replacing a structure combining a DC/DC converter and a DC/AC inverter by a new topology of

inverters. This structure named by its architect, an impedance source inverter (ZSI).

Z-source-related research has grown rapidly; it was firstly proposed in 2002 by Prof. **Feng Zheng Peng**. The ZSI is an alternative power conversion topology, which is based on Z-source network, can buck and boost the output AC voltage, which is not possible using traditional voltage source or current source inverters. It not only converts a continuous signal into an alternating signal but also has the elevating function allowing it to raise the source voltage to a higher level so, Z-source can have greater output AC voltage than the input, which is not possible using traditional voltage source or current source inverters.

Z-source inverter can utilize the shoot-through states to boost the output voltage, which improves the inverter reliability greatly, and provides an attractive single stage DC to AC conversion that can buck and boost the voltage. The shoot-through duty cycle is used for controlling the DC link voltage boost and hence the output voltage boost of the inverter.

Aims of Project:

The main objective of this project are the illumination of the way to design and understand Z-Source inverter; in order to know the function's principle of Z-Source Inverter. In addition, the develop and simulation of the Three-Phase Z-Source inverter used to boost the output voltage of this inverter by using MATLAB/Simulink software. The last objective is the comparative result of ZSI with the traditional voltage source inverters.

Project organization:

This project consists of general introduction, four chapters, general conclusion and future works.

In the beginning, the general introduction discusses the general information of the subject. In addition, the objectives of project, scopes of study, the problem statement and project structure are presented.

The first chapter summarized the background study and the current status of the renewable energies exactly photovoltaic solar energy; and Z-Source inverter.

In addition, the chapter covers the photovoltaic systems and general information on Z-source converter. It is covers also the Z-Source inverter topologies.

The second chapter discusses the modeling of photovoltaic panels and *MPPT* control. Is divided into two parts; the first section summarized the modeling of photovoltaic panels, and the second parts covers the converter dc/dc and MPPT control. In addition, the chapter discusses the characteristic of SOLKAR make 36 W PV module with using MATLAB/Simulink.

The third chapter summarized the modeling and simulation of z-source inverter. In addition, the chapter discusses; the topology, configuration and operating of a three-phase inverter with Z-Source structure. It is covers also the Control strategies for Z-source inverter with PWM techniques. Design of model it using MATLAB/Simulink.

The fourth chapter present the final results and analysis of the global model Z-Source three phase inverter connected with induction motor by using Space PWM Method.

Finally, the general conclusion consists the results of this project for control of the Z-Source three phase inverter applied to a photovoltaic system and recommendations for future works.

CHAPTER I:

Background Study and Current Status

I.1 Introduction:

Solar energy is one of the most renewable energy. It plays a very important role in meeting energy demands in the near future, since it is a clean type of energy with a multiplicity of applications like solar cell.

With rapid growth of solar photovoltaic (PV) and energy storage systems, there is high demand for efficient and reliable power converter solutions. Different families of power transformers aim to connect the renewable solar resource with different applications. One of the most popular topologies for converting power electronics is the Z-source inverter (ZSI).

In this chapter, we will firstly introduce the different kinds of renewable energy, focusing on photovoltaic solar energy, and then we will study the integration of one of the new power electronics converters in photovoltaic solar production which is the Z-source inverter. Finally, some topologies will be given to show how advanced this type of converter is.

I.2 Renewable energies:

Renewable energy uses energy sources that are continually replenished by nature the sun, the wind, water, the Earth's heat, and plants. Renewable energy technologies turn these fuels into usable forms of energy most often electricity, but also heat, chemicals, or mechanical power.

Renewable energy is abundant, and the technologies are improving all the time. There are many ways to use renewable energy. Most of us already use renewable energy in our daily lives.

I.2.1 The different types of renewable energy:

I.2.2.1 Solar energy:



Figure I.1: Solar energy resources [GSH 17].

Solar energy is an important source of renewable energy and its technologies are generally characterized as either passive solar or active solar depending on how they capture and distribute solar energy or convert it into solar power. Solar energy is radiant light and heat from the Sun that can be recovered by two methods, as shown in figure (I.2)

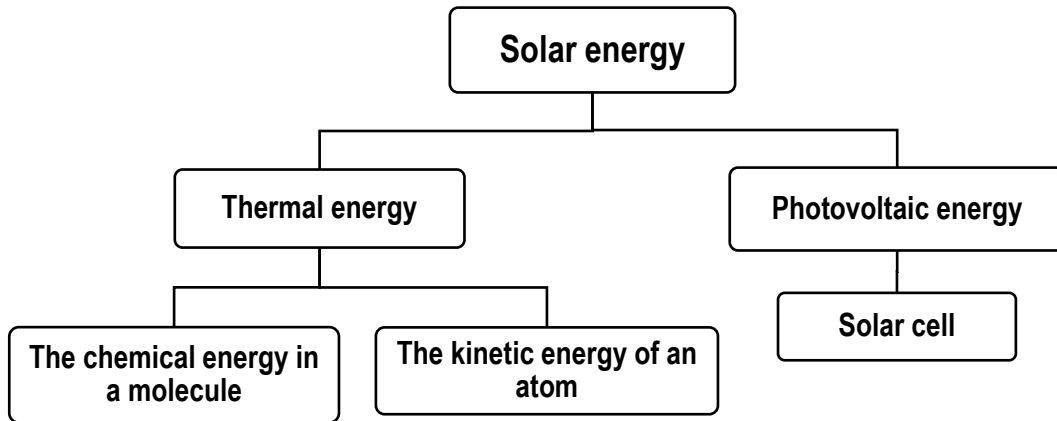


Figure I.2: Solar energy types.

A. Typical technologies of solar energy:

Solar power is one of the best renewable energy sources available because it is one of the cleanest sources of energy. Solar power plants use one of two technologies:

- **Photovoltaic (PV) systems** use solar panels made from silicon or other materials, either on rooftops or in ground-mounted solar farms, converting sunlight directly into electric power.
- **Concentrated solar power (CSP)**, also known as "concentrated solar thermal") plants use solar thermal energy to make steam that is thereafter converted into electricity by a turbine [1].

B. Applications of solar energy:

The major application of solar energy is: Solar water heating, solar pumping, solar heating of buildings, solar distillation, solar drying of agricultural and animal products, solar furnaces, solar cooking, solar electric power generation, solar thermal power production and solar green houses.

I.2.2.2 Wind energy:

Wind is used to produce electricity using the kinetic energy created by air in motion. This is transformed into electrical energy using wind turbines or wind energy conversion systems. Wind first hits a turbine's blades, causing them to rotate and turn the turbine connected to them. That changes the kinetic energy to rotational energy, by moving a shaft which is connected to a generator, and thereby producing electrical energy through electromagnetism [2].



Figure I.3: Wind Turbines [GSH 17].



Figure I.4: Modern Wind Turbines [GSH 17].

I.2.2.3 Geothermal energy:

Geothermal heat is the only renewable energy source created naturally by the Earth itself. Geothermal energy is heat resulting within the sub-surface of the earth. Water and/or steam carry the geothermal energy to the Earth's surface.



Figure I.5: Geothermal energy resources [GSH 17].

There are different geothermal technologies with different levels of development, technologies for direct uses like district heating, geothermal heat pumps, greenhouses, and for other applications are widely used and can be considered mature. The technology for electricity generation from hydrothermal reservoirs with naturally high permeability is also mature and reliable, and has been operating since 1913 [2].

I.2.2.4 Hydropower:

Hydropower or water power is power derived from the energy of falling water or fast running water, which may be harnessed for useful purposes. Flowing water creates energy that can be captured and turned into electricity. This is called hydroelectric power or hydropower.

The most common type of hydroelectric power plant uses a dam on a river to store water in a reservoir [GSH 17].



Figure I.6: Hydropower resources [GSH 17].

The necessary principle of hydropower is using water to drive turbines. Hydropower plants consist of two essential configurations: with dams and reservoirs, or without [2].

I.2.2.5 Marine energy:

Marine and hydrokinetic energy systems, a new generation of water power Technologies offer the possibility of generating electricity from water without the need for dams and diversions [GSH 17].

The ocean can produce two types of energy:

- Thermal energy from the sun's heat.
- Mechanical energy from the tides and waves.

The three most well-known generating technologies for deriving electrical power from the ocean are:

- Tidal power
- Wave power
- Ocean thermal energy conversion (OTEC).



Figure I.7: Tidal Turbines Technology for generation of water power [GSH 17].

I.2.2.6 Bioenergy:

One of the promising sources of renewable energy is biomass. Biomass is the feedstock used to produce bioenergy. Bioenergy use falls into two main categories: “traditional” and “modern”.

- Traditional use refers to the combustion of biomass in such forms as wood, animal waste and traditional charcoal.
- Modern bioenergy technologies include liquid biofuels produced from bagasse and other plants, bio-refineries, biogas produced through anaerobic digestion of residues, wood pellet heating systems, and other technologies [2].

I.3 Photovoltaic solar energy:

The word photovoltaic consists of two words: photo, a Greek word for light, and voltaic, which defines the measurement value by which the activity of the electric field is expressed, i.e. the difference of potentials. Photovoltaic systems use cells to convert sunlight into electricity. Converting solar energy into electricity in a photovoltaic installation is the most known way of using solar energy [3].

The particles of light are called photons. Photons are mass less particles, moving at light speed. The energy of the photon depends on its wavelength and the frequency, and we can calculate it by the Einstein's law, which is:

$$E = h * V \quad (I.1)$$

Where [3]:

- E: photon energy
- h :Planck's constant = 6.626×10^{-34} Js
- V: photon frequency

I.3.1 Solar radiation:

A solar radiation sensor measures solar energy from the sun. Solar radiation is radiant energy emitted by the sun from a nuclear fusion reaction that creates electromagnetic energy. The spectrum of solar radiation is close to that of a black body with a temperature of about 5800 K. About half of the radiation is in the visible short-wave part of the electromagnetic spectrum. The other half is mostly in the near-infrared part, with some in the ultraviolet part of the spectrum. The units of measure are Watts per square meter [4].

I.3.1.1 Radiation components:

There is three radiation components can be distinguished at the surface: direct, diffuse, and global solar radiation [5].

- **Direct radiation:** Direct radiation is received from sun rays travelling in a straight line from sun to the earth. [BYA 17].

- **Diffuse radiation:** Diffuse radiation does not have any fixed direction. When sun rays are scattered by particles present in the atmosphere, these scattered sun rays account for the diffuse radiation [BYA 17].

- **Reflected radiation:** Reflected radiation is the component of radiation which is reflected from surfaces other than air particles [BYA 17].

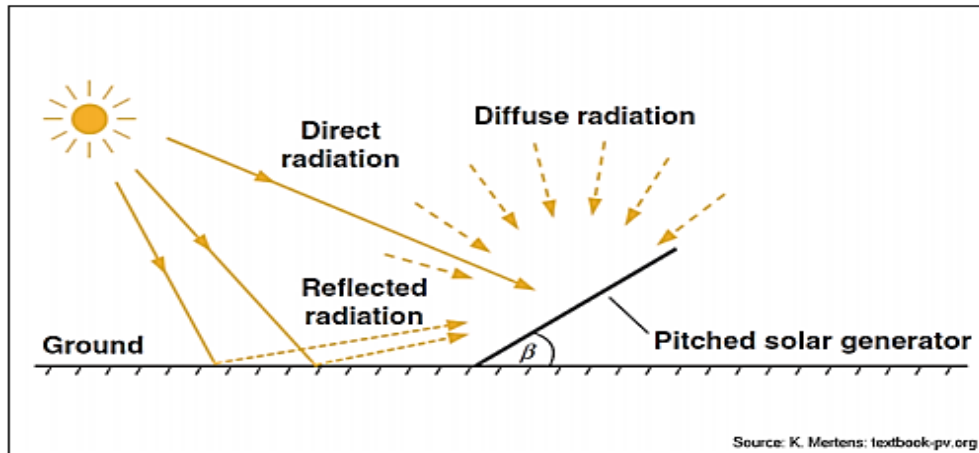


Figure I.8: Solar radiation types [BYA 17].

- **Global radiation:** Global radiation is the sum of direct, diffuse and reflected radiation.

Global radiation is measured with pyranometers, which are radiometers designed for measuring the total (global) irradiance on a plane surface.



Figure I.9: The pyranometers [URERMS 2020].

I.3.2 Principle of the photoelectric conversion:

The photoelectric conversion in the PV junction (diode) is a boundary between two differently doped semiconductor layers; one is a P-type layer (excess holes), and the second one is an N-type (excess electrons). At the boundary between the P and the N area, there is a spontaneous electric field, which affects the generated electrons and holes and determines the direction of the current [3].

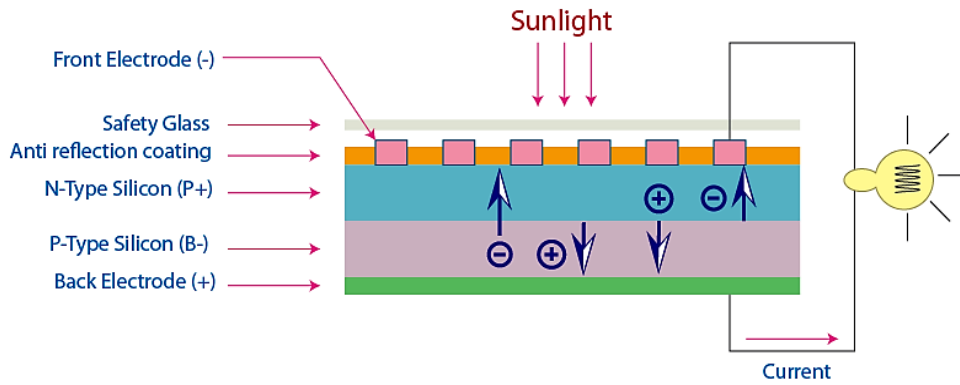


Figure I.10: Photoelectric conversion.

The operation of a photovoltaic (PV) cell requires 3 basic attributes:

1. The absorption of light, generating either electron-hole pairs or exactions.
2. The separation of charge carriers of opposite types.
3. The separate extraction of those carriers to an external circuit.

I.3.3 Photovoltaic cell:

A Solar cell, or photovoltaic cell, is an electrical device that converts the energy of light directly into electricity by the photovoltaic effect. It is a form of photoelectric cell, defined as a device whose electrical characteristics, such as current, voltage, or resistance, vary when exposed to light. Solar cells are the building blocks of photovoltaic modules, otherwise known as solar panels.



Figure I.11: Photovoltaic cell.

I.3.3.1 Historical Development:

The photovoltaic effect has been discovered in the first half of the 19th the century. In 1839, a young French physicist Alexandre Edmond Becquerel observed a physical phenomenon or effect that allows the conversion of light into electricity [5].

- ✚ **1839 – 1899:** Discovery of Basic Phenomena and Properties of PV Materials.
- ✚ **1900 – 1949:** Theoretical Explanation of the PV Effect and First Solar Cells.
- ✚ **1950 – 1969:** Intensive Space Research.
- ✚ **1970 – 1979:** Establishment of Large Photovoltaic Companies.
- ✚ **1980 – 1989:** First Large Utility-Scale Photovoltaic Systems.
- ✚ **1990 – 1999:** Large-Scale Solar Cell Producers.
- ✚ **2000 – 2009:** Multi MW Utility-Scale PV Power Plants.

I.3.3.2 Photovoltaic Cells Technologies:

The most important material for solar cells production is silicon. At the time being it is almost the only material used for solar cell mass production. As the most often used semiconductor material it has many important advantages. In nature it can be easily found in large quantities. Silicon oxide forms one thirty of the Earth's crust. It is not poisonous, and it is environment friendly, its waste does not represent any problems [6].

Due production technology used solar cells can be divided into silicon solar cells, produced from Si wafers, and thin-film solar cells produced with vacuum technologies [6].

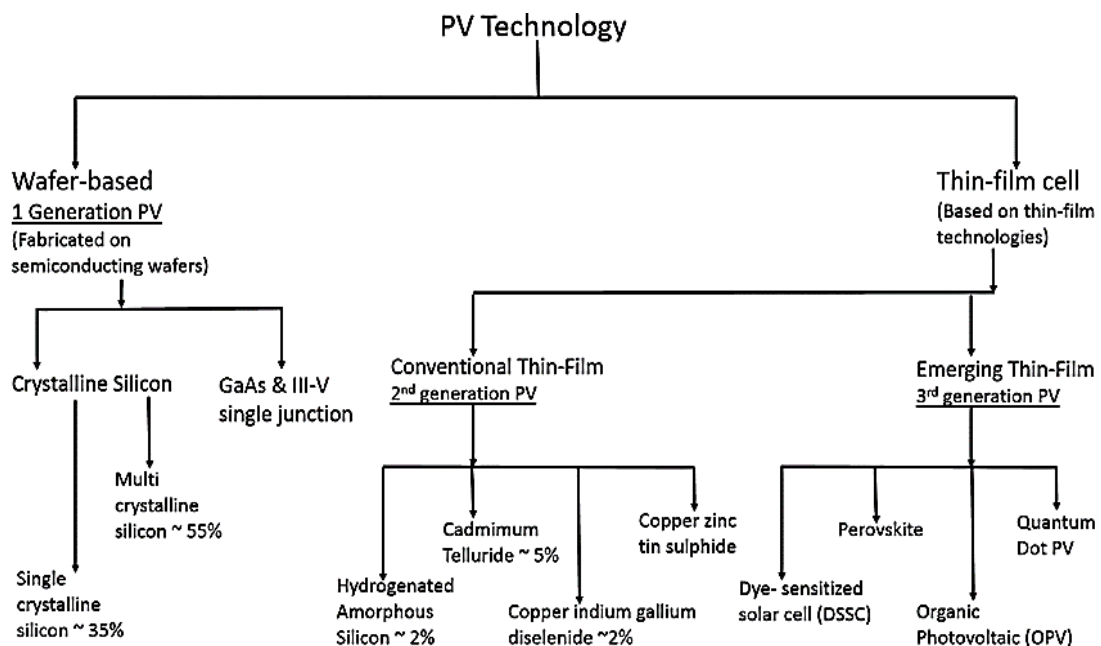
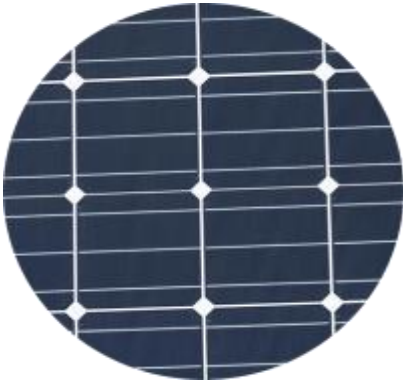
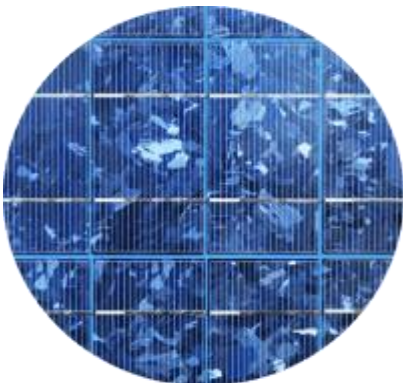



Figure I.12: Classification of PV technologies with their current market share in percentage.

According to the crystalline structure: amorphous, poly-crystalline and single-crystalline solar cells are distinguished, as shown in Table (I.1):

Table I.1: Classification of Solar panels according to the crystalline structure.

<ul style="list-style-type: none"> • Monocrystalline Solar Panels (Mono-SI): Monocrystalline Solar Panels (Mono-SI) This type of solar panels (made of monocrystalline silicon) is the purest one. You can easily recognize them from the uniform dark look and the rounded edges. The silicon's high purity causes this type of solar panel has one of the highest efficiency rates, with the newest ones reaching above 20% [7]. 	
<ul style="list-style-type: none"> • Poly-crystalline Solar Panels (Poly-SI): You can quickly identify these panels because this type of solar panels has squares, its angles are not cut, and it has a blue, speckled look. They are made by melting raw silicon, which is a faster and cheaper process than that used for monocrystalline panels. This leads to a lower final price but also lower efficiency (around 15%) [7]. 	
<ul style="list-style-type: none"> • Amorphous Silicon Solar Cell (A-Si): Amorphous silicon is the non-crystalline form of silicon used as semiconductor material for A-SI solar cells, or thin-film silicon solar cells. Amorphous silicon cells generally feature low efficiency (from 7 to 10%), but are one of the most environmentally friendly photovoltaic technologies, since they do not use any toxic heavy metals [8]. 	

- As a second-generation thin-film solar cell technology, amorphous silicon was once expected to become a major contributor in the fast-growing worldwide photovoltaic market, but has since lost its significance due to strong competition from conventional crystalline silicon cells and other thin-film technologies such as **CdTe** (Cadmium telluride) and **CIGS** (copper indium gallium selenide) [8].

- **Organic solar cells (OSC):**

Organic solar cells have become a subject of attention over time due to their prospects for low cost active layer materials, low-cost substrates, low energy input and the ease of up-scaling to the industrial level [GCU 10]. They have the potential to provide Earth-abundant and low-energy production PV solutions. They use small molecules of organic compounds or polymer to absorb light and consist mostly of Earth-abundant elements that can be fabricated into thin films using inexpensive deposition methods such as thermal evaporation and inkjet printing [JNJ 15].

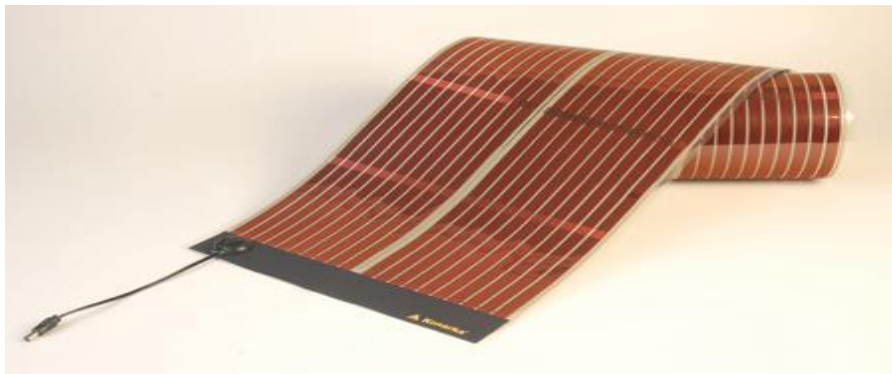


Figure I.13: Organic solar cells.

I.3.3.3 Photovoltaic module:

PV Module or Solar PV Module is an assembly of photovoltaic (PV) cells, also known as solar cells. To realize a required voltage and current, a group of PV modules (also called PV panels) are wired into large array that called PV array.

A PV module is the essential component of any PV system that converts sunlight directly into direct current (DC) electricity. PV modules can be wired together in series and/or parallel to deliver voltage and current in a particular system requires [9].

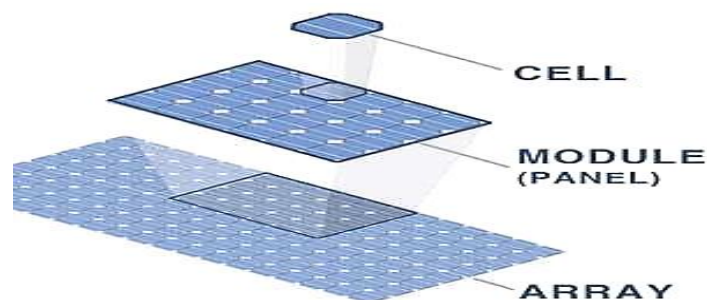


Figure I.14: PV array.

I.4 Photovoltaic systems:

A photovoltaic system uses one or more solar panels to convert PV energy into electricity. It consists of photovoltaic module, mechanical, electrical connections and mounting for regulating and/or modifying the electrical output [DKS 15]. Photovoltaic power systems have increasing roles in modern electric power energy mix due to the continuing decline in the world's conventional sources of energy [LDC 16].

The major advantages associated with PV power systems are [LDC 16]:

- They have no moving parts.
- Do not produce any noise.
- Require little or no maintenance, are non-polluting.
- Are renewable.
- Are highly modular.
- Are highly reliable.
- Can be installed almost anywhere.

PV systems are classified into three distinct types: stand-alone systems, grid-connected systems, and solar PV hybrid system [MSG 16].

I.4.1 Stand-alone systems:

Stand-alone systems where the power is generated and consumed in the same place and which does not interact with the main grid [BDP 14].

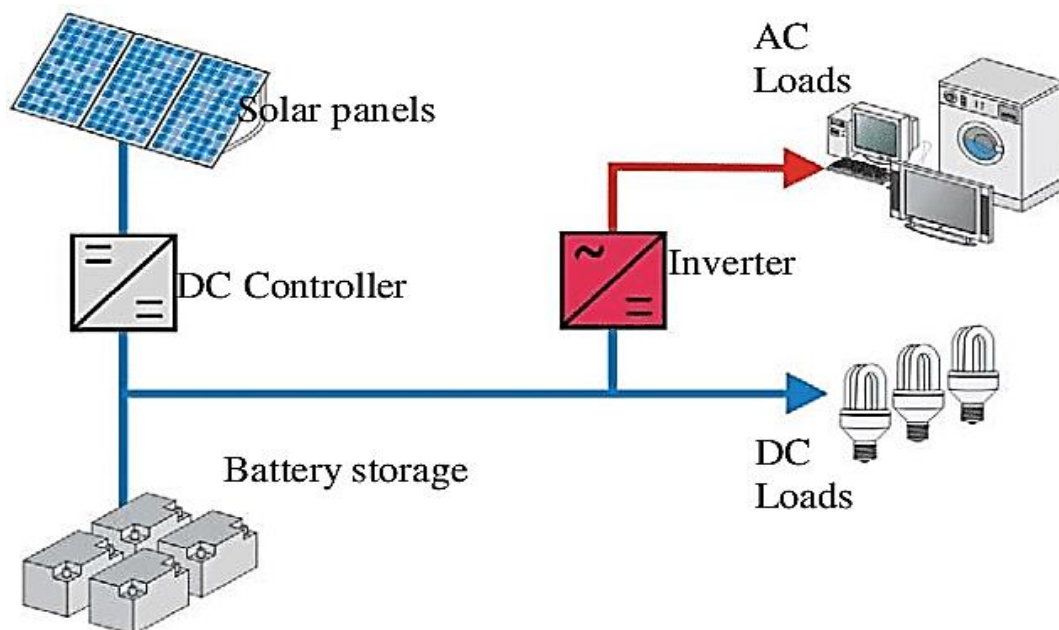


Figure I.15: Stand-alone system.

I.4.2 Grid-connected systems:

Nowadays, it is usual practice to connect PV systems to the local electricity grid. This means that, during the day, the electricity generated by the PV system can either be used immediately (which is normal for systems installed in offices, other commercial buildings, and industrial applications) or be sold to one of the electricity supply companies (which is more common for domestic systems, where the occupier may be out during the day). In the evening, when the solar system is unable to provide the electricity required, power can be bought back from the grid [KSA 13].

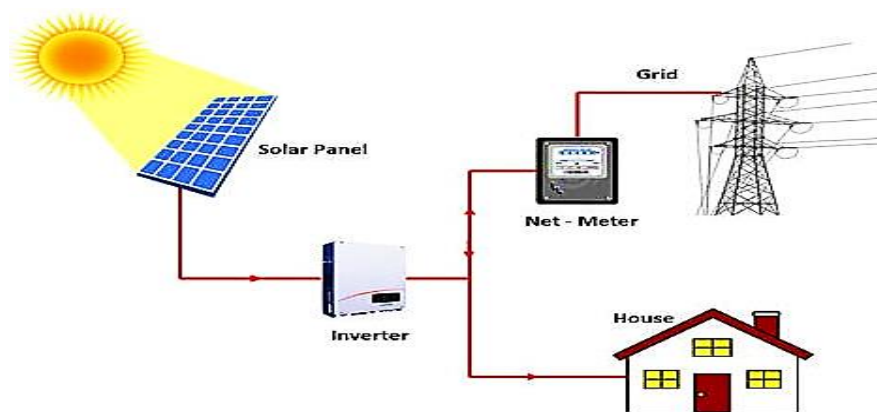


Figure I.16: Grid-connected systems.

I.4.3 Hybrid Systems:

In a hybrid system another source of energy, such as wind, biomass or diesel, can be hybridized to the solar PV system to provide the required power. Here the objective is to bring more reliability into the overall system at an affordable way by adding one or more energy source(s) [BDP 14].

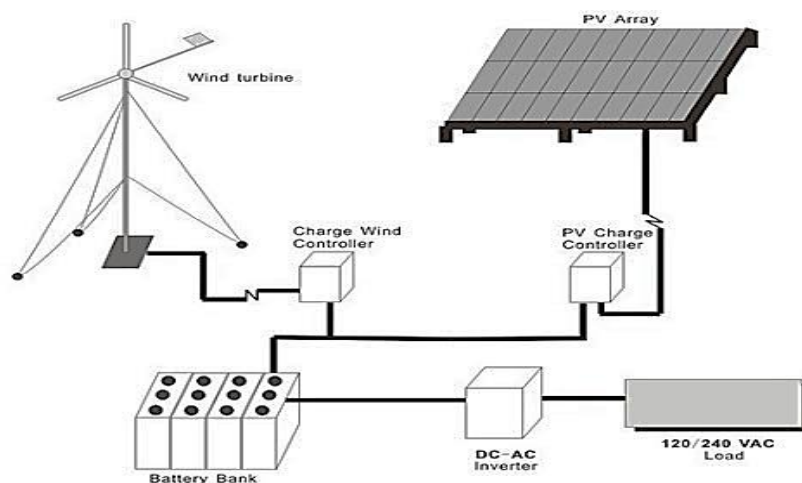


Figure I.17: Hybrid system (Solar/wind).

I.5 General information on Z-source converters:

Photovoltaic systems have been the worldwide fast growing energy source because of the increase in energy demand [SAK 10]. Solar PV system have given lot of importance particularly in the area where grid connected electricity is not available [PFZ 03]. Therefore, PV array is used as an input source, a Photovoltaic system is directly converts sunlight into electricity [SAK 10].

Solar PV fed converter system requires buck-boost capability to satisfy the load requirement. It requires two stage power conversion. This two-stage power conversion increases volume, cost and degrades the reliability of system. For reducing cost and volume single stage VSI topology called Z-Source inverter (ZSI) was proposed in [AER 17].

I.5.1 Converter:

A power converter is an electrical circuit that changes the electric energy from one form into the desired form optimized for the specific load. A converter may do one or more functions and give an output that differs from the input. The converter acts as the link or the transforming stage between the power source and the power supply output [10].

There are several types of converters based on the source input voltage and the output voltage and these falls into four categories namely [10]:

- ✚ The AC to DC converter known as the rectifier.
- ✚ The AC to AC converter known as the changer or transformer of cycloconverter.
- ✚ The DC to AC converter known as the inverter.
- ✚ The DC to DC converter known as the chopper (buck, boost or buck-boost).

I.5.2 Solar Inverter:

Solar Inverter or PV inverter, is a type of electrical converter which converts the output direct current (DC) of a PV solar panel into a utility frequency alternating current (AC) that can be fed into a commercial electrical grid or used by a local off-grid electrical network. Solar power inverters have special functions adapted for use with photovoltaic arrays, including maximum power point tracking and anti-islanding protection [11].

I.5.3 Types of inverters:

Inverters can be classified by their structure into two principal forms: a **Single-phase** and **Three-phase** inverter.

But, inverters are also classified based on the type of input source into two broad types: **voltage source inverter (VSI)** and **current source inverter (CSI)**. The VSI is a voltage step-down/buck inverter while the CSI is a voltage boost/step-up inverter.

A traditional current source and voltage source inverters look like as shown in Figure (I.18). The VSI has a voltage source connected in parallel with a large capacitor while CSI has a constant current source as input, this current source is obtained by connecting a large inductor in series the DC source [SHS 18].

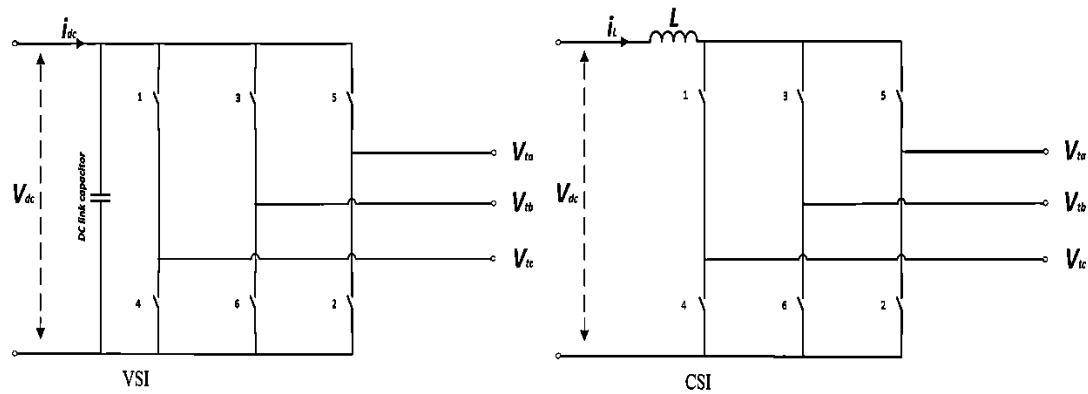


Figure I.18: Schematic diagrams of a Voltage and Current Source Inverter [SHS 18].

Of the two types, VSI is more used than the CSI in industry. In this work also we intend to deal with VSI and later with impedance source inverter (ZSI).

Typical inverters (VSI and CSI) have few disadvantages. They are listed as [13],

- ✚ Behave in a boost or buck operation only. Thus the obtainable output voltage range is limited, either smaller or greater than the input voltage.
- ✚ Vulnerable to EMI noise and the devices gets damaged in either open or short circuit conditions.
- ✚ The combined system of DC-DC boost converter and the inverter has lower reliability.
- ✚ The main switching device of VSI and CSI are not interchangeable.

I.5.4 Z-source Inverter:

In a traditional PWM inverter, the ac output voltage is limited to below the dc input voltage. Therefore, an additional dc-dc boost converter is required to obtain a desired ac output voltage. In order to overcome the limitations of a traditional inverter, a Z-source inverter was introduced in [PFZ 03]. The ZSI is an emerging topology for power electronics DC-AC converters with interesting properties such as buck-boost characteristics and single-stage conversion [EHA 16].

The ZSI is a single stage inverter with crisscross of capacitor and inductor to form an X structure between the DC source and the inverter. The special network of two inductor and two capacitors uses shoot through state to achieve buck and boost in the same configuration as per the need. In case of a shoot-through state, the switches in the phase leg are simultaneously shorted. It could be one phase leg at a time, two phase legs or even all of the three [SHS 18].

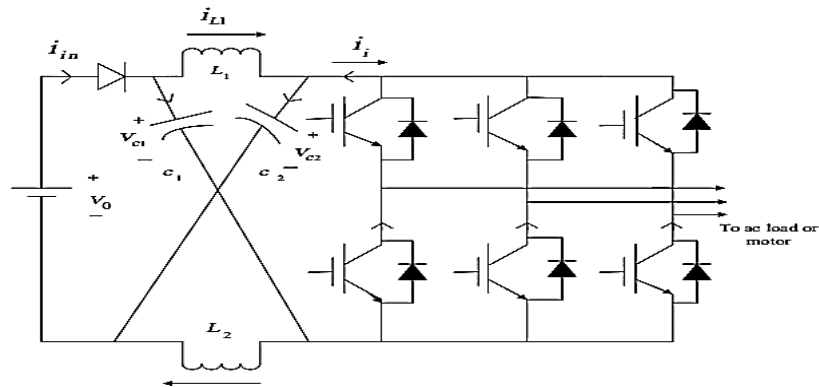


Figure I.19: Schematic diagram of a Z-source Inverter [BKP 17].

The ZSI advantageously uses the shoot-through (ST) state to boost the input voltage, which improves the inverter reliability and enlarges its application fields.

In comparison with other power electronics converters, it provides an attractive single stage dc-ac conversion with buck-boost capability with reduced cost, reduced volume, and higher efficiency due to a lower component number [EHA 16].

I.5.5 Z-source inverter topologies:

Ever since the evolution of Z source inverter, it has been an area of wide research especially due to its application in power generation based on various renewable energy sources. Many improvements are made in the basic topology of ZSI to arrive at numerous topologies, some of them are:

- **Bidirectional-Z source inverter:** A bidirectional ZSI (BZSI) is formed by replacing of input diode D with bidirectional switch S_1 from the traditional version of ZSI [BKP 17].

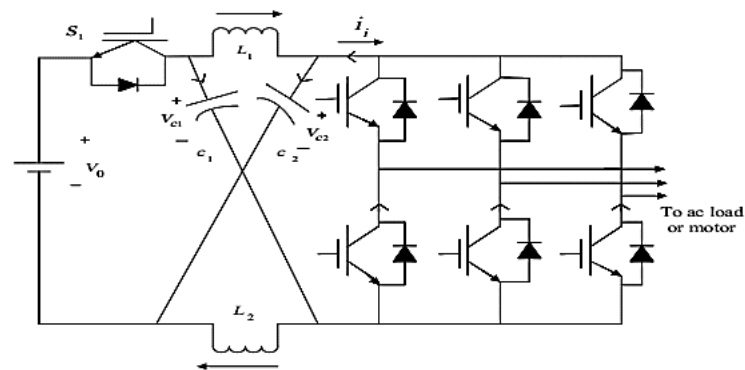


Figure I.20: Bidirectional-Z source inverter [BKP 17].

- **Trans-Z-source inverter:** Trans-Z-source neutral clamped inverter is developed by using a transformer and a capacitor to constitute the Z network. [SAV 17].

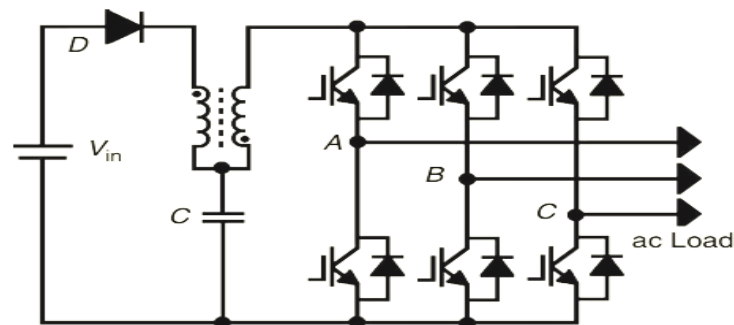


Figure I.21: The transformer-based ZSI topology [EHA 16].

- **Quasi-Z-source inverter:** this type is developed by just adding inductors, capacitors and diodes to the traditional topology to form switched inductor type, two stage network type etc.

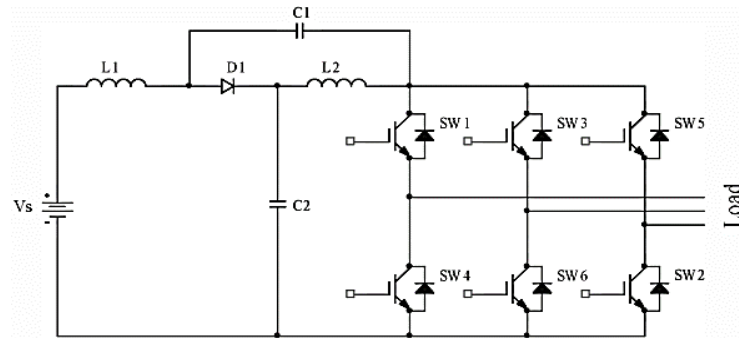


Figure I.22: Quasi Z-source inverter [AUS 13].

I.6 Conclusion:

In this chapter, we have presented a state of the art on photovoltaic systems and the z-source inverter. We started with a definition of renewable energies and their different forms. Thus, photovoltaic energy in details, we presented solar radiation and their different components. Next, we introduced photovoltaic cell and their historical development also their technologies, as well as photovoltaic systems and their various types.

Finally, we presented a general information on the z-source inverter, going through the definitions of: converter, inverter with their general types then the different topologies of this new inverter.

CHAPTER II:
Modeling of PV Panels and MPPT
Control

II.1 Introduction:

PV module represents the fundamental power conversion unit of a Photovoltaic generator system. The output characteristics of a PV module depend on the solar insolation, the cell temperature and the output voltage of the PV module [PNR 11].

For the PV module, to provide its maximum available power, it is necessary to permanently adapt the load with the photovoltaic generator. This adaptation can be achieved by inserting a DC-DC converter (chopper) controlled by a "Maximum Power Point Tracking" (MPPT) mechanism.

This chapter is divided into two parts; the first section is modeling of PV Panels. The SOLKAR make 36 W PV module is taken as the reference module and the PV equations are modeled with Simulink blocks. The next section present the MPPT controller with P&O algorithm, using a boost converter to track the MPP of PV module; at the end, the simulation results are discussed.

PART 1: Modeling Of Photovoltaic Panels

II.2 Basic Functioning Of the Solar Cell:

PV cell is a semiconductor diode whose p-n junction is exposed to light. It is made from several types of semiconductors using different manufacturing processes. Because some of photons have energy lower than what is required, these do not assist the carrier generation. Thus, the energy associated with these photons is transformed into heat. The photons that have energy more than what is required generate the electric current.

II.2.1 Photovoltaic Modules Interconnection:

PV cell convert solar energy to electricity when exposed to sunlight. In order to get required amount of current (Ampere) and voltage (volts) many PV cells are interconnected into a single unit called a PV module.

A. Connection of Modules in Series:

Series wiring is when the voltage of a solar array is increased by wiring the positive of one solar module to the negative of another solar module.

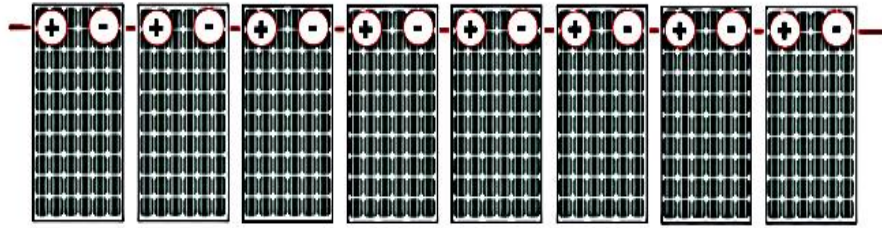


Figure II.1: Connection of Modules in Series.

B. Connection of Modules in Parallel Combination:

Parallel wiring increases the current (amps) output of a solar array while keeping the voltage the same.

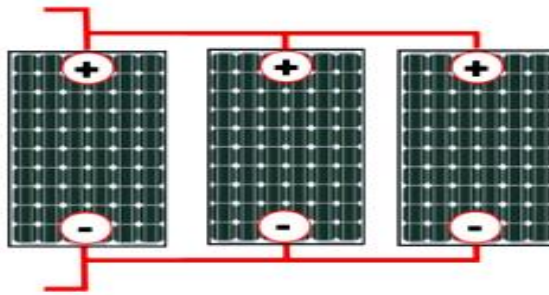


Figure II.2: Connection of Modules in Parallel.

C. Connection of Modules in Series and Parallel (Mixed Combination):

Solar PV panels connected in series and in parallel to meet both current and voltage requirements.

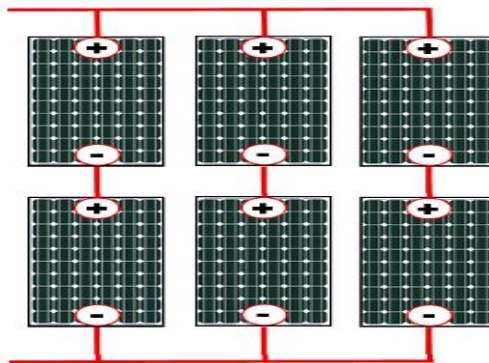


Figure II.3: Connection of Modules in Series and Parallel.

II.3 Mathematical model for a PV module:

A single solar cell can be represented as a component of an electrical circuit. It contains a p–n junction called as a diode, a photocurrent generator represented a generation of current from light and two resistors, one is arranged in series and

another one is in parallel which described the Joule effect and recombination losses. Then this combination is called as a single diode solar cell model [KRS 18]. The solar PV device can be represented as an ideal solar cell in Figure (III.4).

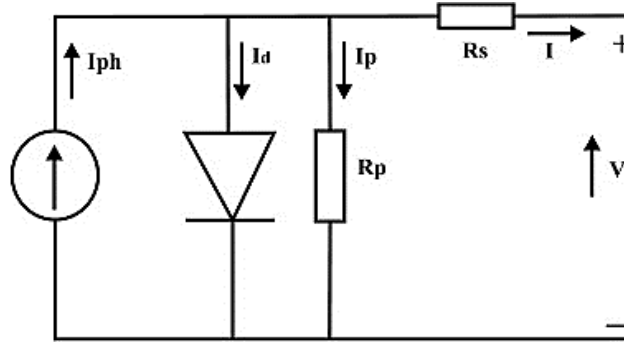


Figure II.4: PV modeled as diode circuit.

The current source I_{ph} represents the cell photocurrent. R_p and R_s are the intrinsic parallel and series resistances of the cell, respectively. Usually the value of R_p is very large and that of R_s is very small, hence they may be neglected to simplify the analysis.

By using the Kirchoff's first law the output current of an ideal solar cell is described in equation (II.1).

$$I = I_{ph} - I_d \quad (II.1)$$

The Shockley's diode current equation as illustrated in equation (II.2):

$$I_d = I_s \left(\exp\left(\frac{qV}{N_s K A T_0}\right) - 1 \right) = I_s \left[\exp\left(\frac{q(V + IR_s)}{N_s K A T_0}\right) - 1 \right] \quad (II.2)$$

Considering the PV cells coupled in a series-parallel manner, the current output of PV module is:

$$I = N_p * I_{ph} - N_p * I_s \left(\exp\left(\frac{q(V + IR_s)}{N_s K A T_0}\right) - 1 \right) \quad (II.3)$$

Module photo-current (I_{ph}):

$$(II.4) I_{ph} = [I_{sc} + K_i(T_0 - T_{ref})] * \frac{G}{G_{ref}}$$

Module reverse saturation current (I_{rs}):

$$I_{rs} = I_{sc} / \left[\exp\left(\frac{qV_{oc}}{N_s K A T_0}\right) - 1 \right] \quad (II.5)$$

Module saturation current (I_s):

$$I_s = I_{rs} \left[\frac{T_0}{T_{ref}} \right]^3 \exp \left[\left(\frac{qE_g}{AK} \right) \left(\frac{1}{T_{ref}} - \frac{1}{T_0} \right) \right] \quad (\text{II.6})$$

The ideality factor A and energy band gap E_g obtained from the selected model, which is taken from the manufacturer of the selected module.

II.4 Reference Model:

Modeling is basic tool of the real system simulation. For modeling, it is necessary to analyze the influence of different factors on the photovoltaic cells and to take in consideration the characteristics given by the producers.

SOLKAR make 36 W PV module is taken as the reference module for simulation and the datasheet details are given in Table (II.1).

Table II.1: Electrical characteristics of the SOLKAR 36 W PV module [PNR 11].

Description	Rating
Rated power	37.08 W
Voltage at Maximum power (V_{mp})	16.56 V
Current at Maximum power (I_{mp})	2.25 A
Open circuit voltage (V_{oc})	21.24 V
Short-circuit current (I_{sc})	2.55 A
Total number of cells in series (N_s)	36
Total number of cells in parallel (N_p)	1

The performance of solar cell is normally evaluated under the standard test condition (STC), where an average solar spectrum is used, the irradiance is normalized to 1000 W/m², and the cell temperature is defined as 25°C.

PART 2: Converter DC/DC and MPPT control:

II.5 Optimization of the performance of the GPV:

The efficiency of a solar cell is very low. In order to increase the efficiency, methods are to be undertaken to match the source and load properly. One such method is the Maximum Power Point Tracking (MPPT). This is a technique used

to obtain the maximum possible power from a varying source. In photovoltaic systems the I-V curve is non-linear, thereby making it difficult to be used to power a certain load. This is done by utilizing a boost converter whose duty cycle is varied by using an MPPT algorithm [SAS 12].

II.5.1 DC-DC converter (chopper):

A DC / DC converter or chopper is a static converter using semiconductor components which can supply loads with an adjustable DC voltage, from a constant DC voltage source [KDJ 18]. These converters must be chosen to be able to match the maximum power point (MPP) of PV module when climatic conditions change with different resistive load values. So DC-DC converters must be used with MPPT controller in order to reduce losses in the global PV system [KSB 14]. For our study, we choose the step-up chopper " Boost converter ".

II.5.1.1 Boost converter (step-up converter):

Boost converter also called as high efficiency step-up converter or parallel chopper, which has an output DC voltage greater than its input DC voltage. It consists of two semiconductor switches and one storage element [KVN 13]. Figure (II.5) shows the circuit diagram of a boost converter. It consists of an inductor, an IGBT switch, a fast switching diode and a capacitor.

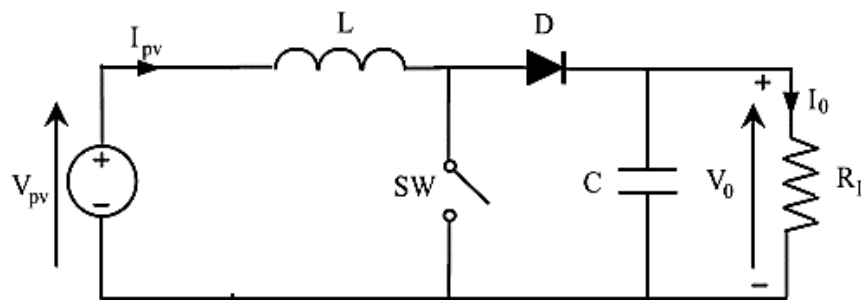


Figure II.5: Circuit diagram of a Boost converter.

The configurations of the boost converter circuit during switching ON and OFF intervals are shown in Figures (II.6) and (II.7) respectively.

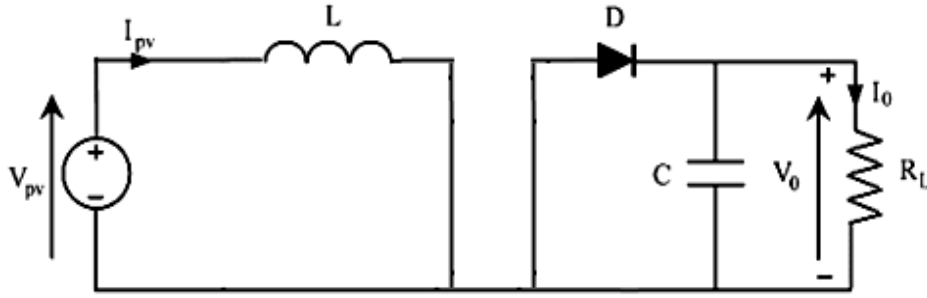


Figure II.6: ON state of the IGBT switch.

- When the IGBT is switched ON, the inductor is directly connected to the input voltage source. In this case, the inductor current rises charging it and the inductor is storing energy while the diode is reverse biased disconnecting the load (R_L) and output capacitor (C) from the source voltage. During this interval, the pre-charged capacitor assures constant voltage across the load terminals [EAO 10].

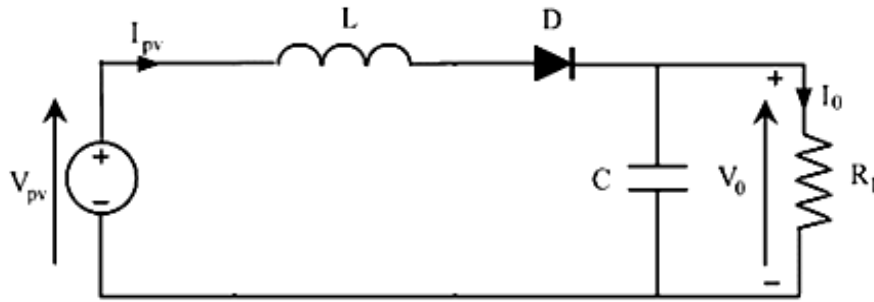


Figure II.7: OFF state of the IGBT switch.

- When the IGBT is switched OFF, the diode is forward biased and both the source and the charged inductor are connected to the load. The inductor releases the energy stored in it. This energy is transferred to the load in the form of voltage that adds to the source voltage. Hence, the converter has boosts the input voltage [EAO 10].

The voltage and current of the load in the case of continuous conduction are given by:

$$\begin{cases} V_o = \frac{1}{1-D} V_{in} \\ I_o = (1-D) \cdot I_{in} \end{cases} \quad / \quad V_{in} = V_{pv} \quad , \quad I_{in} = I_{pv} \quad (II.7)$$

The current ripple is:

$$\Delta I_L = \frac{V_{PV}}{L f} D \quad (II.8)$$

The voltage ripple is:
$$\Delta V_o = \frac{1}{fC} DI_o \quad (\text{II.9})$$

With D : the converter duty cycle.

f : the switching frequency of the converter.

II.5.1.2 Buck converter (step-down converter):

The buck converter (or series chopper) is also called voltage step-down chopper, it allows to have an average output voltage lower than that of input, used for the speed control of DC machines and in battery chargers. The basic switch used is a unidirectional static current switch, controlled on opening and closing [KDJ 18], the circuit diagram of this converter is shown in Figure (II.8).

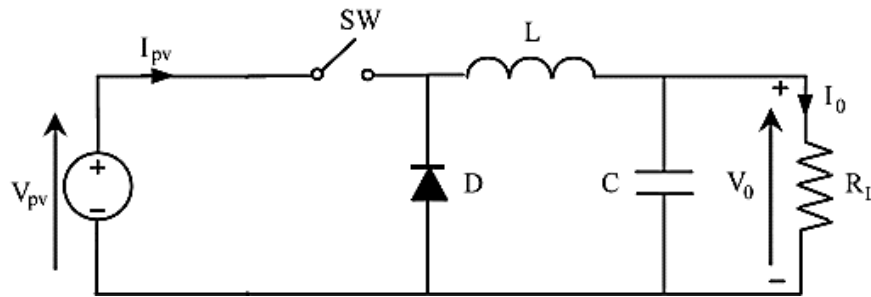


Figure II.8: Circuit diagram of a Buck converter.

II.5.1.3 Buck-Boost converter (step-to-step converter):

The step-to-step converter combines the properties of the two previous converters, it is used as an ideal transformer of any input voltage for any desired output voltage [BEF 16]; its basic diagram is illustrated by the figure (II.9).

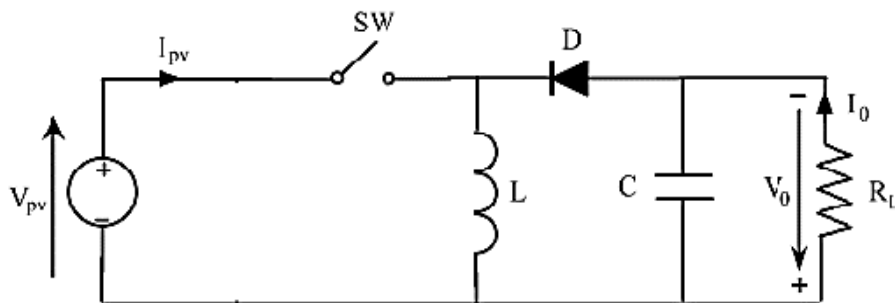


Figure II.9: Circuit diagram of a Buck-Boost chopper.

Buck-Boost converter is considered as an adaptation stage, and it also makes it possible to carry out the operations of charge and discharge considering its

reversibility in current. Thus, it is a voltage step-up converter for the discharge, and a voltage step-down converter for the charge [KDJ 18].

II.5.2 The MPPT Control Technique:

II.5.2.1 Definition:

The MPPT (Maximum Power Point Tracking) command is an essential command for optimal functioning of the PV system. The principle of this control is based on the automatic variation of the duty cycle (D) by bringing it to the optimal value so as to maximize the power delivered by the PV panel [ACM 13]. A maximum power point (MPP) is used for extracting the maximum power from the solar panel and transferring maximum power from the PV module to the load. A dc to dc converter which interface between load and module, serve the purpose of transferring maximum power from PV module to the load.

II.5.2.2 Converter For the continuation of the maximum power point:

A Boost converter is a DC to DC converter with an output voltage greater than the source voltage, it must be designed to be connected between the PV generator and the load, and perform operation to search the maximum power point (MPPT). In order to track MPP, the converter must be operated with duty cycle corresponding to it, the MPPT system is illustrated in Figure (II.10).

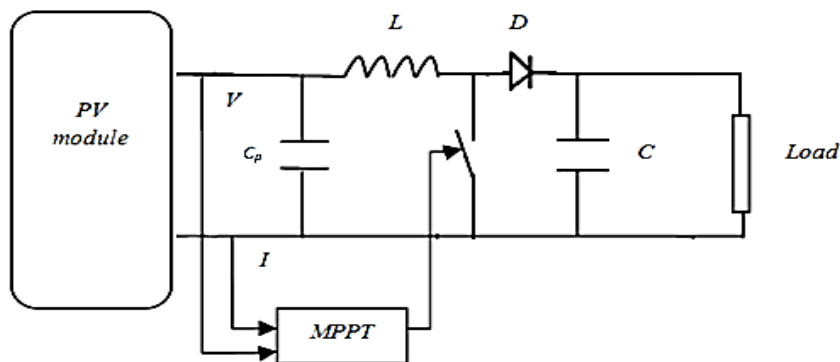


Figure II.10: PV system with DC-DC Boost converter.

The main application and benefits of MPPT in solar power system to increase the efficiency and power of solar cells and help to enable them to be competitive solution in an increasingly energy market [KVT 13].

II.5.2.3 Principle of finding the maximum power point:

The MPPT control varies the duty cycle of the static converter, using an appropriate electrical signal, to get the most power that the GPV can provide. The MPPT algorithm can be more or less complicated to find the MPP.

In general, it is based on the variation of the duty cycle of the Boost converter according to the evolution of the input parameters of the latter (I and V and consequently of the power of the GPV) until being placed on the MPP [FBN 16].

II.5.2.4 MPPT research methods:

The characteristic of the solar cell V-I is not linear and varies according to the illumination and the temperature. There is a point on the curve V-P, V-I we call the maximum power point, this point is not known, but it can be calculated. There are many algorithms and methods used for maximum power point tracking a few are listed below:

- Perturb and Observe method.
- Incremental Conductance method.
- Parasitic Capacitance method.
- Constant Voltage method.
- Constant Current method

II.5.2.5 Perturb and observe (P&O) method:

This method is the most common. P&O is an iterative method of MPPT control methods. This method has an advantage of not requiring solar panel characteristics. The P&O algorithm flowchart is shown in Figure (II.11)

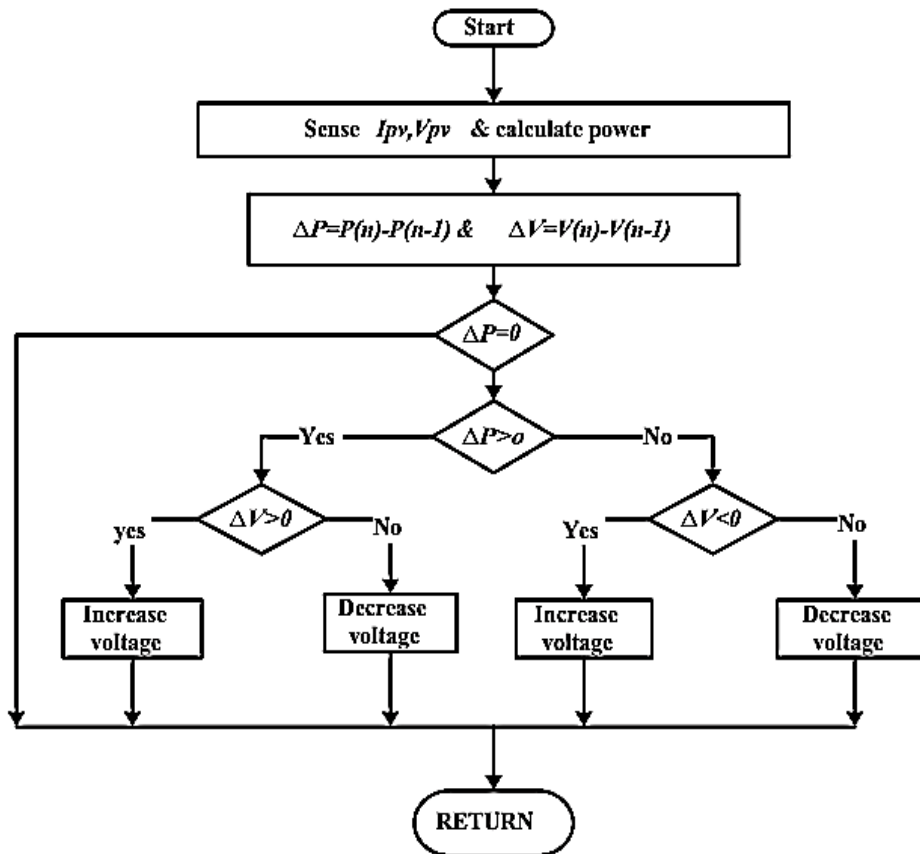


Figure II.11: P&O algorithm.

PV panel output voltage V_{PV} and output current I_{PV} are detected. Then power $P(n)$ is calculated and compared with the power measured in the previous sample $P(n-1)$ in order to get ΔP . Then according to the sign of ΔP and ΔV , the duty cycle of the converter is changed to track MPP, this process continues till ΔP , $\Delta V=0$ [BPR 13].

II.6 Simulation Model:

II.6.1 Simulink model PV cell:

The mathematical model of solar PV module is developed in step by step procedure under MATLAB/Simulink system using the above-described modeling equations (II.1) to (II.6). All the simulation results for this model of PV cell are compared with [PNR 11].

Figure (II.12) depicts the PV modeling of SOLKAR 36 W PV. The desired PV model is equipped with subsystems and these subsystems are developed and connected to each other [see Annex A].

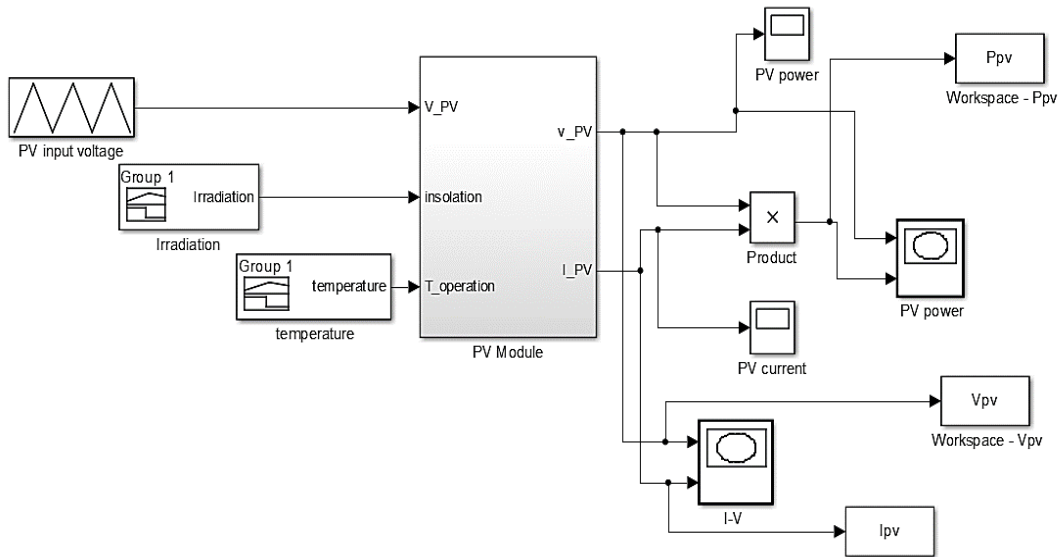


Figure II.12: External view of PV module in Simulink window.

II.6.2 Simulink model of Step-up DC/DC Converter:

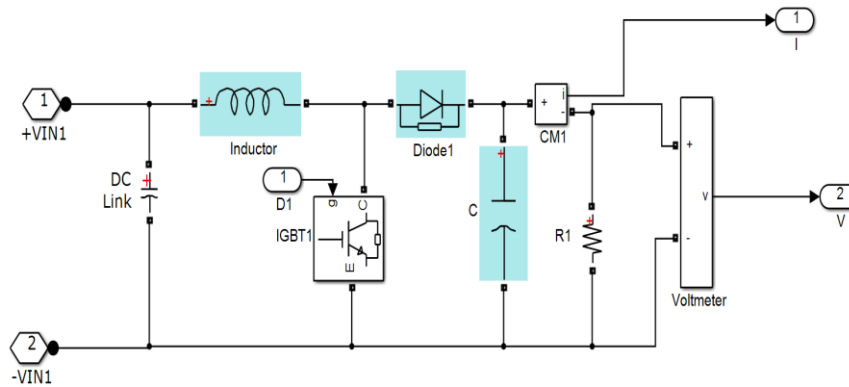


Figure II.13: Model of Boost Converter.

II.6.3 Simulink Block diagram of P&O MPPT:

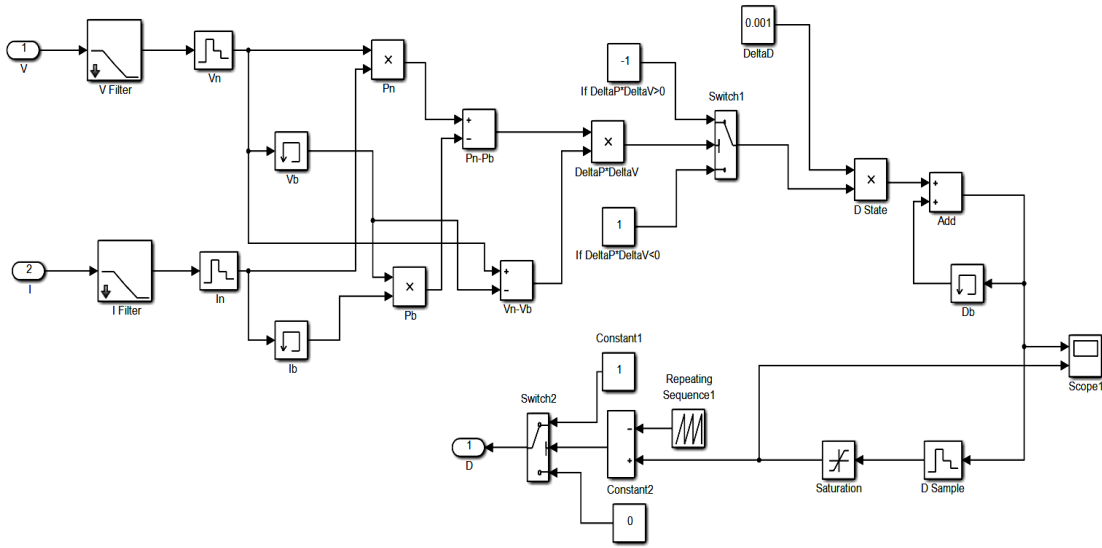


Figure II.14: Simulink Block diagram of P&O MPPT.

II.6.4 Simulink Block of PV model with P&O MPPT:

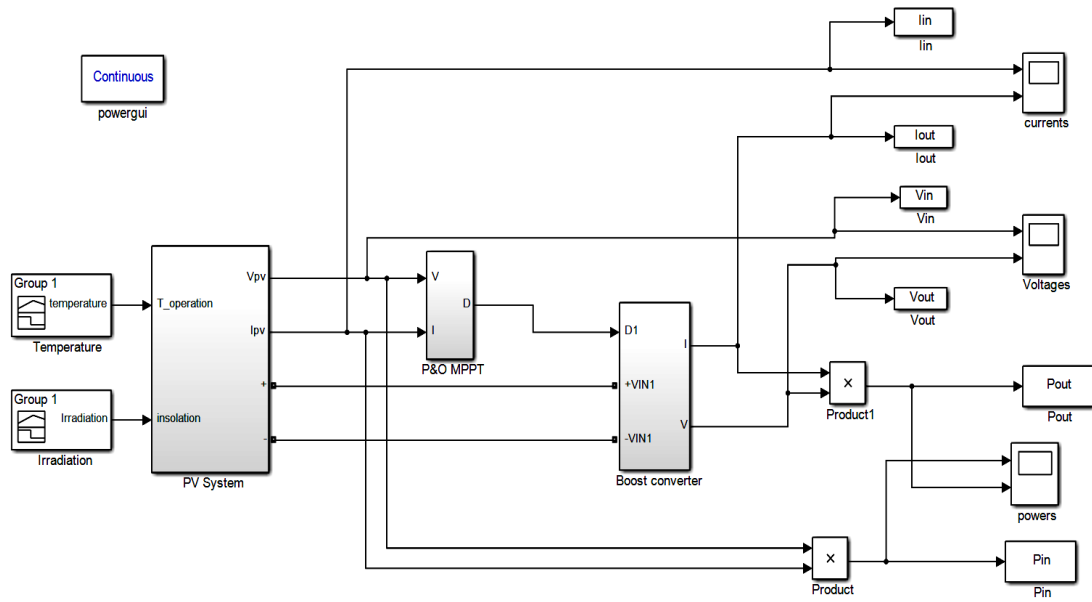


Figure II.15: MPPT System used for simulation.

II.7 Simulation Results:

II.7.1 Solar cell simulation results:

The simulation of a solar cell was done using MATLABSIMULINK. The I-V and P-V curves from the simulation are as shown in figures (II.16) and (II.17).

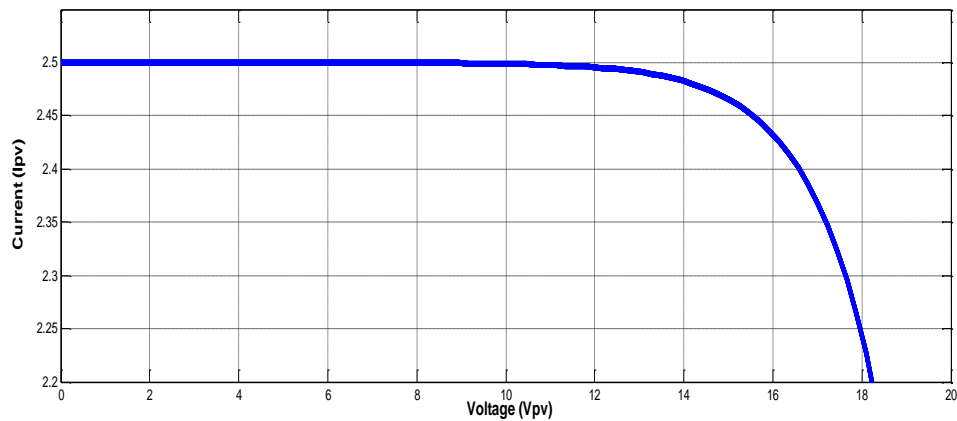


Figure II.16: I-V characteristics of a solar cell.

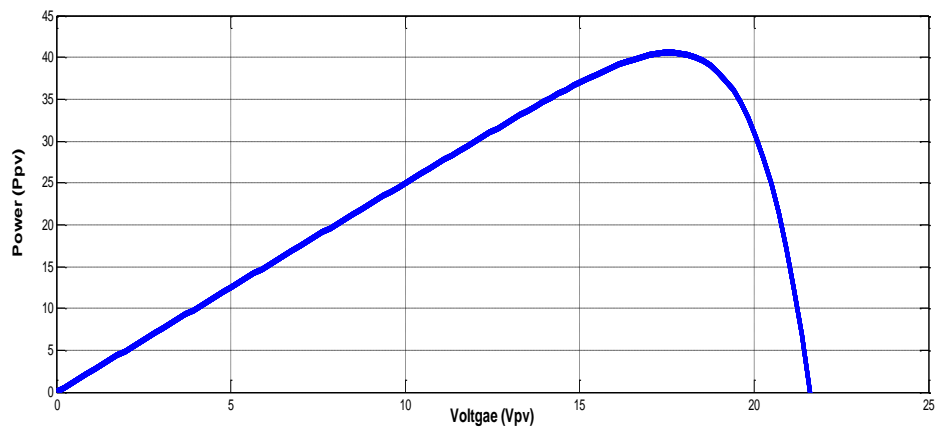


Figure II.17: P-V characteristics of a solar cell.

II.7.1.1 Effect of Variation of Solar Irradiation:

I-V and P-V characteristics under varying irradiation with constant temperature are obtained in Figures (II.20) and (II.21):

In Figure (II.18), the input irradiation is shown. Between 0 and 1(s), the irradiation is 200W/m^2 , between 1 and 2(s) it is 600 W/m^2 , while from 2(s) onwards it is 1000W/m^2 .

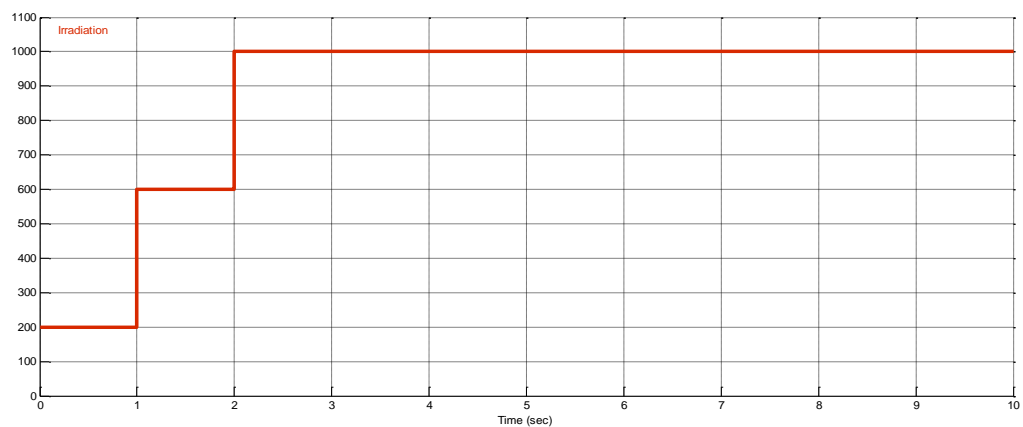


Figure II.18: Input – Time varying irradiation.

In figure (II.19), the input temperature is shown which is constant at 25°C.

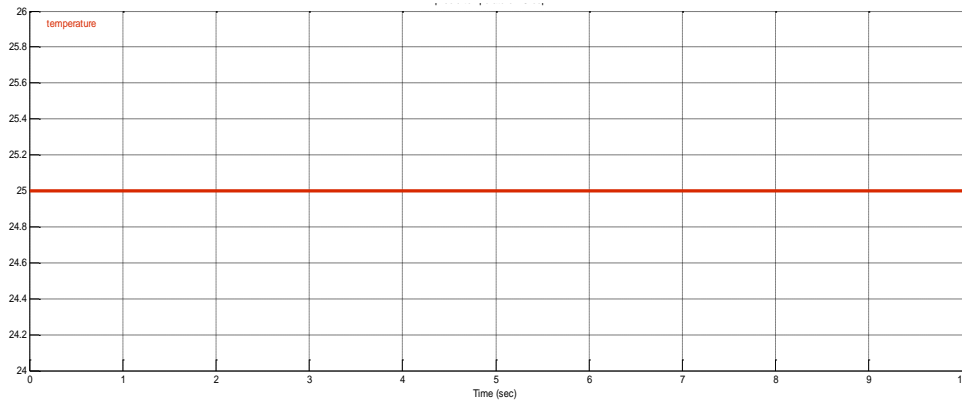


Figure II.19: Input - Constant temperature – 25°C.

The I-V output characteristics of PV module with varying irradiation at constant temperature of 25°C are shown in figure in figure (II.20).

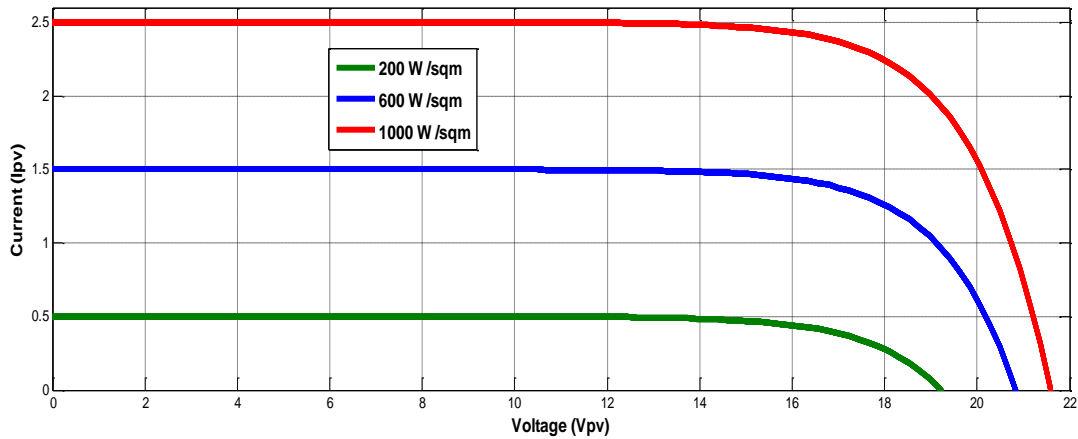


Figure II.20: Output – I-V characteristics with varying irradiation.

The P-V output characteristics of PV module with varying irradiation at constant temperature of 25°C are shown in figure in figure (II.21).

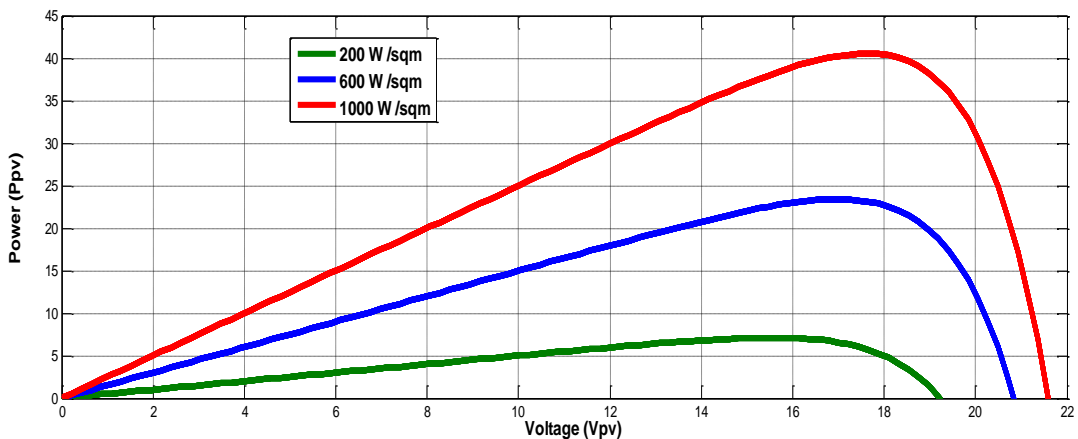


Figure II.21: Output – P-V characteristics with varying irradiation.

II.7.1.2 Effect of Variation of Temperature:

I-V and P-V characteristics under varying temperature with constant Irradiation are obtained in Figures (II.24) and (II.25):

In Figure (II.22), the time varying temperature signal is shown. Between 0 and 1 second, the temperature of 25°C is applied and it is increased to 50 and 75°C.

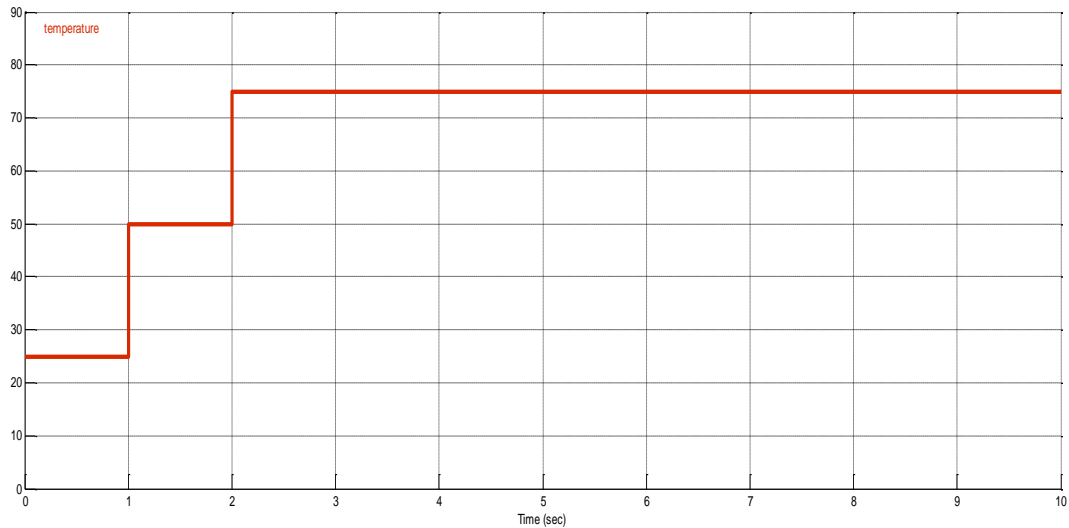


Figure II.22: Input – Time varying temperature.

In figure (II.23), the input irradiation is shown which is constant at 1000 W/m².

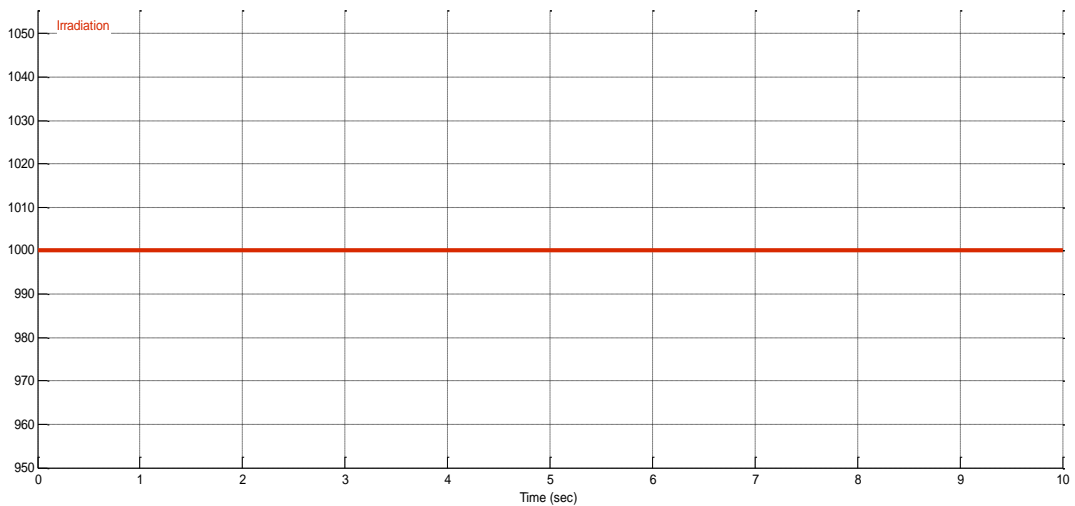


Figure II.23: Input – Constant irradiation at 1000 W/m².

The I-V output characteristics of PV module with varying temperature at constant irradiation of 1000W/m² are shown in figure in figure (II.24).

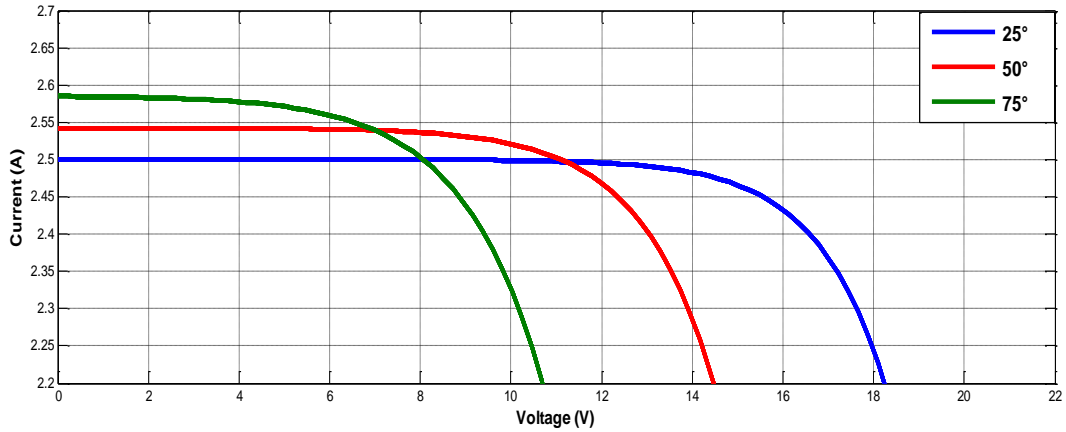


Figure II.24: Output – I-V characteristics with varying temperature.

The P-V output characteristics of PV module with varying temperature at constant irradiation of $1000W/m^2$ are shown in figure (II.25).

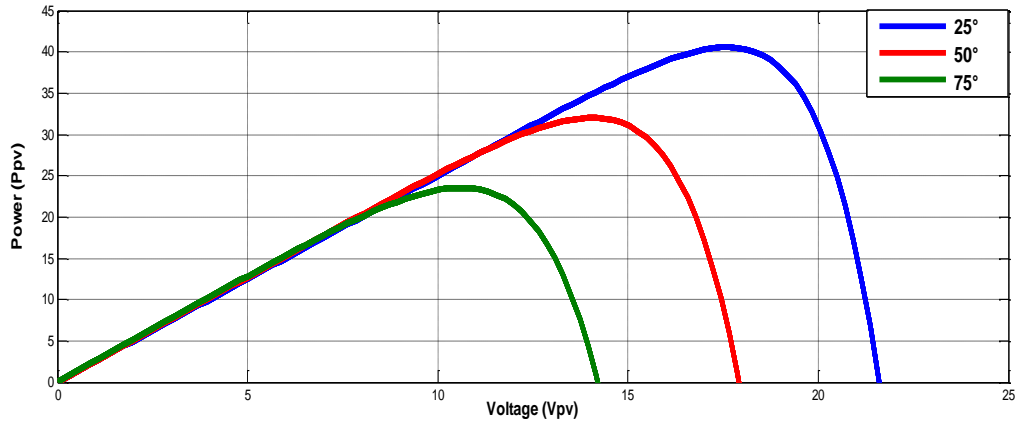


Figure II.25: Output – P-V characteristics with varying temperature.

II.7.2 Simulation Results of MPPT and the Converter Model:

The simulations were carried out in Simulink and the various voltages, currents and power plots were obtained.

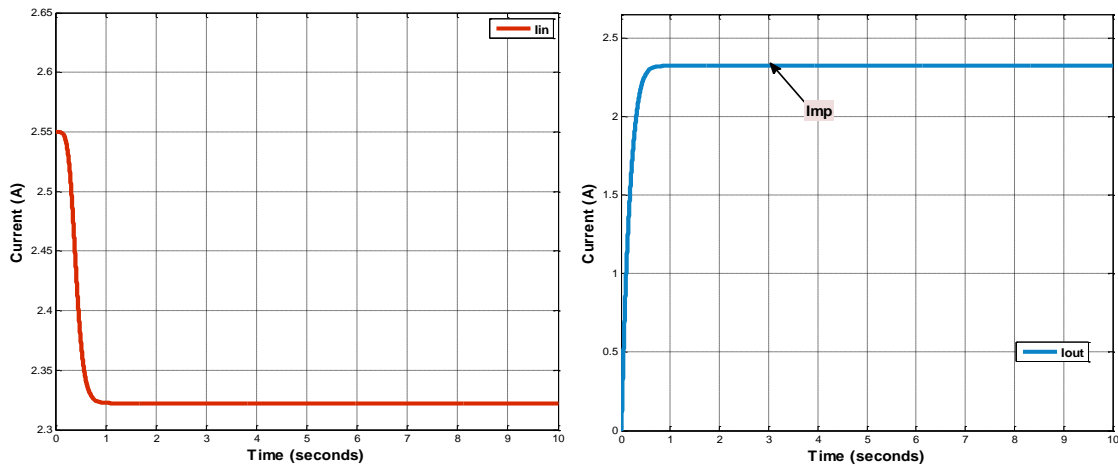


Figure II.26: Input current (the output current of PV) and output current of Boost converter.

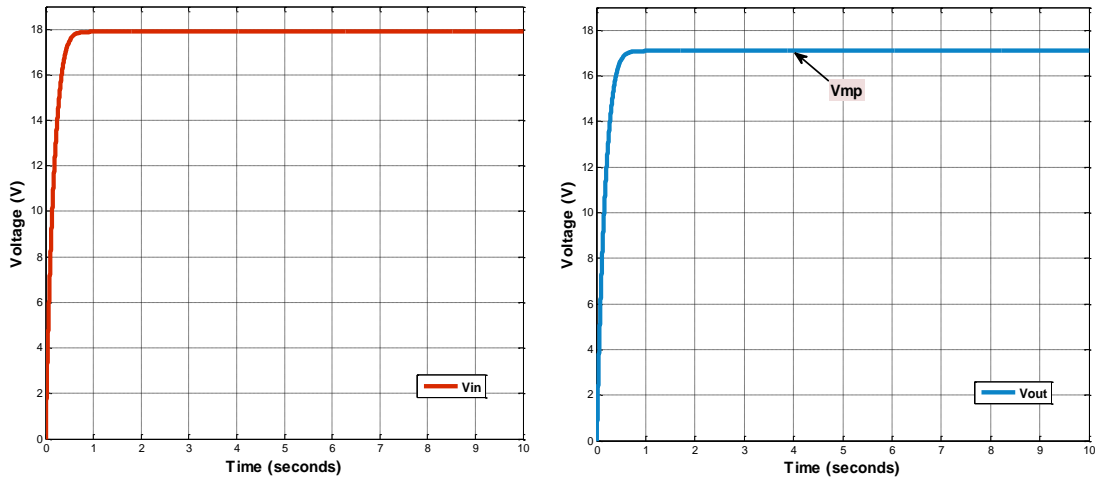


Figure II.27: Input voltage (the output voltage of PV) and output voltage of Boost converter.

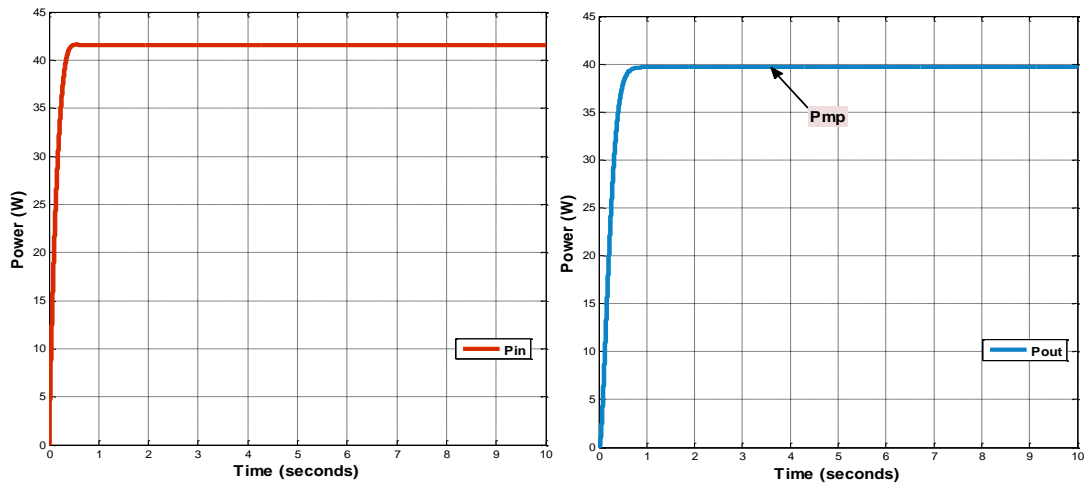


Figure II.28: Input power (the output power of PV) and output power of Boost converter.

II.7.3 Analyze and discuss:

✚ The simulation results of PV modeling:

- From figures (II.20) and (II.21) it is seen that as the irradiation increases, the current and voltage outputs also increase. Hence, the power output of the PV module increases with increase in irradiation when the temperature remains constant at 25° C.

- From Figures (II.24) and (II.25) it is seen that at constant irradiation at 1000 W/m², with the increase in operating temperature of the PV module, the current output increases marginally. However, the voltage output decreases drastically. This results in a net reduction in the power output for increase in the temperature.

- From the results of modeling of Equation (II.6), it can be seen that the PV current I_{ph} is a function of the solar irradiation and is the only energy conversion process in which the light energy is converted to electrical energy.

Interpretation of the simulation results of MPPT:

- We note that the point of operation at maximum power is reached after a few seconds of applying the MPPT P&O algorithm. The results obtained are satisfactory, they clearly show that the extraction of energy from solar panels being maximized and independent of weather conditions.

- There is a small loss of power from the solar panel side to the boost converter output side. This can be attributed to the switching losses and the losses in the inductor and capacitor of the boost converter. This can be seen from the plots of the respective power curves.

II.8 Conclusion:

The physical equations governing the PV module were elaborately presented with numerical values of the module saturation current at various temperatures and solar irradiations. The characteristics curves obtained from this model have been matched with the theoretical prediction which ensures the validity of this model.

P&O MPPT method is implemented with MATLAB-SIMULINK for simulation. The MPPT method simulated in this chapter is able to improve the dynamic and steady state performance of the PV system simultaneously. Through simulation it is observed that the system completes the maximum power point tracking successfully despite of fluctuations.

CHAPTER III:
Modeling and Simulation of Z-
Source Inverter

III. 1 Introduction

Traditional voltage source inverter (VSI) and current source inverter (CSI) technology has advanced to the new Z-source inverter (ZSI) with a built-in impedance network, with modification to the traditional pulse width modulated (PWM) signal.

In this chapter, two models (SPWM and SVPWM) have been built with MATLAB/Simulink and Simscape. In addition, these control methods will be used in the traditional VSI and the Z-source inverter. Both of their results have been compared and analyzed.

III. 2 Inverter:

An inverter is a DC/AC power electronic converter that transforms direct (DC) voltage or current to alternating (AC) voltage or current of different of variable frequency and amplitudes. This is the reverse function of a rectifier.

A typical DC/AC converter system is shown in figure (III.1). Input is from DC source (voltage or current) and the output is desired to be a sinusoidal voltage or current with a zero DC component.

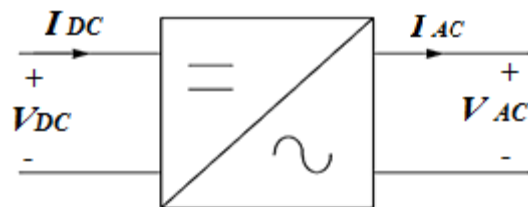


Figure III.1: General block diagram of DC-AC converter.

III. 3 Traditional voltage source inverter (VSI):

VSI is a three-phase bridge inverter fed from DC voltage source (or) AC voltage source with diode rectifier as shown in figure (III.2). A large capacitor is connected at the input terminals tends to make the input DC voltage constant. Six switches are used in the main circuit; each composed of power transistor and an antiparallel diode to provide bidirectional current flow and unidirectional voltage blocking capability [LNS 12].

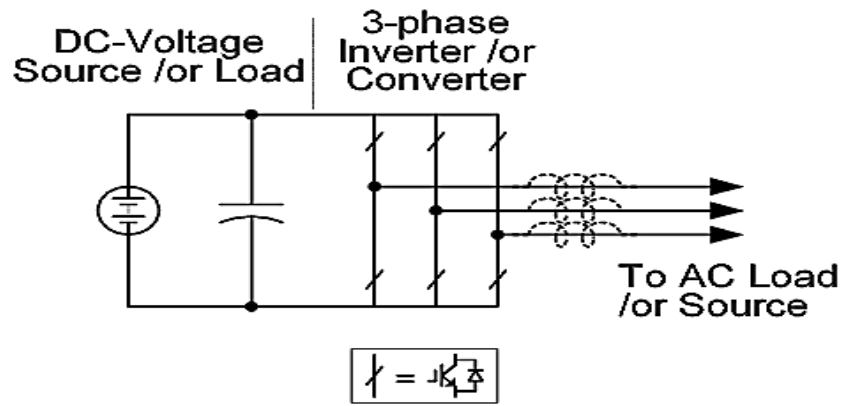


Figure III.2: Voltage Source Inverter.

A DC to AC inverter system usually has two high switching frequency stages. The first stage of the inverter system is a DC to DC converter regulating the input voltage to the second stage is a three-phase voltage source inverter (Figure III.3).

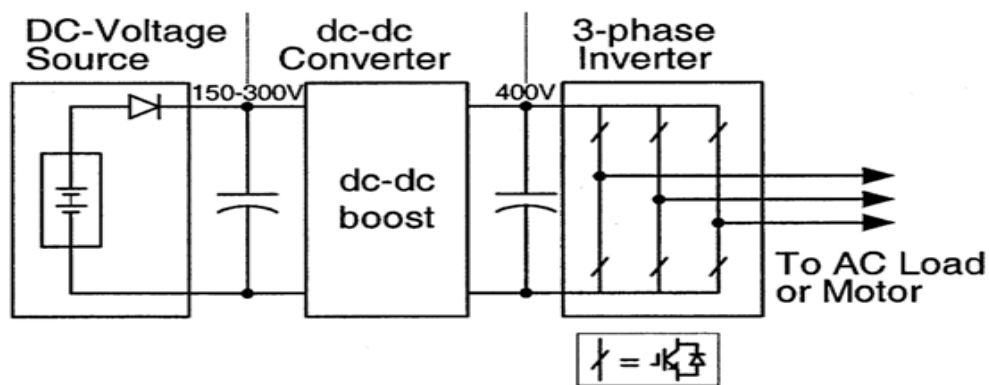


Figure III.3: Traditional two-stage DC/AC power conversion.

It has the following conceptual and theoretical barrier:

- The AC output voltage is limited below and cannot exceed the DC input voltage.
- External equipment is needed to boost up the voltage, which increases the cost and lowers the overall system efficiency.
- There is a possibility for the occurrence of short through which destroys the devices.

Given previous hurdles related to VSI, a new power conversion concept is proposed in, and it is shown in Figure (III.4).

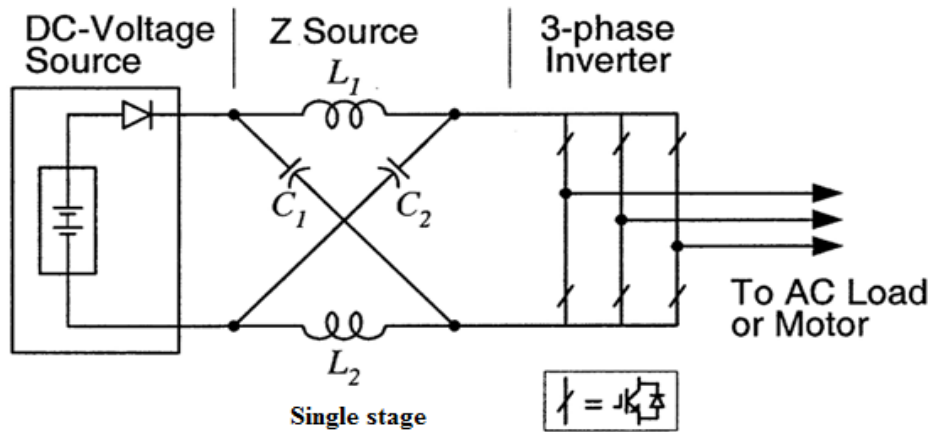


Figure III.4: Single stage DC/AC power conversion.

III. 4 Z-Source converter (ZSC):

Z-source converter is an innovative technology presented in recent years. It's a new type of converters besides the other two kinds of traditional converters: the voltage-source and the current-source converters. It employs a unique impedance network to couple the main circuit of the converter to the power source. Figure (III.5) shows the general Z-source converter structure.

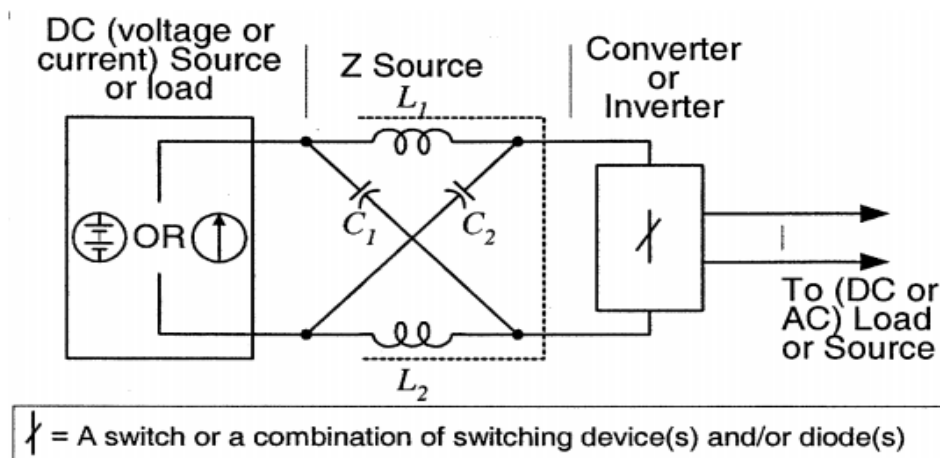


Figure III.5: General structure of the Z-source converter.

It has a valuable feature due to two particular ideas added to the basic Voltage Source converter [KJS 17]:

- Turning on at least one leg of switches set, a shoot through mode, which is forbidden in conventional converters.
- X-shaped impedance network includes two pairs of capacitors and inductances, maintains energy in the shoot-through state.

III.4.1 Comparison between CSI, VSI and ZSI:

Table III.1: Comparisons of CSI, VSI and Impedance Source Inverter (ZSI) [ZPH 12].

Current Source Inverter	Voltage Source Inverter	Z-Source Inverter
The CSI acts as a constant current source or current stiff since a large inductor is used in series with the voltage source	The VSI acts as a constant voltage source or voltage stiff inverter since a large capacitor is used in parallel with the voltage source.	The ZSI acts as a constant high impedance voltage source. As capacitor and inductor is used in the DC link.
A CSI is capable of withstanding short circuit across any two of its output terminals. Hence momentary short circuit on load.	A VSI is more dangerous situation as the parallel capacitor feeds more powering to the fault.	In ZSI miss-firing of the switches sometimes are also acceptable.
Cannot be used in both buck or boost operation of inverter at the same time.	Cannot be used in both buck or boost operation of inverter at the same time.	Can be used in both buck and boost operation of inverter at the same time.
The main circuits cannot be interchangeable.	The main circuit cannot be interchangeable here also.	Here the main circuits are Interchangeable
It is affected by the EMI noise.	It is affected by the EMI noise.	It is less affected by the EMI noise.
It has a considerable amount of harmonic distortion.	It has a considerable amount of harmonic distortion	Harmonics Distortion in low
Power loss should be high because of filter.	Power loss is high	Power loss should be low
Observed that power loss decreases efficiency here.8	High power loss decreases efficiency here.	Higher efficiency because of less power loss

III. 5 Z-Source inverter:

The Z-source inverter is an alternative power conversion topology that can both buck and boost the input voltage using passive components. It uses a unique LC impedance network for coupling the converter main circuit to the power source, which provides a way of boosting the input voltage, a condition that cannot be obtained in the traditional inverters.

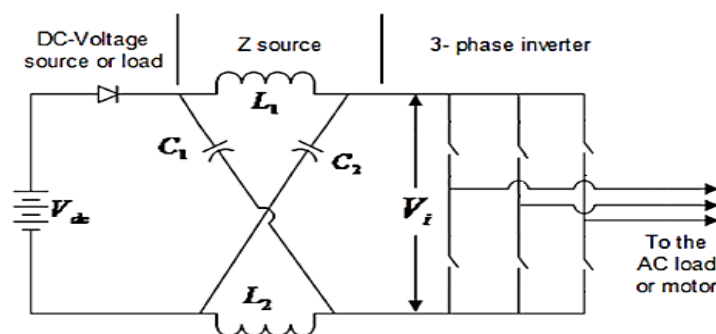


Figure III.6: General structure of a Z-source inverter.

The ZSI consists of a network of impedances Z , comprising two capacitors C_1 and C_2 and two inductors L_1 and L_2 mounted in X and connected to a three-phase inverter as shown in Figure (III.6). Also, a diode is used to prevent the passage of reverse currents.

III.5.1 Topology of a three phase inverter with Z-Source structure:

The three-phase voltage inverter is illustrated in the figure below, it is in the form of a three-phase bridge consisting of 3 arms connected to the voltage source via a Z-Source impedance network as well as a protective diode which is used to prevent the discharge of the two capacitors in the DC voltage source [RYO 17].

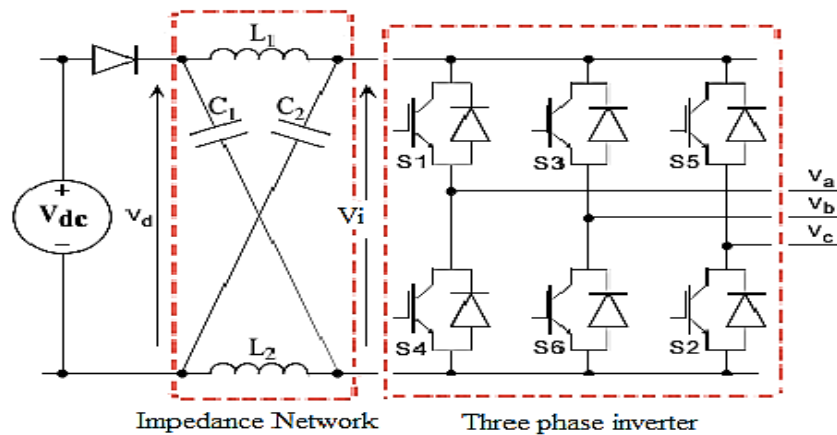


Figure III.7: Topology of a three phase inverter with Z-Source structure.

Each arm of the inverter constitutes a switching cell. It consists of two reversible current switches containing of an IGBT transistor and a diode mounted in antiparallel [MOL 17].

The insertion of an impedance network between the DC source and the three-phase inverter, Provides the right to strike two switches in the same arm, something that is impossible in a traditional, which gives rise to a new "Shoot-through State", or "short-circuit state". An inverter arm can replace an independent external switch at the input of the latter, this state is used to control the duty cycle of the z-source impedance network, and thus adjust the ratio between the source voltage and the DC bus at the input of the inverter [RYO 17].

The Z-Source impedance network plays a double role, the first is that of a Boost chopper, once coupled to the three-phase inverter, the whole works in Buck-Boost. The second function is that of a voltage and current filter.

The network impedance is used to reduce current ripples around its average value during a switching period, while the capacitor is intended to absorb these ripples and serves limit voltage fluctuations, and thus provide a more or less stable peak voltage at the input of the three-phase inverter, in order to obtain sinusoidal voltages of fixed amplitude at the output of the inverter.

III.5.2 Configurations of a three-phase inverter with Z-Source structure:

There are (06) six active configurations for a traditional VSI, (06) six configurations where there is a transfer of energy between the source and the load, and (02) two passive configurations where there is no a transfer of power between the source and the load, we can call these states: null configurations.

There is also a ninth state which corresponds to several configurations, dedicated to the control of the Z-source impedance network part. This state is characterized by the short circuit of one or more arms, among the three available arms of the inverter [RYO 17]. All possible configurations of the Z-Source inverter are illustrated in the table below:

Table III.2: Switching states of three-phase Z-source inverter [LPC 04].

(!S_X represents complement of S_X, where X = 1, 3 or 5)

State (Output Voltage)	S ₁	S ₄	S ₃	S ₆	S ₅	S ₂
Active {100} (finite)	1	0	0	1	0	1
Active {110} (finite)	1	0	1	0	0	1
Active {010} (finite)	0	1	1	0	0	1
Active {011} (finite)	0	1	1	0	1	0
Active {001} (finite)	0	1	0	1	1	0
Active {101} (finite)	1	0	0	1	1	0
Null {000} (0V)	0	1	0	1	0	1
Null {111} (0V)	1	0	1	0	1	0
Shoot-Through E1 (0V)	1	1	S ₃	!S ₃	S ₅	!S ₅
Shoot-Through E2 (0V)	S ₁	!S ₁	1	1	S ₅	!S ₅
Shoot-Through E3 (0V)	S ₁	!S ₁	S ₃	!S ₃	1	1
Shoot-Through E4 (0V)	1	1	1	1	S ₅	!S ₅
Shoot-Through E5 (0V)	1	1	S ₃	!S ₃	1	1
Shoot-Through E6 (0V)	S ₁	!S ₁	1	1	1	1
Shoot-Through E7 (0V)	1	1	1	1	1	1

Analysis of the previous table shows that the short-circuit state can be generated by seven (07) possible configurations, distributed as follows:

- Three configurations are obtained by the short circuit of each arm;
- Three configurations are made by the short circuit of two arms;
- A configuration is obtained by the short circuit of the three arms.

The values of the alternating voltages at the output of the inverter are not affected by the insertion of these configurations [BEF 16].

The operation of the device is linked to the behavior of the nonlinear elements surrounding the Z-source continuous stage as shown in the table (III.2).

Table III.3: The states used with the Z-source command [BEF 16].

State of the diode	freewheeling inverter	Active inverter	Z-source short-circuited
Passing	YES	YES	NO
blocked	NO	NO	YES

III.5.3 Operating principle and circuit analysis of Z-source network:

Normally, there are eight switching statuses in the three-phase SPWM control system, but there are total nine statuses in ZSI, eight statuses is as the same with traditional three-phase inverter and one extra zero status.

In this extra zero status, the circuit between inverter and DC source are shorted by upper and lower switches turn on at same time in any one bridge, any two bridges or all bridges [HZH 14]. Figure (III.8) shows the equivalent circuit of the Z-source inverter.

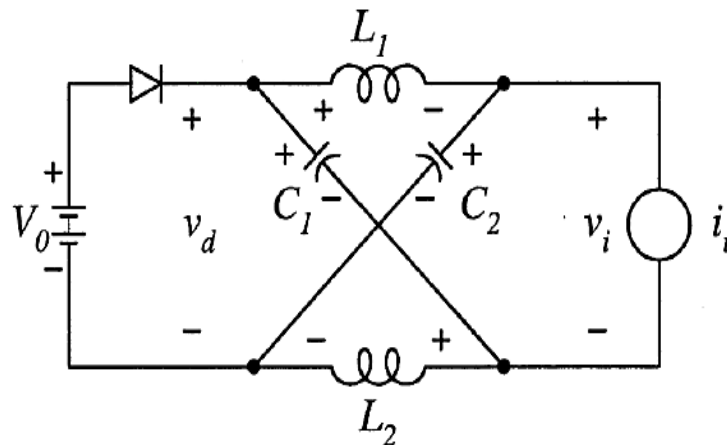


Figure III.8: Equivalent circuit of the Z-source inverter viewed from the dc link.

From Figure (III.8), we can assume all the inductors L_1 , L_2 and capacitors C_1 , C_2 have the same value in the Z-Network:

$$\begin{cases} V_{L1} = V_{L2} = V_L \\ \text{and} \\ V_{C1} = V_{C2} = V_C \end{cases} \quad (III.1)$$

The figures shown below are the equivalent circuit of Z-source inverter in different states.

III.5.3.1 Shoot-Through State:

The ZSI advantageously utilizes the shoot-through states to boost the dc bus voltage by gating on both the upper and lower switches of a phase leg [SUU 11].

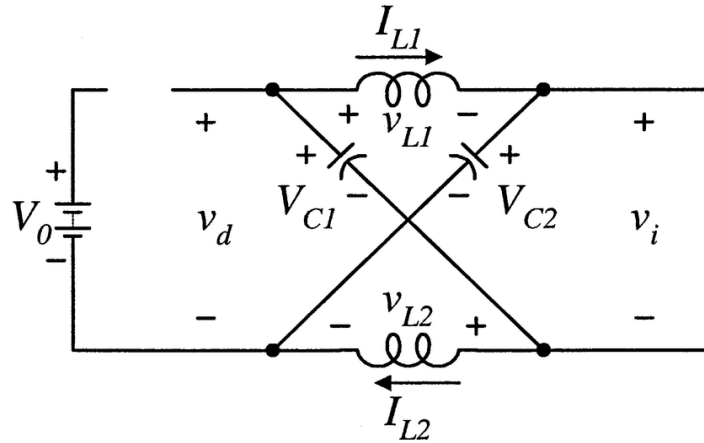


Figure III.9: Equivalent circuit shoot-through zero state of the ZSI viewed from the dc link.

The circuit is in a shoot-through zero state, as a result the capacitor voltage is boosted during this state, the sum of the two capacitors' voltage is greater than the dc source voltage ($V_{C1}+V_{C2} > V_0$), the diode is reverse biased, and the capacitors charge the inductors. The voltages across the inductors are [SZP 05]:

$$\begin{cases} V_{L1} = V_{C1} \\ \text{and} \\ V_{L2} = V_{C2} \end{cases} \quad (III.2)$$

The inductor current increases linearly assuming the capacitor voltage is constant during this period. Because of the symmetry ($L_1=L_2=L$) and ($C_1=C_2=C$) of the circuit, ($V_{L1}=V_{L2}=V_L$), ($I_{L1}=I_{L2}=I_L$) and ($V_{C1}=V_{C2}=V_C$) [SZP 05].

Through the above, we get:

$$V_C = V_L \quad , \quad V_D = 2V_C \quad \text{and} \quad V_i = 0 \quad (III.3)$$

III.5.3.2 Active States (Non shoot-Through State):

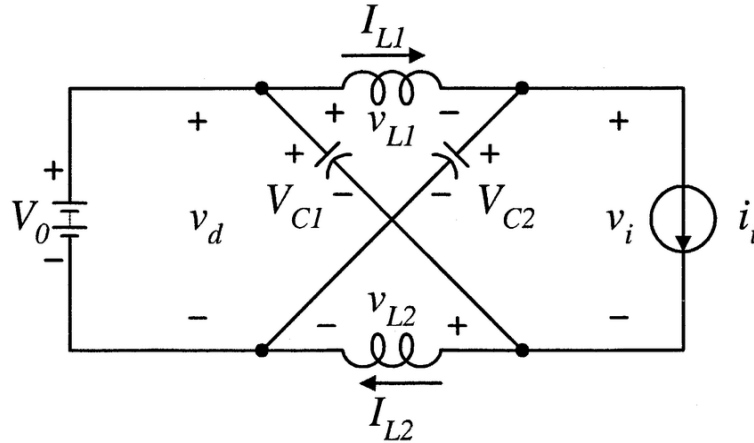


Figure III.10: Equivalent circuit non shoot-through switching states of the ZSI viewed from the dc link.

The inverter is in a non-shoot through state (one of the 6 active states and 2 traditional zero states) and the inductor current meets the following equation

$$I_L > \frac{1}{2}L_I \quad (\text{III.4})$$

Again because of the symmetry of the circuit, the capacitor current I_{C1} and I_{C2} and the inductor current I_{L1} and I_{L2} should be equal to each other respectively. In this mode, the input current from the dc source becomes:

$$I_{in} = I_{L1} + I_{C1} = I_{L1} + (I_{L2} - I_i) = 2I_L - I_i > 0 \quad (\text{III.5})$$

Therefore, the diode is conducting and the voltage across the inductor is:

$$V_L = V_0 - V_c \quad (\text{III.6})$$

$$V_D = V_0 \quad (V_0 \text{ is DC source voltage}) \quad (\text{III.7})$$

As time goes on, the inductor current keeps decreasing to a level that no longer the condition of (III.4) can be met. At this point, the input current I_{in} or the diode current is decreased to zero [SZP 05].

In addition to the previous two types, a ZSI have new modes that may exist for small inductance and high ripple of the inductors [see Annex B].

III.5.4 Calculation of the Elevation Factor β :

Set non-shoot-through states for an interval of T_1 , in one switching cycle T , we have $T=T_0+T_1$. So from Figure (III.10) equivalent circuit, we have [HZH 14]:

$$V_i = V_C - V_L \quad (\text{III.8})$$

According to relationship (III.6) we have:

$$V_i = 2V_C - V_0 \quad (\text{III.9})$$

The relationship with switching period and voltage of capacitor and dc source is:

$$\frac{V_C}{V_0} = \frac{T_1}{T_1 - T_0} \quad (\text{III.10})$$

The peak dc-link voltage across the inverter bridge is expressed in (III.3) and can be rewritten as:

$$V_i = V_C - V_L = 2V_C - V_0 = \frac{T}{T_1 - T_0} V_0 = \beta \cdot V_0 \quad (\text{III.11})$$

- β is boosting factor: $\beta = \frac{T}{T_1 - T_0} = \frac{1}{1 - 2 \left(\frac{T_0}{T}\right)} \geq 1$ (III.12)

Where T is total time period, T_0 is the shoot through period, and D_0 is the ST duty ratio.

$$D_0 = \frac{T_0}{T_S} \quad (\text{III.13})$$

The output peak phase voltage from the inverter can be expressed as:

$$V_{AC} = M \frac{V_i}{2} = M \cdot \beta \frac{V_0}{2} \quad (\text{Where } M \text{ is the modulation index}) \quad (\text{III.14})$$

From this equation, we know the output AC voltage can be controlled by the value of M and β , the boost factor [HZH 14].

III. 6 Control strategies for Z-source inverter:

Pulse-width modulation (PWM) technique is a method to generate variable voltage magnitudes and difference forms by control the pulse duration in every full period [HZH 14]. PWM technique is also very common in DC/AC conversion. Using this high frequency switching technique, it is possible to eliminate the undesirable low frequency harmonics and high frequency switching harmonics are easy to filter [ZPH 12].

The three-phase Z-source structure inverter can be controlled by several control strategies, these strategies are developed from sinusoidal and vector Pulse Width Modulation (PWM) control techniques used in conventional inverters.

III.6.1 Sinusoidal Pulse Width Modulation (SPWM):

SPWM technique is one of the earliest modulation signals for carrier-based PWM, the main idea of SPWM is using sinusoidal modulation signal compare with a carrier signal (normally is ramp wave) to produce. The ON/OFF duration time of the six switches in the inverter system is depending on the intersections between the reference waveform (sinusoidal wave) and the carrier waveform [HZH 14].

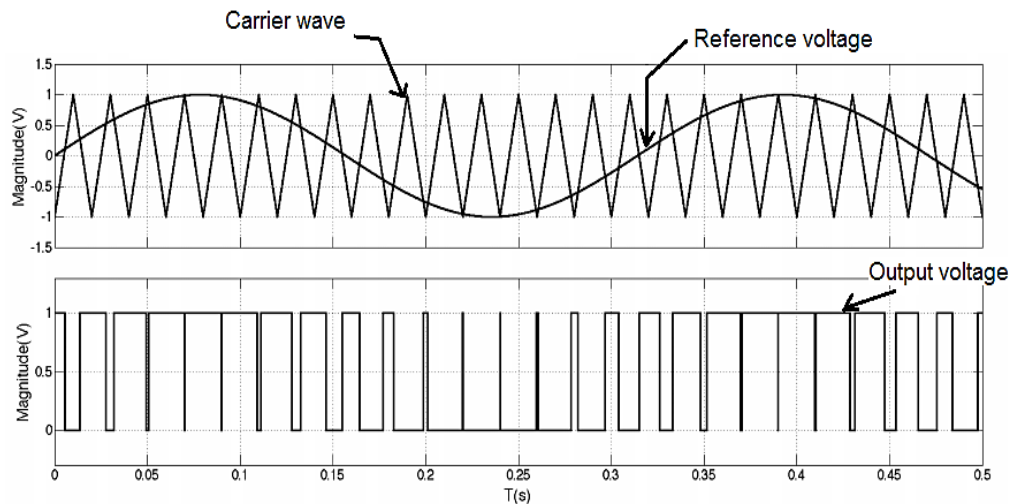


Figure III.11: SPWM signal produce: reference voltage and carrier wave vs. output voltage.

The modulation index (M) which is the principle control component and it is expressed as:

$$M = \frac{V_{ref}}{V_{car}} \quad (III.15)$$

The relation of modulation index and output voltage is produced by under modulation index ($M < 1$).

SPWM control can be investigated under three separate headings. These are: simple boost control, maximum boost control and the maximum constant boost control.

Simple Boost Control (SBC):

In this system, gating pulses are generated by correlating the three sine reference signals and two constant voltage envelopes with the carrier triangular wave. The reference signals are phase difference by 120 degrees and amplitude of two envelopes is same as to peak amplitude of reference signals [RKA 17].

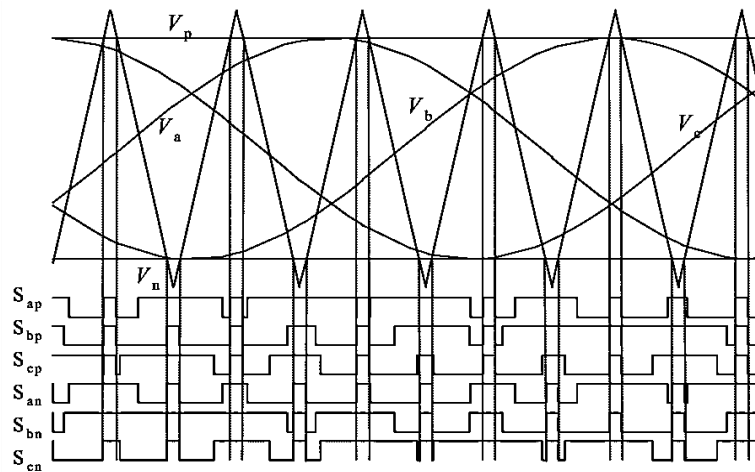


Figure III.12: Simple Boost PWM Control.

✚ Maximum Boost Control (MBC):

In this strategy, the circuit is in shoot through state when the triangular carrier wave is either greater than the maximum curve of the references (V_a , V_b , V_c) or smaller than the minimum of the references.

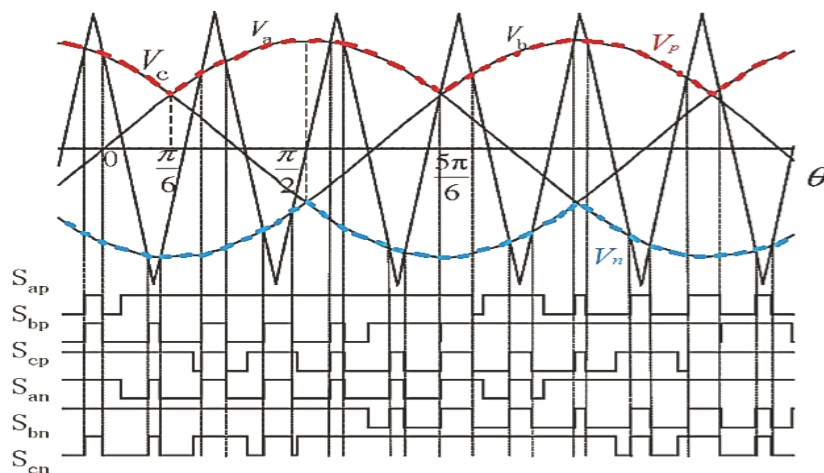


Figure III.13: Maximum Boost PWM Control.

In case of MBC, the total zero-state time period is converted into the shoot through state, which causes better result than SBC.

✚ Maximum Constant Boost Control (MCBC):

In order to reduce the volume and cost, it is important always to keep the shoot-through duty ratio constant. Figure (III.14) shows the sketch map of the MCBC method, which achieves the maximum voltage gain while always keeping the shoot-through duty ratio constant [SHM 04].

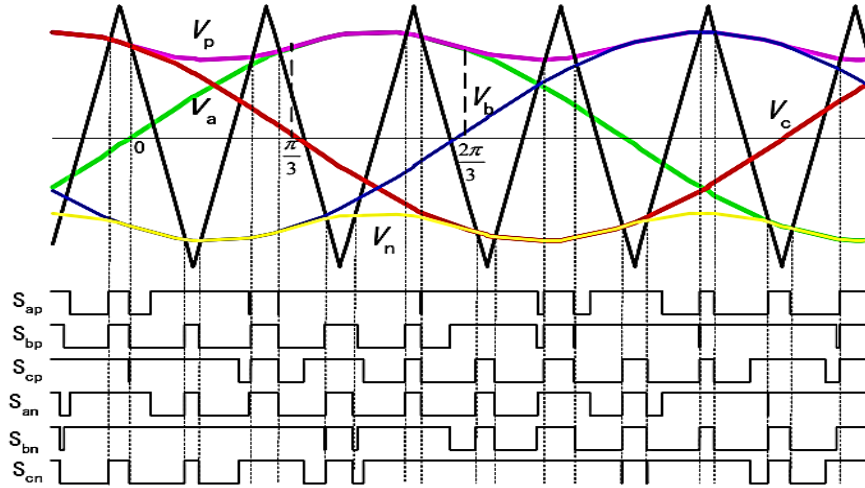


Figure III.14: Maximum Constant Boost PWM Control [SHM 04].

There are five modulation curves in this control method: three reference signals, V_a , V_b and V_c , and two shoot-through envelope signals, V_p and V_n . When the carrier triangle wave is greater than the upper shoot-through envelope, V_p , or lower than bottom shoot-through envelope V_n , the inverter is turned to a shoot through state. In between, the inverter switches in the same way as in the traditional carrier-based PWM control [RKH 09].

For the first half-period, $(0, \pi/3)$ in Figure (III.14), the upper and lower envelope curves can be expressed by following equations respectively:

$$V_{p1} = \sqrt{3}M + \sin\left(\theta - \frac{2\pi}{3}\right)M \quad 0 < \theta < \frac{\pi}{3} \quad (\text{III.16})$$

$$V_{n1} = \sin\left(\theta - \frac{2\pi}{3}\right)M \quad 0 < \theta < \frac{\pi}{3} \quad (\text{III.17})$$

And for the second half-period $(\pi/3, 2\pi/3)$ are expressed respectively as:

$$V_{p2} = \sin(\theta)M \quad \frac{\pi}{3} < \theta < \frac{2\pi}{3} \quad (\text{III.18})$$

$$V_{n2} = \sin(\theta)M - \sqrt{3}M \quad \frac{\pi}{3} < \theta < \frac{2\pi}{3} \quad (\text{III.19})$$

Third harmonic injection is commonly used in a three-phase inverter system to increase the modulation index range. This can also be used here to increase the range of so as to increase system voltage gain range [PMZ 05]. The sketch map is shown in Figure (III.15).

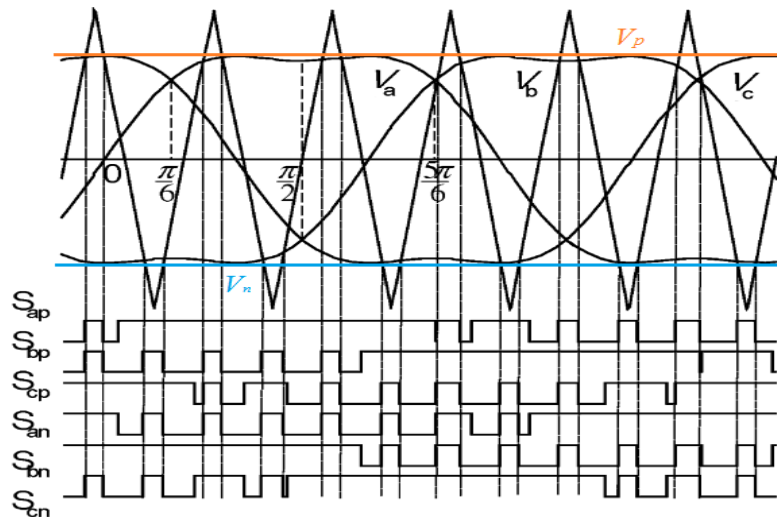


Figure III.15: Maximum Constant Boost PWM Control with third-harmonic injection [PMZ 05].

The operation principle is identical to the previous case, the only difference is that the modulation waveform is changed. In this control, the maximum modulation index can be achieved at third harmonic injection [PMZ 05].

III.6.2 Space Vector Pulse Width Modulation (SVPWM) Control:

Space vector PWM (SVPWM) is a technique designed for three phase ac motor inverter control, it work depending on their special switching sequence and effect of combination of different pulse width. As a result, the windings in the ac motor will generate the three-phase sinusoidal waves which have 120° phase shifts and less harmonics [HZH 14].

Compared with SPWM, SVPWM is widely used for variable frequency drive applications because of its various advantages such as:

- Higher dc voltage utilization
- Higher fundamental component and fewer harmonic.
- SVPWM is better control the ac motor by digital control system.

III.6.2.1 Modified Space Vector PWM (MSVPWM):

The output voltage control by SVPWM consists of switching between the two active and one zero voltage vector in such a way that the time average within each switching cycle corresponds to the voltage command. In order to apply this concept for Z-source inverter, a novel modified SVPWM is needed to introduce the shoot-through states into the zero vectors without compromising the active states [USK 11].

III.6.2.2 Rotating Transformation:

The space vector concept, which is derived from the rotating field of induction motor, is used for modulating the inverter output voltage. In this modulation technique the three phase quantities can be transformed to their equivalent two-phase quantity either in synchronously rotating frame (or) stationary frame. From these two-phase components, the reference vector magnitude can be found and used for modulating the inverter output [KVI 10].

The performance of three-phase motor is described by their voltage equations. Let U_m as the peak value of three-phase sinusoidal voltage and $\omega = 2\pi f$ is the radian frequency, so the three-phase sinusoidal mathematical system can be represented:

$$\begin{cases} V_a = U_m \cos(\omega t) \\ V_b = U_m \cos(\omega t - \frac{2\pi}{3}) \\ V_c = U_m \cos(\omega t - \frac{4\pi}{3}) \end{cases} \quad (\text{III.20})$$

When this three-phase voltage is applied to the AC machine it produces a rotating flux in the air gap of the AC machine. This rotating resultant flux can be represented as single rotating voltage vector. The magnitude and angle of the rotating vector can be found by means of Clark's Transformation as explained below in the stationary reference frame.

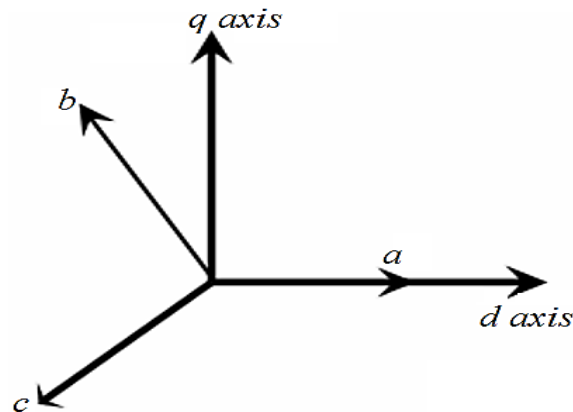


Figure III.16: The relationship of abc reference frame and stationary dq reference frame.

Transform three-phase domain to two-phase domain is expressed by:

$$\begin{pmatrix} V_a \\ V_b \\ V_c \end{pmatrix} = \begin{pmatrix} 1 & 0 \\ -1/2 & -\sqrt{3}/2 \\ -1/2 & \sqrt{3}/2 \end{pmatrix} \begin{pmatrix} U_\alpha \\ U_\beta \end{pmatrix} \quad (\text{III.21})$$

Then exchange $\alpha\beta$ items and abc items from matrix (III.22), (Clark or α - β transformation):

$$\begin{pmatrix} U_\alpha \\ U_\beta \end{pmatrix} = \frac{2}{3} \begin{bmatrix} 1 & -\frac{1}{2} & -\frac{1}{2} \\ 0 & \sqrt{3}/2 & -\sqrt{3}/2 \end{bmatrix} \begin{pmatrix} V_a \\ V_b \\ V_c \end{pmatrix} \quad (III.22)$$

From the Clarke transformation we can derive the Park transformation: (dp0 transform):

$$\begin{pmatrix} U_d \\ U_q \end{pmatrix} = \frac{2}{3} \begin{pmatrix} \cos \theta & \cos(\theta - \frac{2\pi}{3}) & \cos(\theta + \frac{2\pi}{3}) \\ \sin \theta & \sin(\theta - \frac{2\pi}{3}) & \sin(\theta + \frac{2\pi}{3}) \end{pmatrix} \begin{pmatrix} V_a \\ V_b \\ V_c \end{pmatrix} \quad (III.23)$$

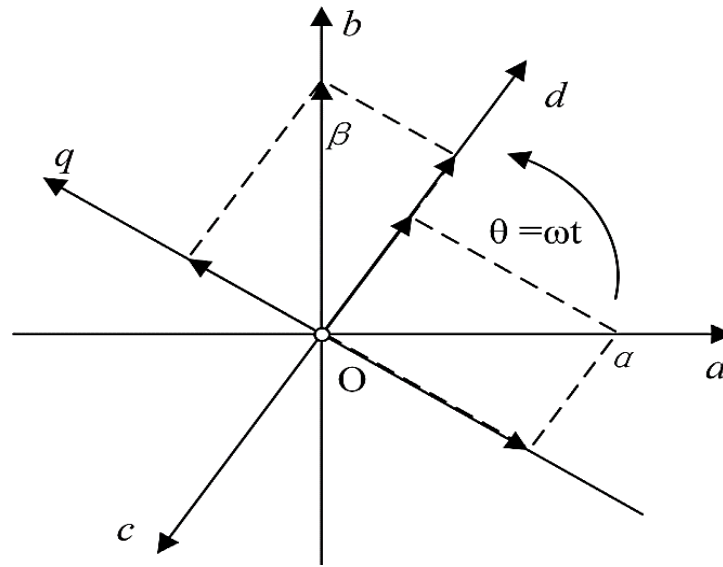


Figure III.17: Park transformation from three-phase to rotating dq0 coordinate system.

III.6.2.3 Principle of SVPWM:

The output phase voltages of the inverter depend on the relationship between the switching variables $[S_1; S_3; S_5]$ and the DC voltage as follows:

$$\begin{bmatrix} V_{an} \\ V_{bn} \\ V_{cn} \end{bmatrix} = \frac{V_{dc}}{3} \begin{bmatrix} 2 & -1 & -1 \\ -1 & 2 & -1 \\ -1 & -1 & 2 \end{bmatrix} \begin{bmatrix} S_1 \\ S_3 \\ S_5 \end{bmatrix} \quad (III.24)$$

SVPWM works on the principle that when upper switch is ON; corresponding lower switch is OFF. The ON and OFF state of the upper switches (S1, S3, S5) evaluates the output voltages. Switching states, On-state switches and vector definition are shown in table (III.4).

Table III.4: Space Vectors, Switching States, and On State Switches.

Space Vector	Switching State	On-state Switches	Vector Definition
\vec{V}_0	[000]	S_4, S_6, S_2	$\vec{V}_0 = 0$
\vec{V}_1	[100]	S_1, S_6, S_2	$\vec{V}_1 = \frac{2}{3}V_{dc}e^{j0}$
\vec{V}_2	[110]	S_1, S_3, S_2	$\vec{V}_2 = \frac{2}{3}V_{dc}e^{j\frac{\pi}{3}}$
\vec{V}_3	[010]	S_4, S_3, S_2	$\vec{V}_3 = \frac{2}{3}V_{dc}e^{j\frac{2\pi}{3}}$
\vec{V}_4	[011]	S_4, S_3, S_5	$\vec{V}_4 = \frac{2}{3}V_{dc}e^{j\frac{3\pi}{3}}$
\vec{V}_5	[001]	S_4, S_6, S_5	$\vec{V}_5 = \frac{2}{3}V_{dc}e^{j\frac{4\pi}{3}}$
\vec{V}_6	[101]	S_1, S_6, S_5	$\vec{V}_6 = \frac{2}{3}V_{dc}e^{j\frac{5\pi}{3}}$
\vec{V}_7	[111]	S_1, S_3, S_5	$\vec{V}_7 = \frac{2}{3}V_{dc}e^{j0}$

The SVPWM strategy approximates the reference voltage vector V_{ref} during each modulation period by a combination of eight vectors, each relating to a given configuration or state of the inverter, the six active vectors divides the plane into six sectors, (60° or $\pi/6$) for each sector, V_{ref} must be generated during each modulation period by two adjacent active vectors (V_1 to V_6) and two vectors of zero states (V_0 or V_7) [RYO 17].

Space vector diagram for conventional voltage source and impedance source inverter is shown in Figure (III.18).

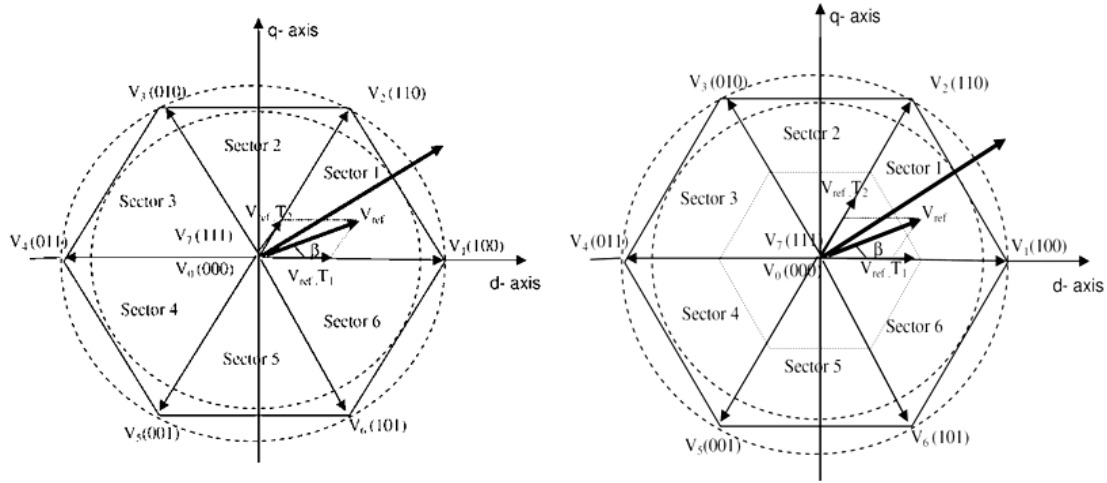


Figure III.18: Voltage vector through conventional SVPWM of VSI.

In order to determine which voltage space vector will be used to generate the synthesized vector \vec{V}_{out} , we need to use the value u_α and u_β in the $\alpha\beta$ coordinate system to determine which sector will work on the active statue. Define three variable values U_{ref1} , U_{ref2} and U_{ref3} in the equation (III.25):

$$\begin{aligned}
 U_{ref1} &= u_\beta \\
 U_{ref2} &= \sqrt{3}u_\alpha - u_\beta \\
 U_{ref3} &= -\sqrt{3}u_\alpha - u_\beta
 \end{aligned}
 \tag{III.25}$$

Then define other three variable values A, B and C, build the relationship like below:

- If $U_{ref1} > 0$, then $A = 1$, otherwise, $A = 0$;
- If $U_{ref2} > 0$, then $B = 1$, otherwise, $B = 0$;
- If $U_{ref3} > 0$, then $C = 1$, otherwise, $C = 0$;

Let: $N = 4 \times C + 2 \times B + A$ (III.26)

Then we can get the relationship between N and sector and already shown in the Table (III.5)

Table III.5: The corresponding relationship between N and sector

N	3	1	5	4	6	2
Sector	I	II	III	IV	V	VI

The switching patterns in the six sectors are illustrated in Figure (III.19) and the algorithm for the conventional SVPWM of VSI is briefed as follows.

The modulation index is:

$$M = \frac{V_{ref}}{\frac{2}{3}V_{dc}} \tag{III.27}$$

Switching time durations for active states are:

$$T_1 = \frac{T_s \cdot M \cdot \sin(\frac{\pi}{3} - \beta)}{\sin(\frac{\pi}{3})} \quad / \quad T_2 = \frac{T_s \cdot M \cdot \sin(\beta)}{\sin(\frac{\pi}{3})} \tag{III.28}$$

Switching time duration for zero state is:

$$T_0 = T_s - (T_1 + T_2) \tag{III.29}$$

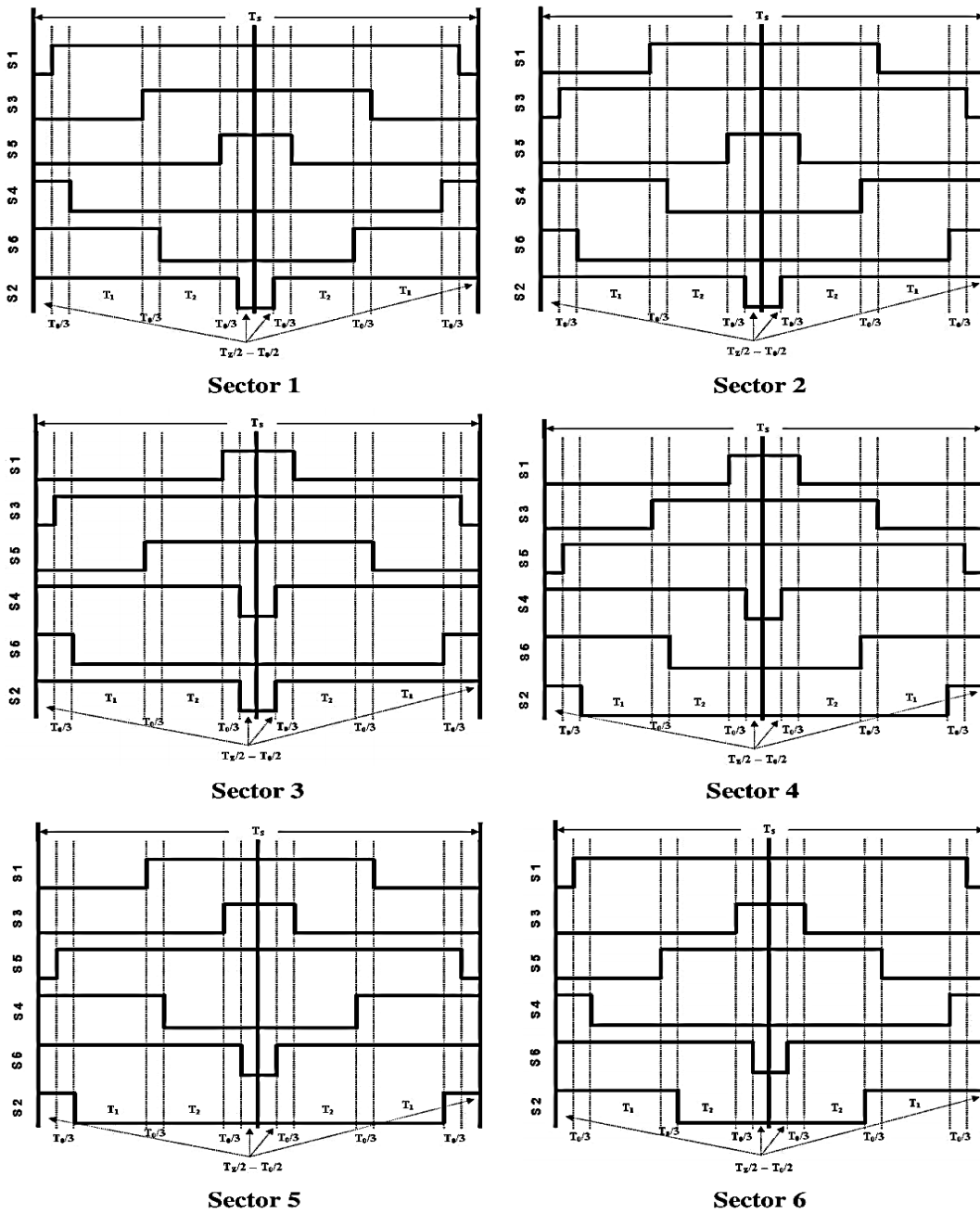


Figure III.19: Switching patterns and placement of ST states in all sectors by SVPWM.

The SVPWM is suitable to control the shoot-through time in ZSI. If the reference voltage vector V_{ref} is located between the arbitrary vector V_i and V_{i+1} , the reference voltage vector is divided into the two adjacent voltage vectors (V_i and V_{i+1}) and zero vectors (V_0 and V_7). In one sampling interval, V_i and V_{i+1} are applied at times T_1 and T_2 , respectively, and the zero vector is applied at time T_0 .

Consequently, the reference voltage vector V_{ref} can be obtained as [TQV 07]:

$$V_{ref} = V_i T_1 + V_{i+1} T_2 \tag{III.30}$$

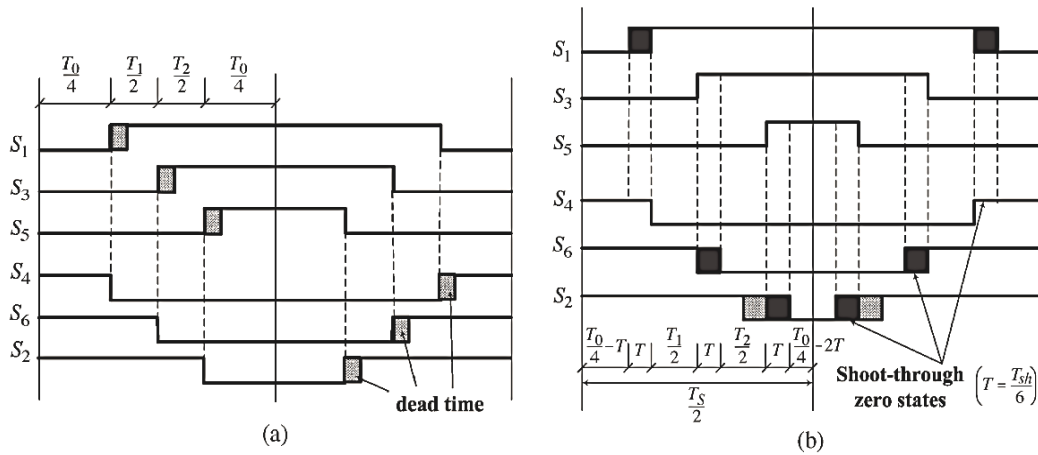


Figure III.20: PWM switching patterns at sector I.

(a) Switching patterns for traditional SVPWM.(b) Switching patterns for modified SVPWM.

Figure (III.20) shows the PWM switching patterns for both the traditional SVPWM and the MSVPWM when the reference voltage vector is at sector I.

✚ Unlike the traditional SVPWM, the MSVPWM has an additional shoot-through time T_{sh} for boosting the dc link voltage of the inverter beside time intervals T_1 , T_2 , and T_0 . The shoot-through states are evenly assigned to each phase with $T_{sh}/6$ within zero voltage periods T_0 , as shown in Figure (III.20 (b)). The zero voltage periods should be diminished for generating a shoot-through time, and the active states periods T_1 and T_2 are unchanged. So, the shoot-through time does not affect the PWM control of the inverter, and it is limited to the zero state time T_0 . The six PWM signals in the MSVPWM scheme should be controlled independently [TQV 09].

The reference voltage vector V_{ref} can be obtained as:

$$V_{ref} = V_1 T_1 + V_2 T_2 \tag{III.31}$$

III.7 Simulation Model:

III.7.5 Simulink model of hardware circuit:

Figure (III.21) shows a three-phase inverter hardware model, there are consist of DC power supply, switches circuit, LC filter circuit and, and series RL branch, both of them build with Simscape software.

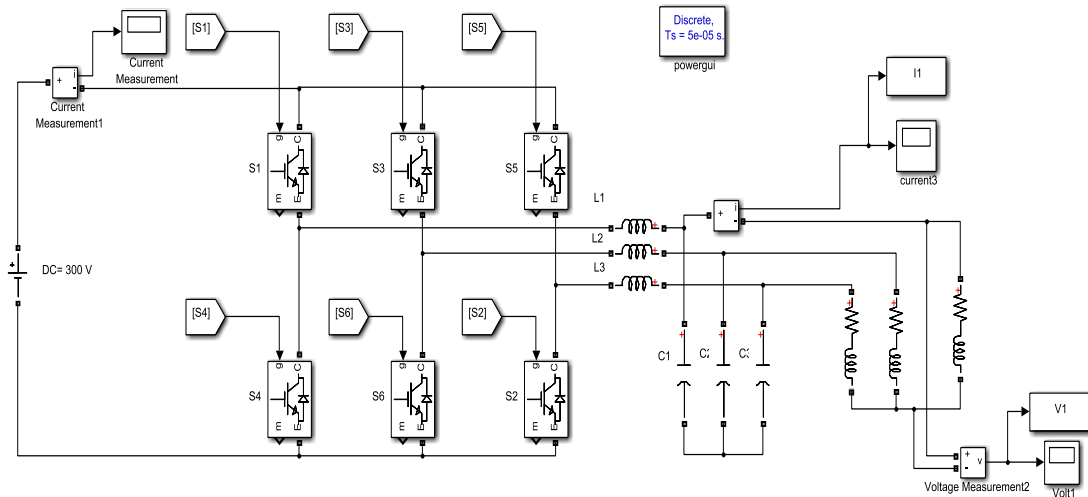


Figure III.21: Simulink model of three-phase full bridge inverter system

- **Three-phase LC filter:** In order to decrease the harmonic current, a three-phase LC filter is needed. The configuration circuit of LC filter is shown in Figure (III.22).

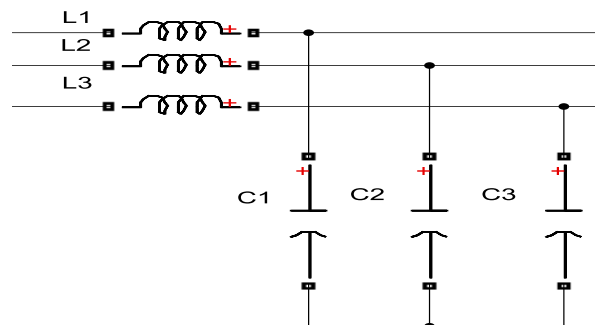


Figure III.22: Simulink model of the LC filter.

In this system, the fundamental frequency generate by inverter is 50 Hz, therefore, the LC filter resonant frequency is calculated by equation below:

$$f_0 = \frac{1}{2\pi\sqrt{LC}} = 50Hz \tag{III.32}$$

Let L=12mH, the capacitor value C can be calculated by the above equation:

$$C=844 \times 10^{-6}F=844\mu F \tag{III.33}$$

III.7.6 Model building of Z-source inverter:

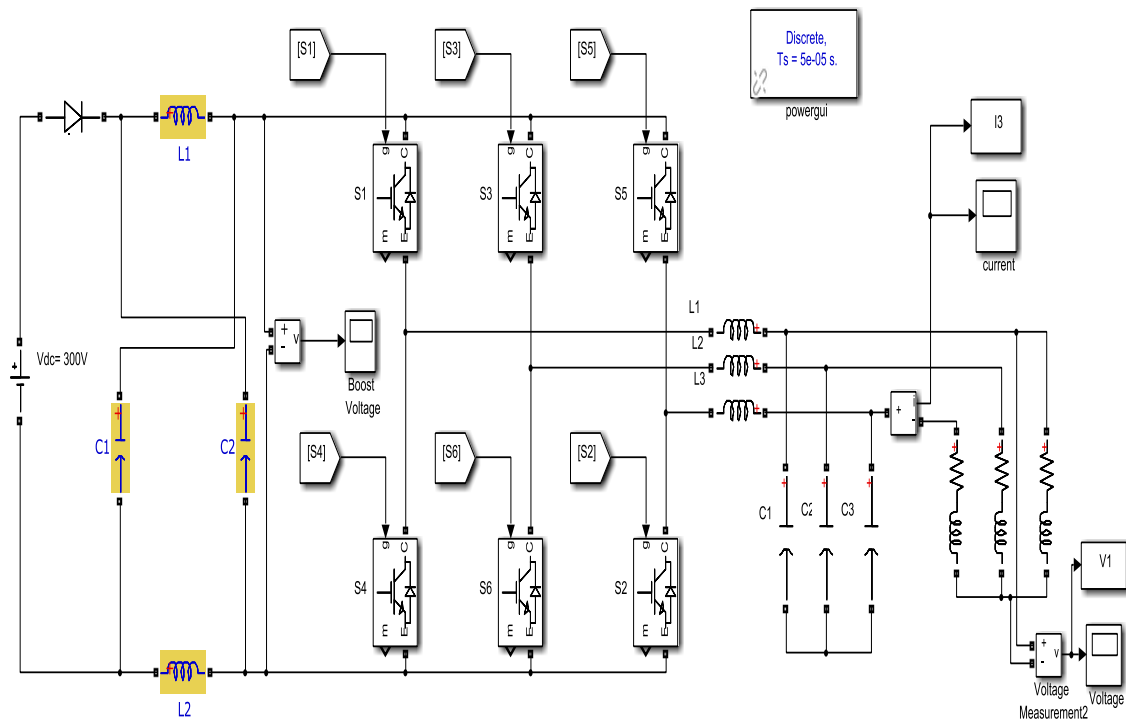


Figure III.23: Simulink model of three-phase full bridge Z-Source inverter system.

III.7.7 Simulink model of SPWM signal generator:

A three-phase Pulse Width Modulation (PWM) switching signal is as shown in Figure (III.24).

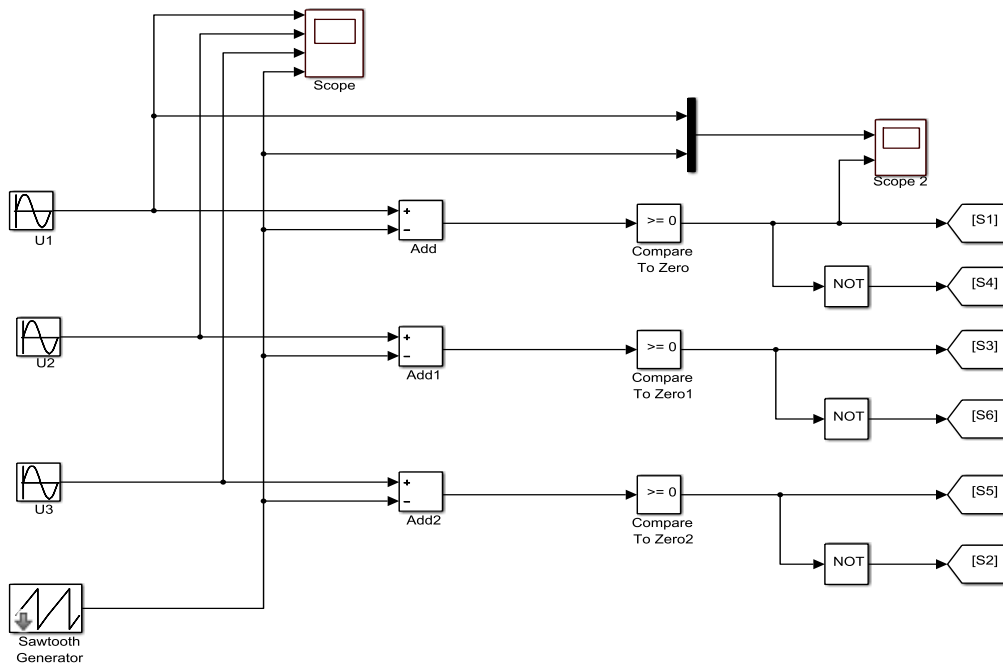


Figure III.24: Three-phase Pulse Width Modulation (PWM).

II.7.8 Simulink model of SVPWM signal generator:

The SVPWM control system model is used to generate the SVPWM control signal for z-source inverter [See annex C]. The whole SVPWM control system is shown in Figure (III.25).

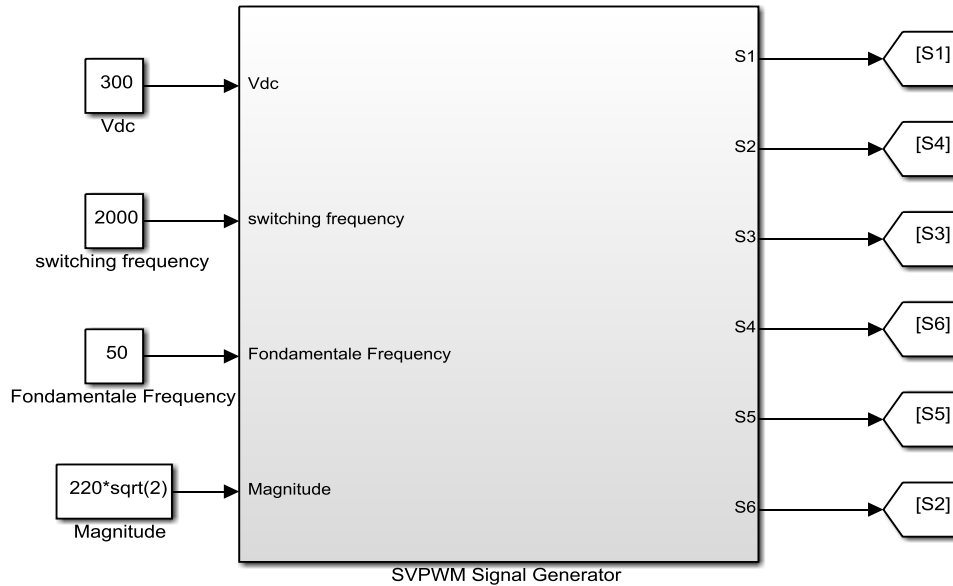


Figure III.25: SVPWM signal generator.

Simulation test beds using MATLAB/Simulink 2013 were constructed to validate the effectiveness of the system models and control algorithms proposed. Parameters used for the simulation are shown in (Table III.6).

Table III.6: Parameters used for simulation.

Parameter	Value
DC bus voltage	300 v
Z-source inductance (L1 and L2)	9.6 mH
Z-source capacitance (C1 and C2)	4700 μ F
Switching frequency	2 KHz
Fundamental frequency	50 Hz
Modulation Index (M)	0.8

III.8 Simulation Results:

III.8.1 The simulation results of SPWM control:

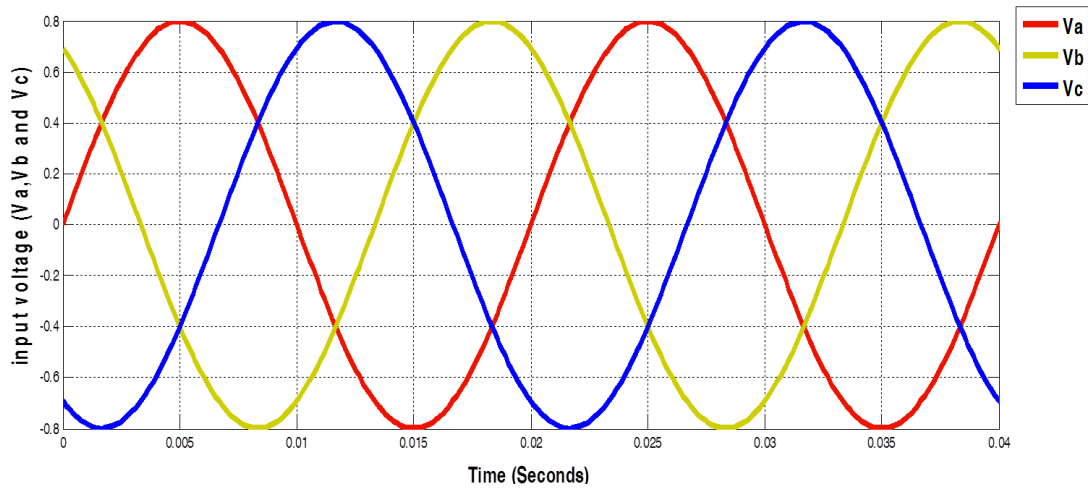


Figure III.26: Three-phase sinusoidal signals (V_a , V_b and V_c) and output waveforms.

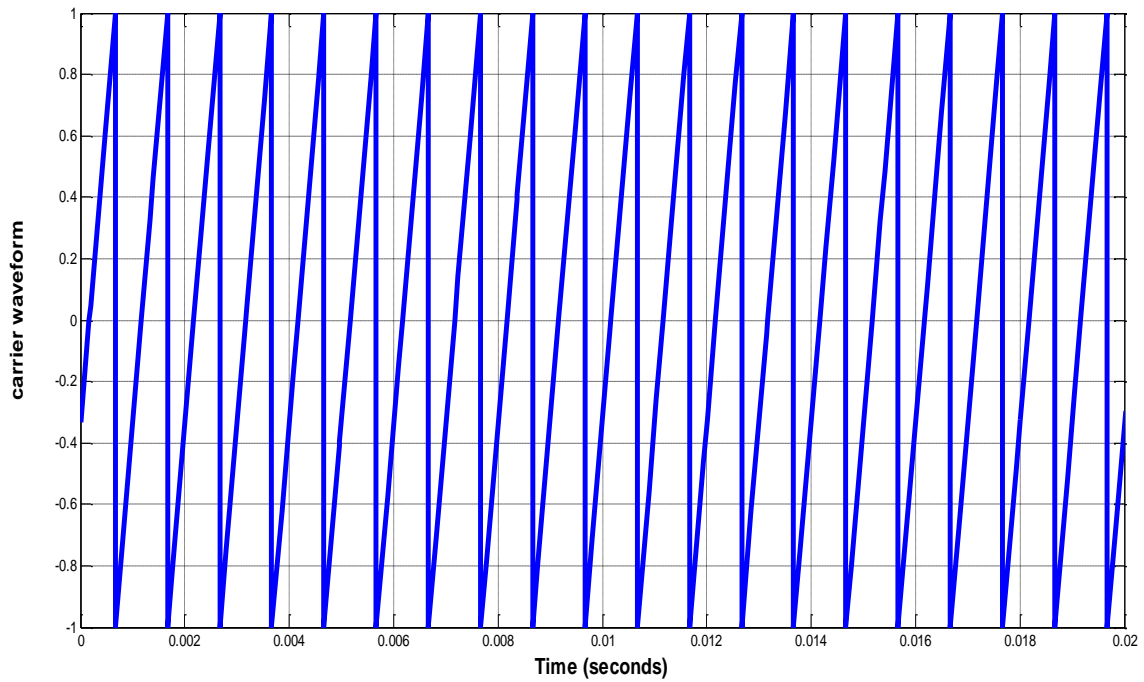


Figure III.27: Pulse Width Modulation (PWM) Control.

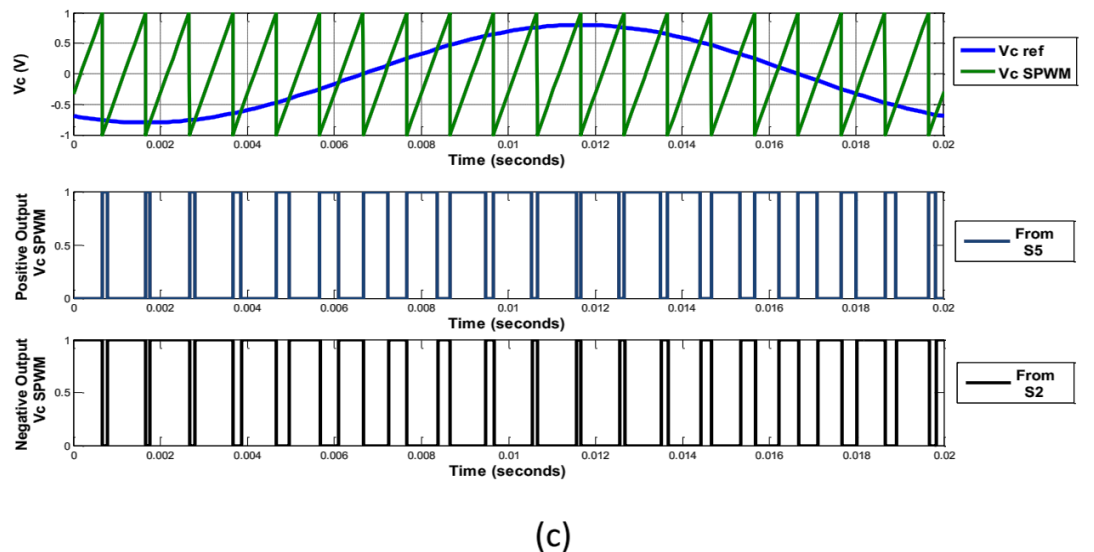
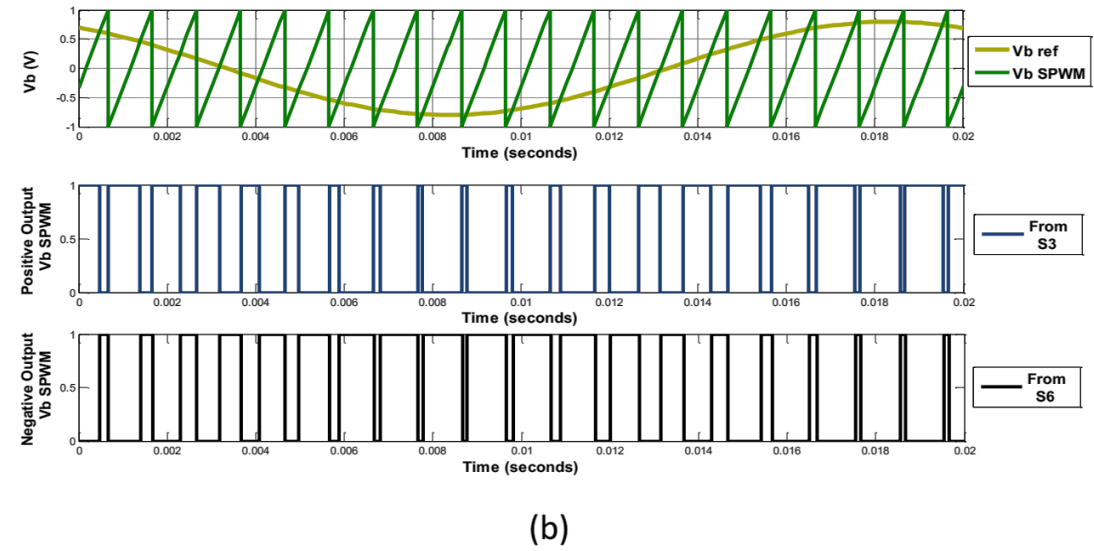
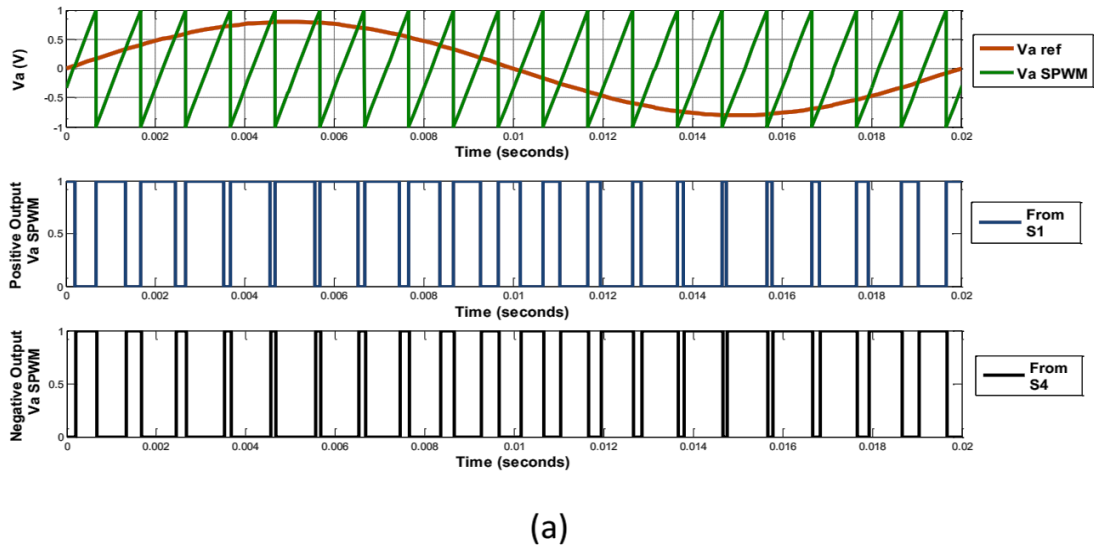


Figure III.28: SPWM signal produce: reference voltage and carrier wave vs. output voltage (upper and lower switches).

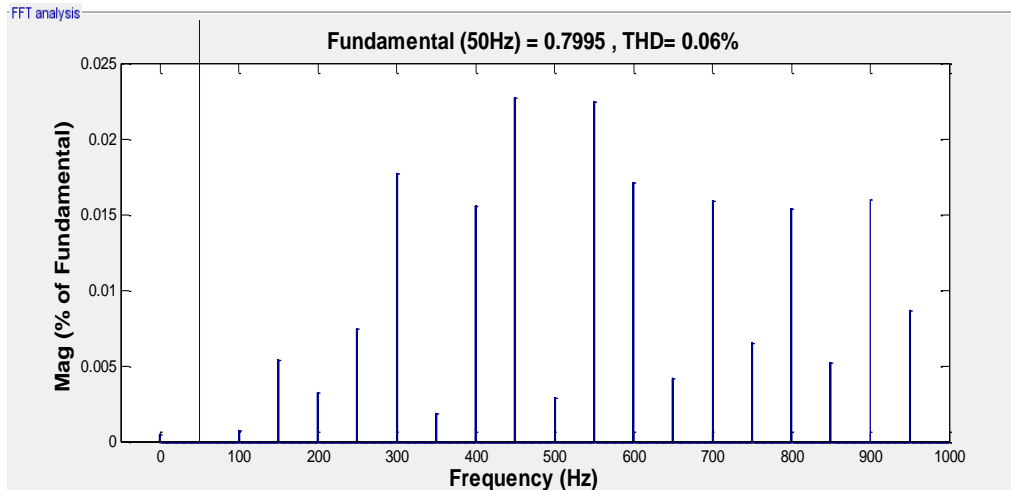


Figure III.29: FFT Analysis of output reference voltage V_a of three- phase inverter with $MI=0.8$.

III.8.2 The simulation results of SVPWM control:

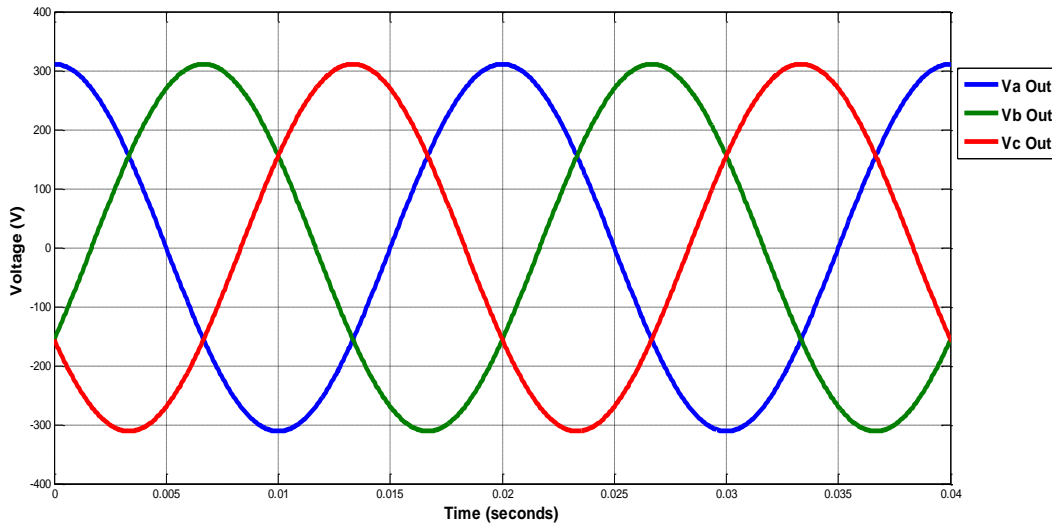


Figure III.30: Three-phase sinusoidal signal generator and output waveform.

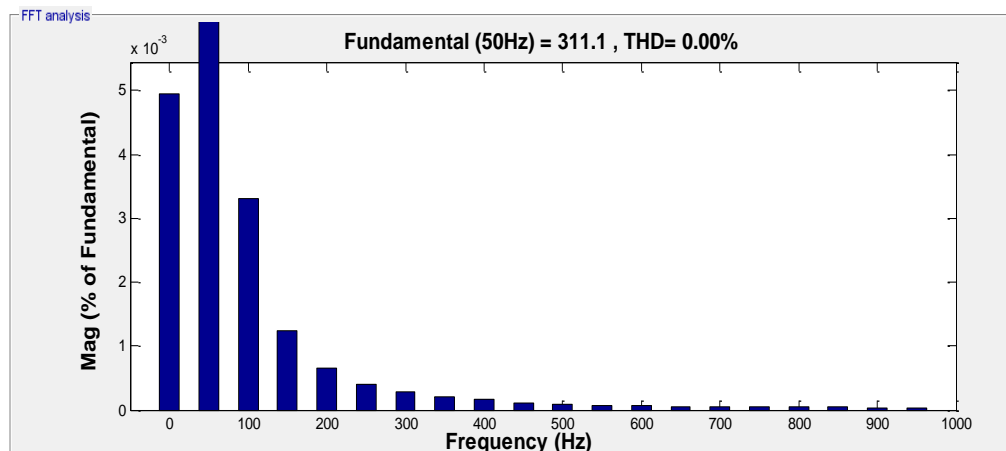


Figure III.31: FFT Analysis of output sinusoidal signal generator.

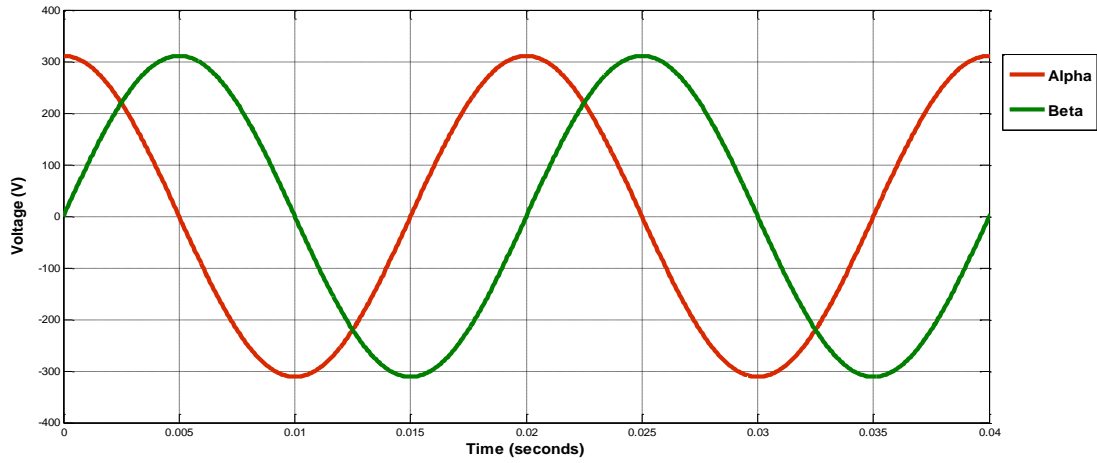


Figure III.32: Clarke transformation block and output waveform.

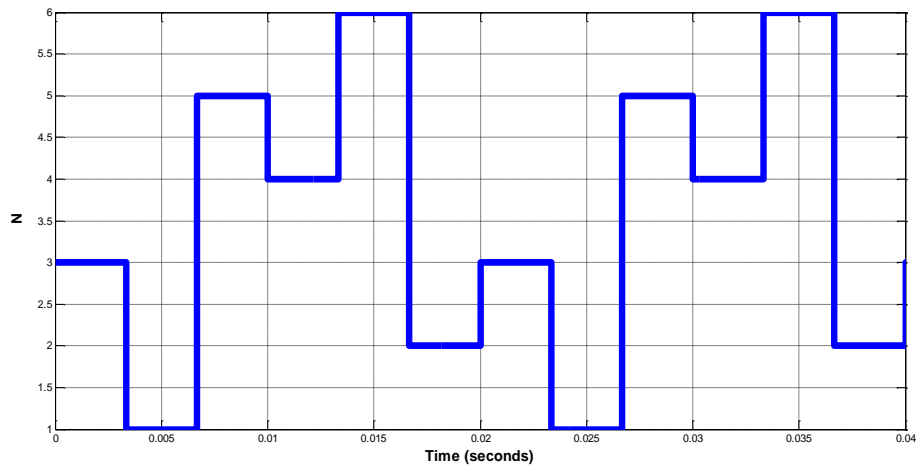


Figure III.33: Reference angel sector block.

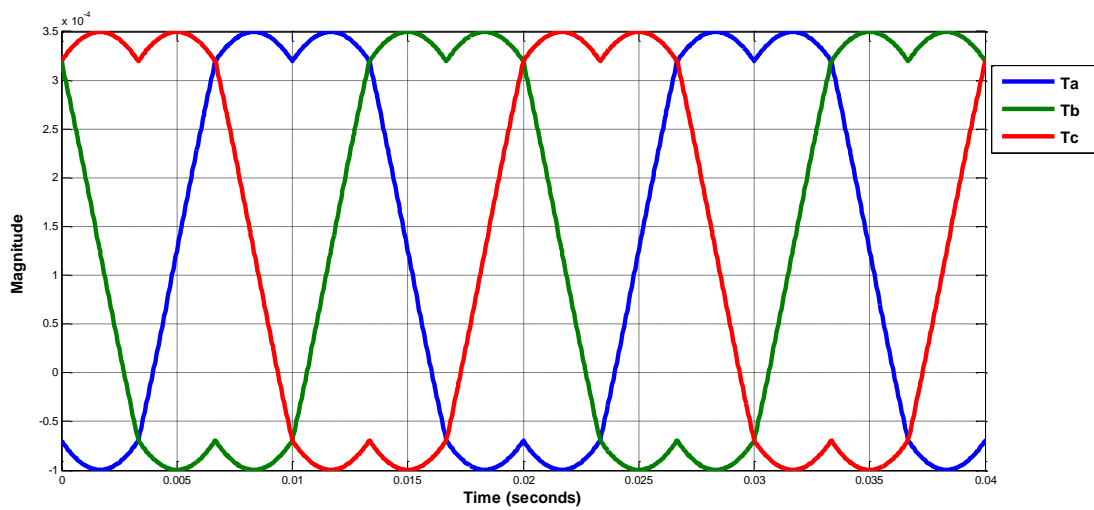


Figure III.34: Space vector modulation signal generator and the output waveform.

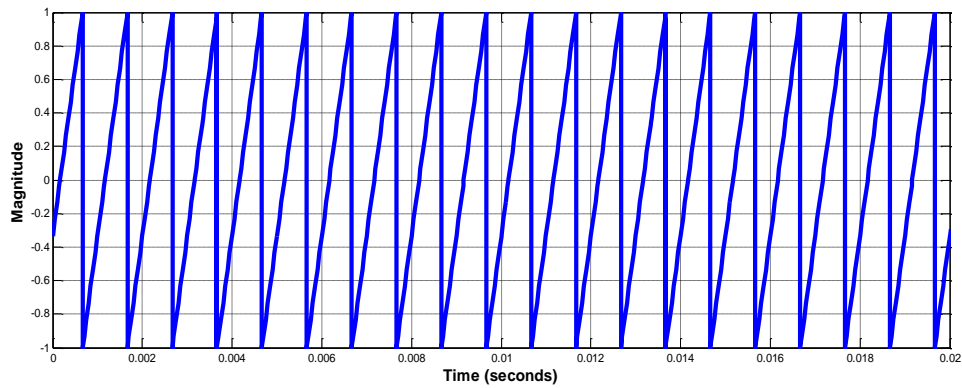


Figure III.35: PWM signal generator.

III.8.3 The three-phase inverter with SPWM control simulation results:

- Test on an RL load: $R=10\Omega$ and $L=1\text{mH}$

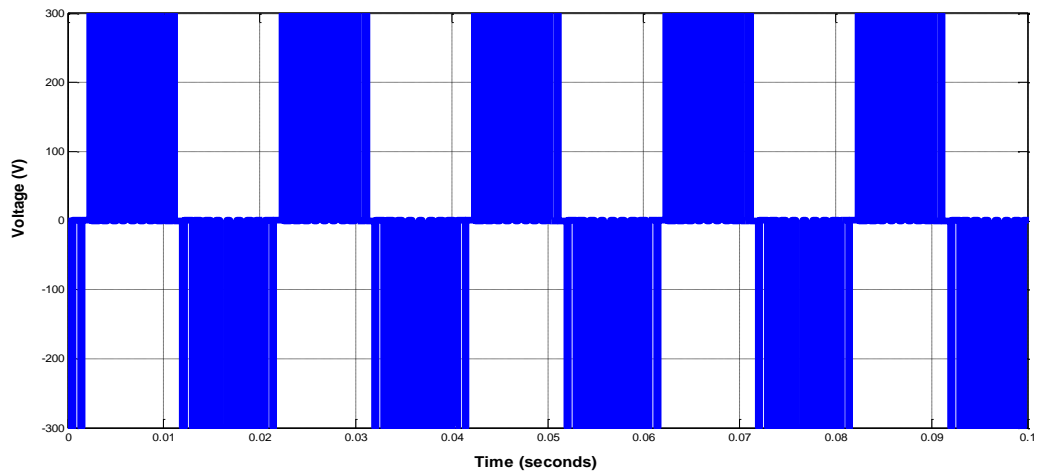


Figure III.36: Output voltage of three-phase inverter at 300 V.

The output three phase load voltage and current wave forms of three phase inverter are shown respectively in figure (III.37) and figure (III.38).

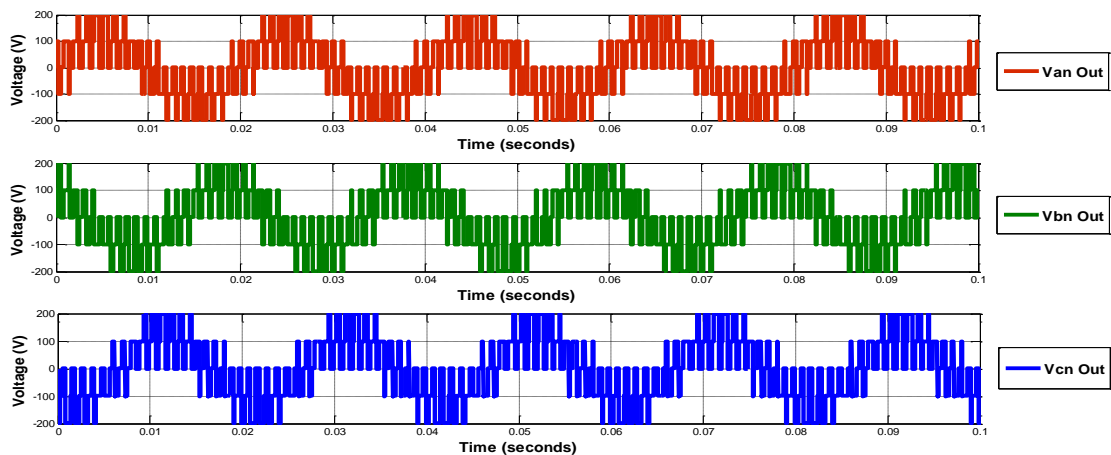


Figure III.37: Three Phase Voltage (Line to Neutral voltage) of three phase inverter across Load for $M_I= 0.8$.

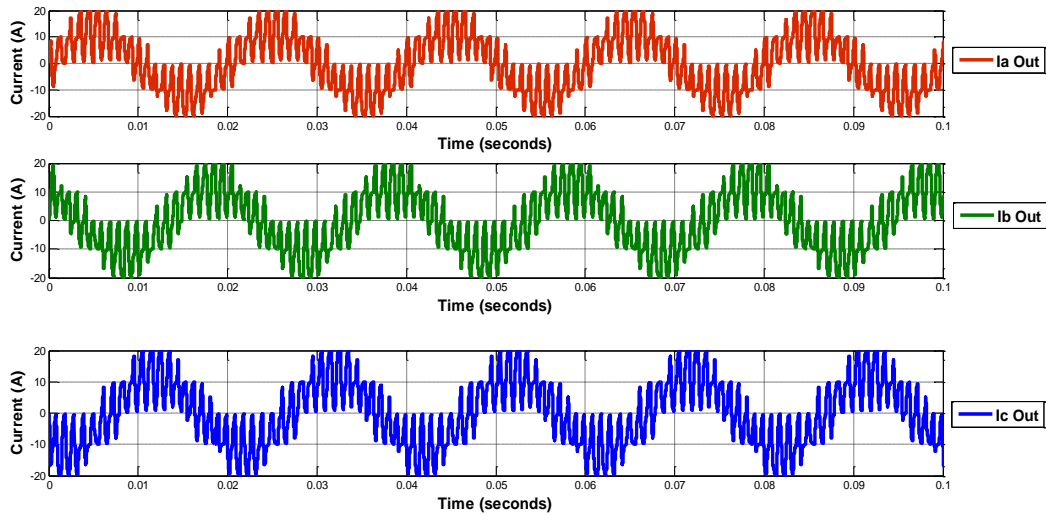


Figure III.38: Three Phase Current waveform of three phase inverter across Load for MI= 0.8.

The FFT analysis results (THD) of the output voltage and output current of the inverter are shown respectively in Figure (III.39) and Figure (III.40).

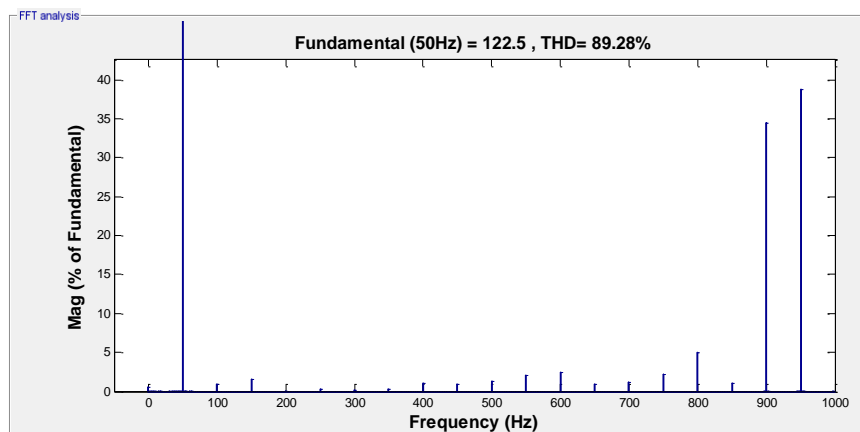


Figure III.39: FFT Analysis of output Voltage (V_a) of three phase inverter with MI= 0.8.

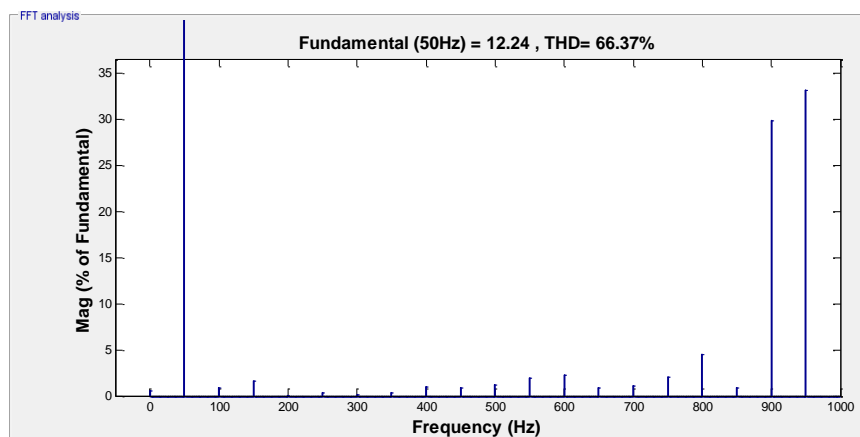


Figure III.40: FFT Analysis of output current (I_a) of three phase inverter with MI= 0.8.

The output three phase load voltage and current wave forms of three phase inverter after LC filter are shown respectively in figure (III.41) and figure (III.42).

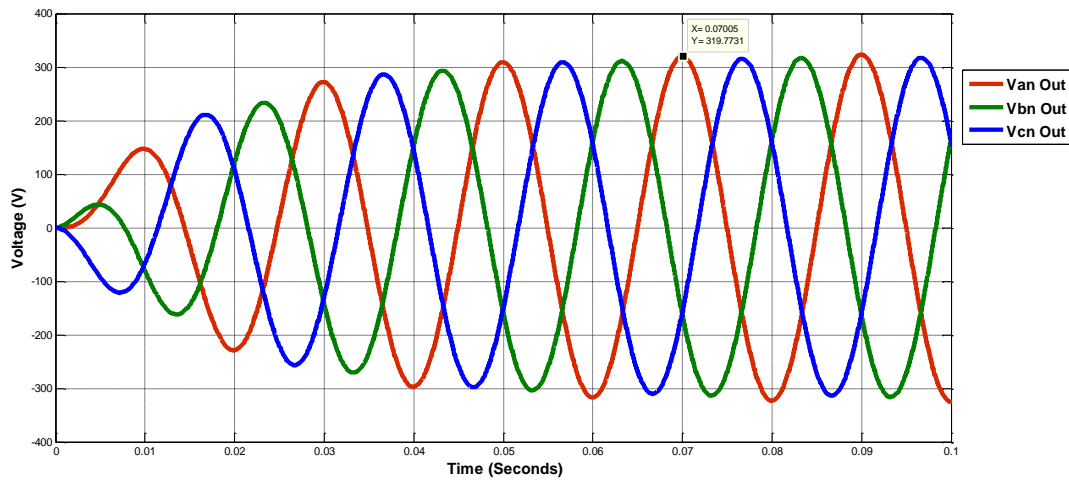


Figure III.41: Three Phase Voltage (Line to Neutral voltage) of three phase inverter across Load for MI=0.8 after filtering.

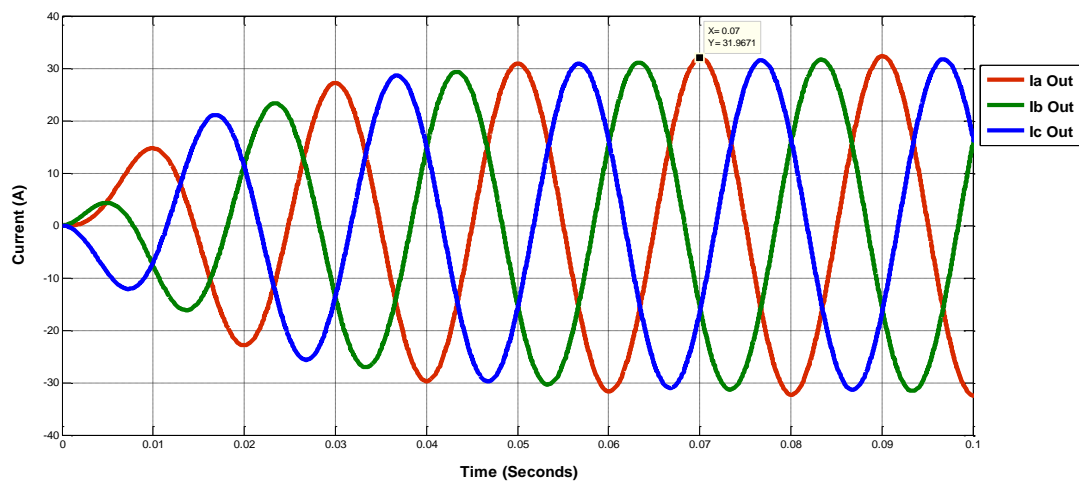


Figure III.42: Three Phase Current waveform of three phase inverter across Load for MI=0.8 after Filtering.

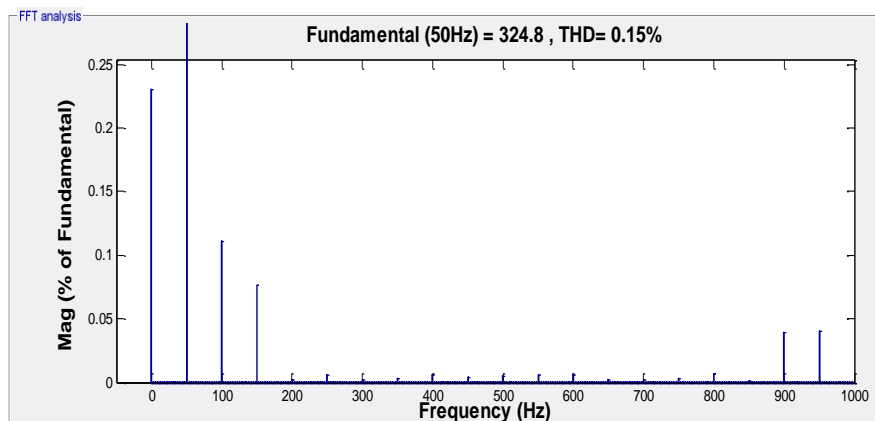


Figure III.43: FFT Analysis of output Voltage (V_a) of three phase inverter after filtering.

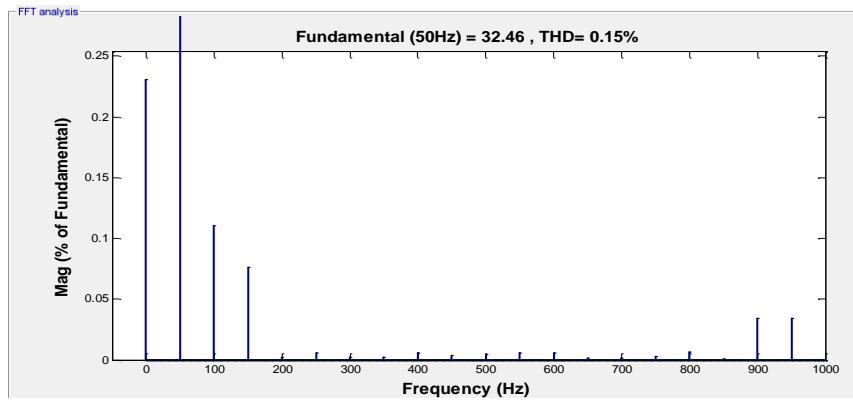


Figure III.44: FFT Analysis of output Current (I_a) of three phase inverter after filtering.

III.8.4 The three-phase ZSI with SPWM control simulation results:

- Test on an RL load: $R=10\Omega$ and $L=1\text{mH}$

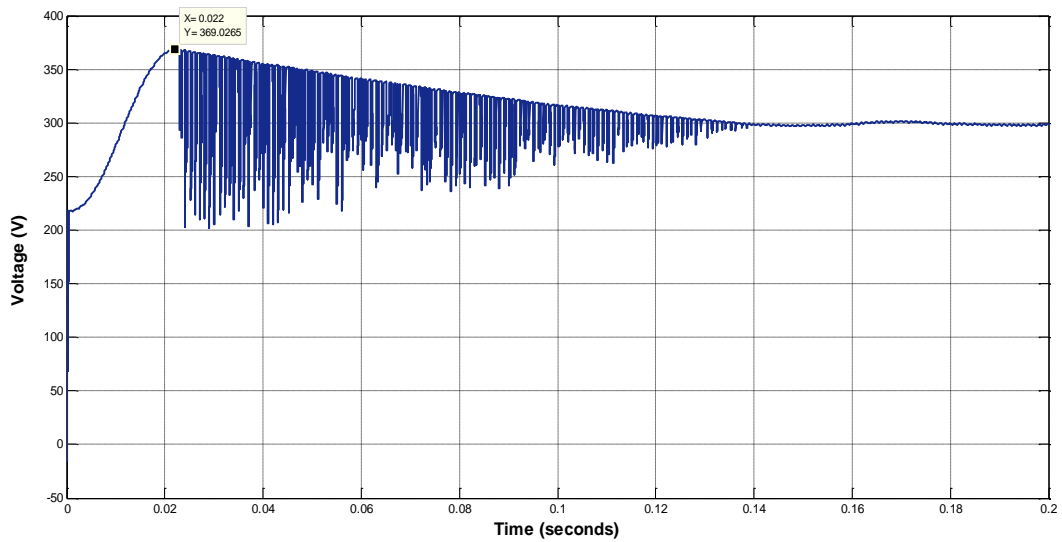


Figure III.45: Voltage across Impedance Network of three- phase ZSI for $MI= 0.8$.

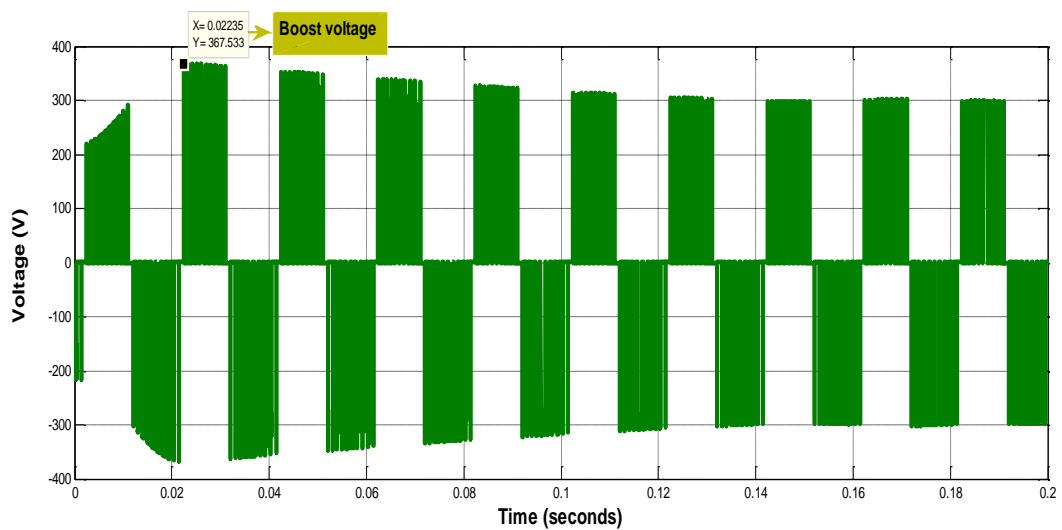


Figure III.46: Output voltage of three- phase Z-Source Inverter.

Appreciated in Figures (III.45) and (III.46), we note that there is an increase in tension at 369 V caused by the LC impedance network effect.

The output three phase load voltage and current wave forms of three phase Z-Source Inverter (ZSI) are shown respectively in figure (III.47) and figure (III.48).

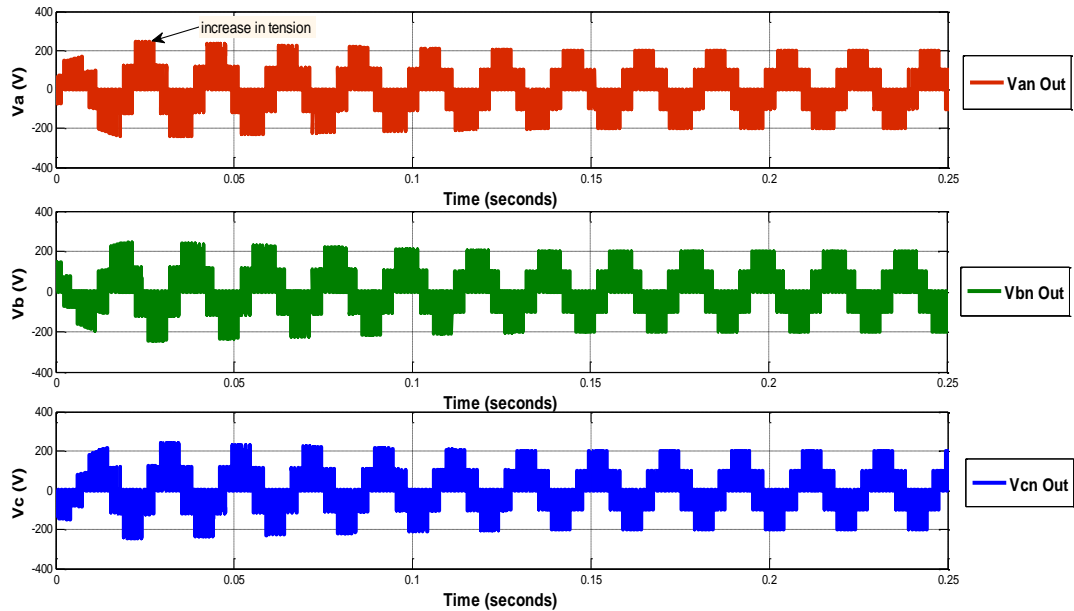


Figure III.47: Three Phase Voltage (Line to Neutral voltage) of three- phase ZSI across Load for $M=0.8$.

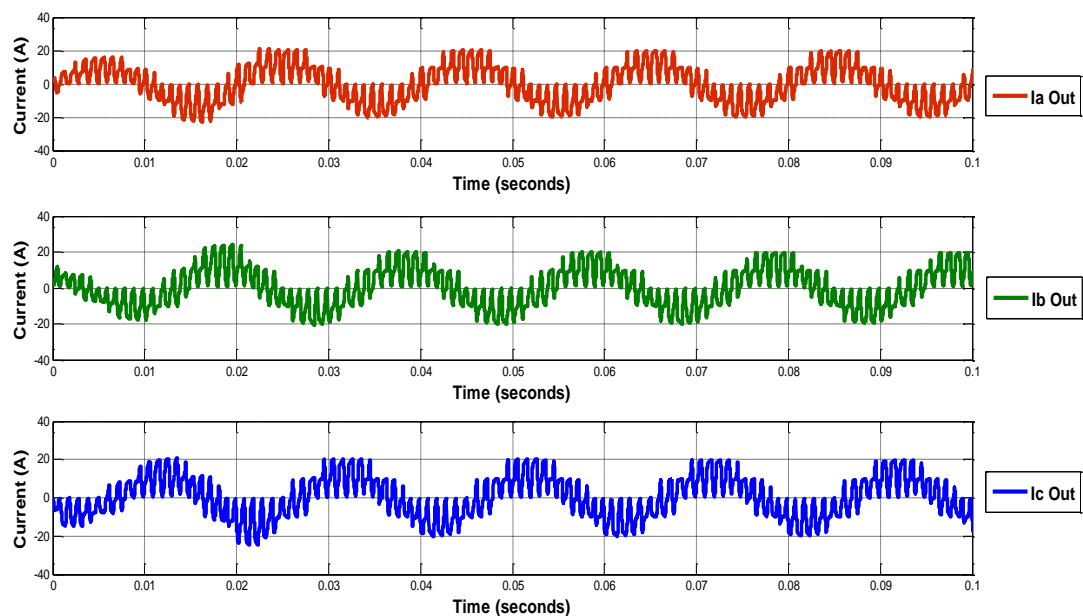


Figure III.48: Three Phase Current waveform of three- phase ZSI across Load for $M=0.8$.

The FFT analysis results (THD) of the output voltage and output current of the Z-Source Inverter are shown respectively in Figure (III.49) and Figure (III.50).

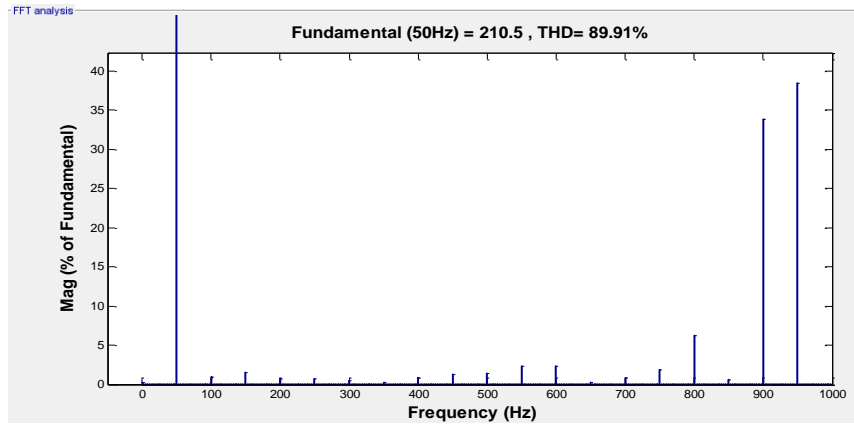


Figure III.49: FFT Analysis of Output Voltage (Va) of three- phase ZSI with MI= 0.8.

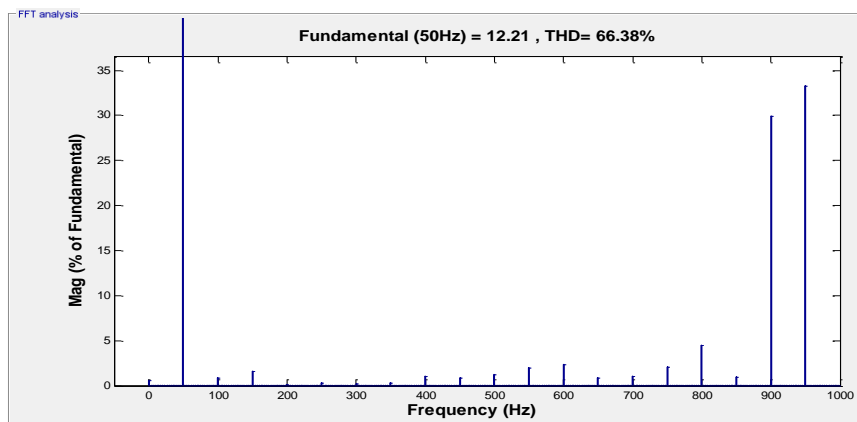


Figure III.50: FFT Analysis of Output Current (Ia) of three- phase ZSI with MI= 0.8.

The output three phase load voltage and current wave forms of three-phase Z-Source Inverter after filtering are shown respectively in figure (III.51) and figure (III.52).

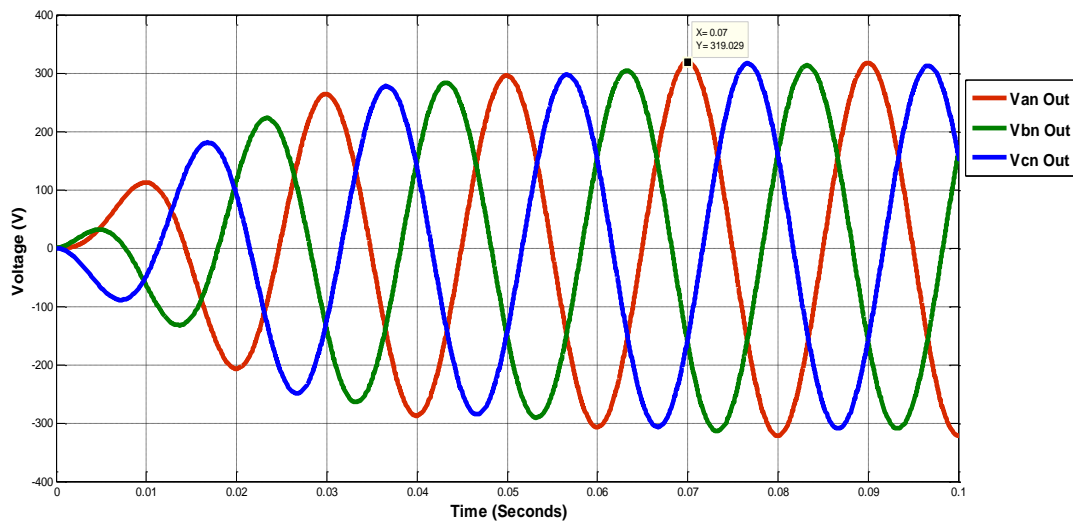


Figure III.51: Three Phase Voltage (Line to Neutral voltage) of three- phase ZSI across Load for MI=0.8 after Filtering.

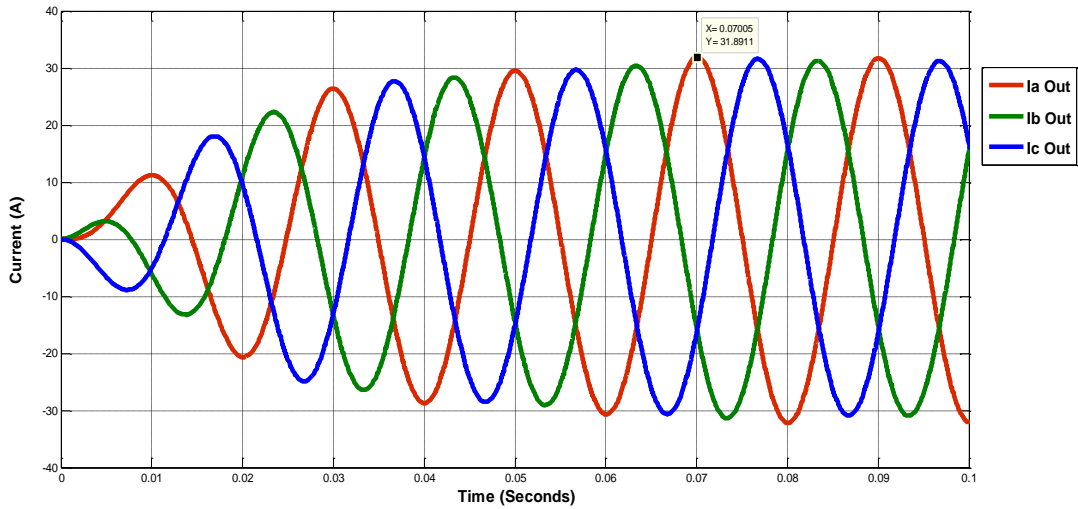


Figure III.52: Three Phase Current waveform of three-phase ZSI across Load for MI=0.8 after Filtering.

The FFT analysis results (THD) of the output voltage and output current of the Z-Source Inverter after filtering are shown respectively in Figure (III.53) and Figure (III.54).

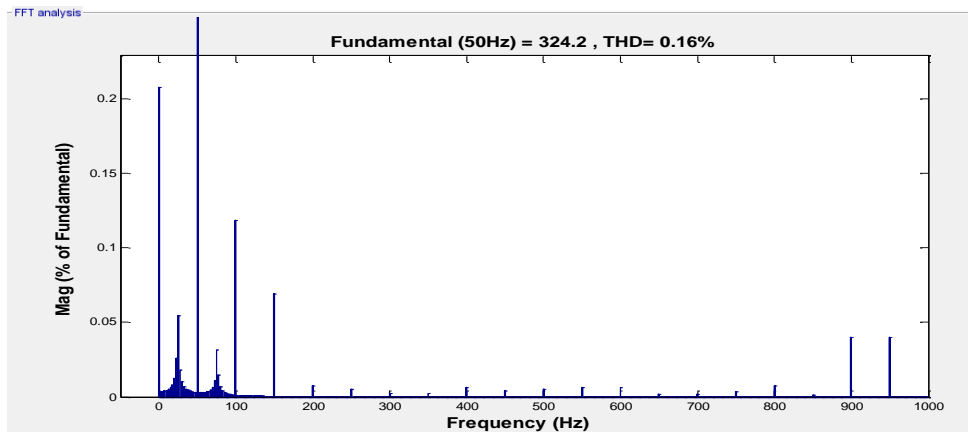


Figure III.53: FFT Analysis of Output Voltage (V_a) of three-phase ZSI with MI= 0.8.

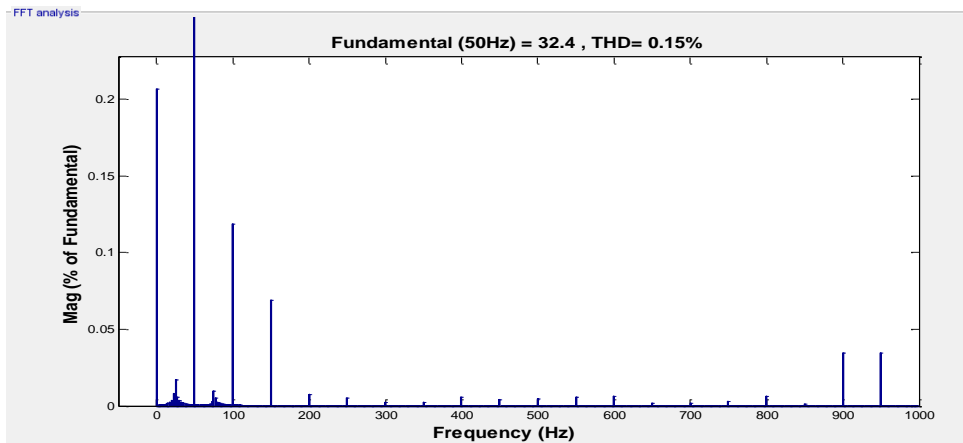


Figure III.54: FFT Analysis of Output Current (I_a) of three-phase ZSI with MI= 0.8.

III.8.5 The three-phase ZSI with SVPWM control simulation results:

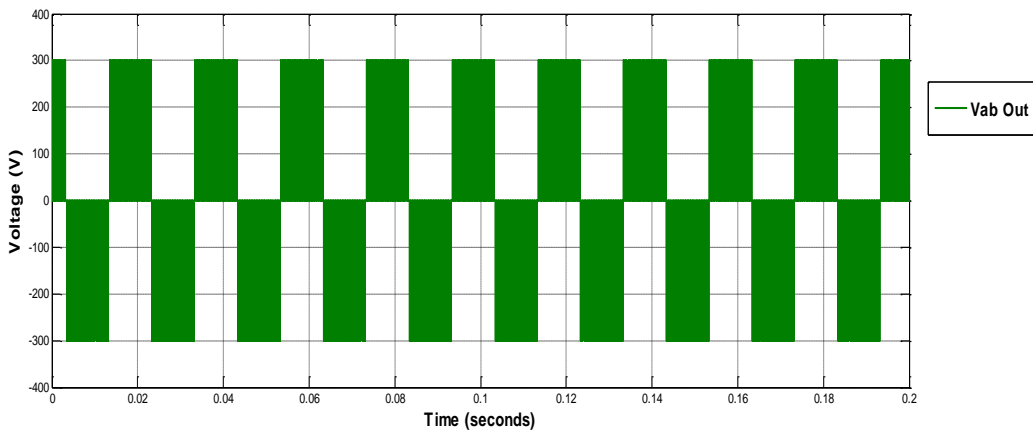


Figure III.55: Output voltage of three- phase Z-Source Inverter.

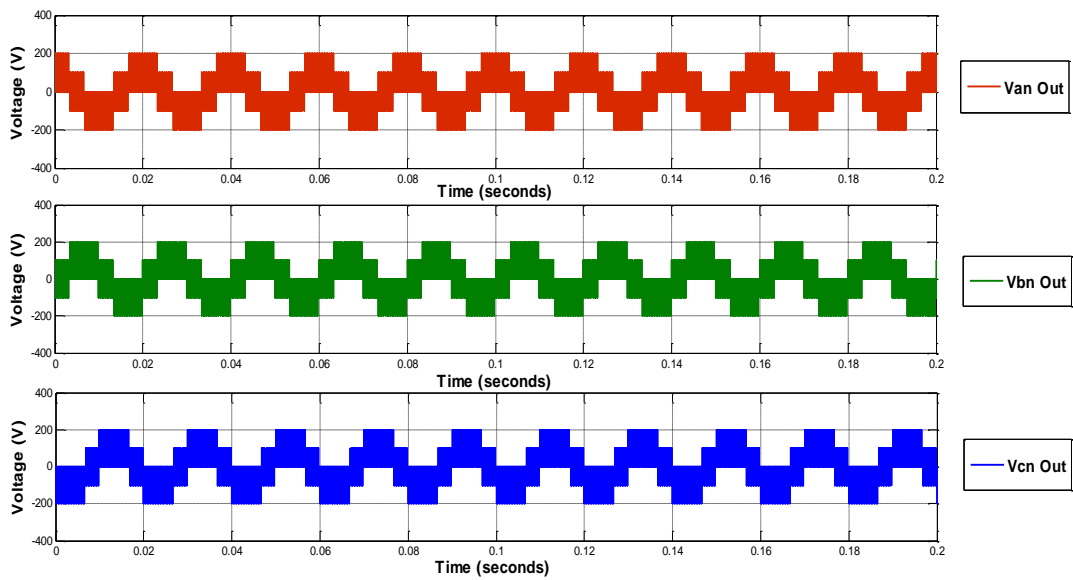


Figure III.56: Three Phase Voltage (Line to Neutral voltage) of three- phase ZSI across Load for $M=0.8$.

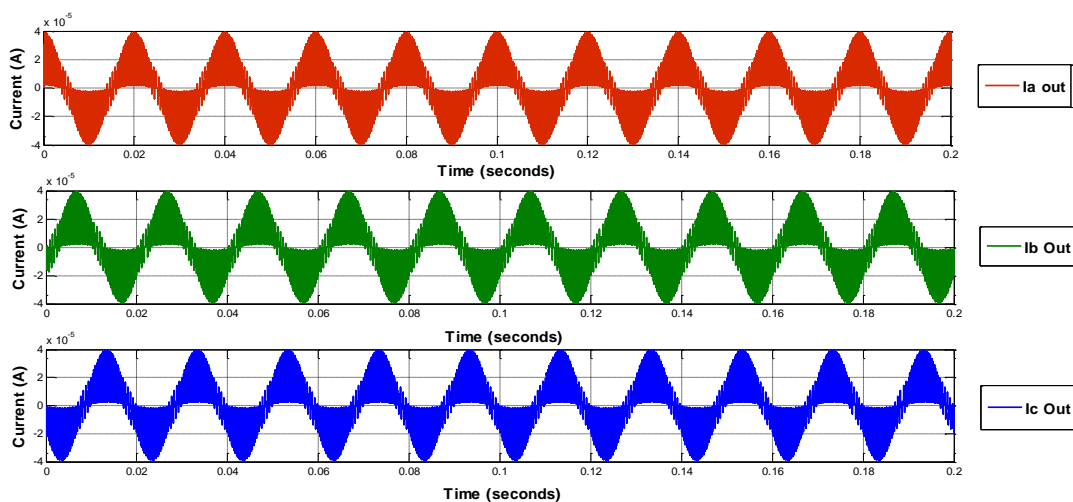


Figure III.57: Three Phase current waveform of three- phase ZSI across Load for $M= 0.8$.

III.8.6 Interpretation of results:

✚ Through the curve of voltage across Impedance Network of three- phase ZSI for modulation index $M= 0.8$ (Figure III.45) we observed the performance of LC network to boost voltage. As results, the enhanced Z-source inverter system provides ride-through capability to reduce capacitor voltage stress, inrush current and extends output voltage range. Therefore, to achieve better performance of inverter, the modulation index should be controlled, and the output voltage has a linear relationship with modulation index.

✚ Figure (III.28) shows the SPWM control signal waveform for three phases switches, the control sequence is very similar with the SVPWM control sequence. The Figures (III.51) and (III.52) shows good results for the output voltage and current, both of them are controlled to a high-quality shape of sinusoidal waveform.

✚ FFT analysis is done in the waveforms of output voltage and current of the three-phase inverter; in order to know about the Total Harmonic Distortion (THD) of the respective waveforms. Here, these two three-phase inverters (Traditional and Z-source Inverter) are compared on the basis of the THD values obtained. Accordingly, the explanation of the results will be based on:

a. From the figure (III.46) shown above, we find the peak value of output phase voltage is 367.355v and is higher than the output without using Z-source network, THD = 0.16% and it's little bit higher than the output without using Z-source network. However, in the real world, the less increasing value of THD can be ignored.

b. We observe a low percentage of THD after filtering. From this, we conclude that passive electronic LC filters block or reduce noise of circuits and systems, and separate or condition the desired signals.

✚ Through all the simulation results, we concluded that the SVPWM has high efficiency than SPWM.

III. 9 Conclusion:

From this chapter we have stressed on the operating principle of the z-source inverter, as well as the different control strategies of this inverter. The z-source inverter offers the advantage of boosting the input voltage without using a step-up converter (boost chopper).

The PWM sequences has been inserted to SPWM and SVPWM controls signal to achieve the shoot-through time in the Z-source network. The comparison results of these control strategies show that the SVPWM control are the most appropriate for controlling the Z-source inverter. However, the SPWM strategy is characterized mainly by remarkable simplicity.

The FFT Analysis is performed to calculate the Total Harmonic Distortion (THD) of the inverters output voltage and current. The experimental shows a significant results for boost dc-link voltage, and the output waveform have a good shape and less THD.

CHAPTER IV:
Z-Source Inverter Connected with
Induction Motor

IV. 1 Introduction:

The use of induction motor is growing day by day because of its superiority and high efficiency over DC machine. So for wide range of use in the industry, this machine requires an efficient drive circuit arrangement. Currently conventional VSI or CSI is dealing as key part in the field of induction motor drive circuit [SML 18].

This chapter represents a description, design and general information of asynchronous motor, and simulation of impedance network connected with induction using SPWM Method.

IV. 2 Asynchronous Motor:

IV.2.1 Definition:

An asynchronous motor or an Induction motor is an AC motor where the rotor current needed to produce torque is induced by electromagnetic induction from the magnetic field of the stator winding [CRA 14]. Induction motors are referred to as ‘asynchronous motors’ because they operate at a speed less than their synchronous speed.

An induction motor is sometimes known as a revolving transformer despite the stator (stationary element) acts as one winding of the transformer and the rotor is the other winding of the transformer factor [MGK 20].

IV.2.2 Types of Induction Motors:

A. Single phase induction motor: The single-phase induction motor is not self-starting. When the motor is connected to a single-phase power supply, the main winding carries an alternating current [12].

B. Three phase induction motor: The three-phase induction motor are widely used as industrial drives because they are self-starting, reliable and economical.

IV.2.3 Parts of Induction Motor:

- a. Stator:** consisting of a steel frame that supports a hollow cylindrical core of stacked laminations. Slots are on the internal circumference of the stator.
- b. Air Gap:** This air gap has a length from 1.25 mm to 2.5 mm.

- c. **Rotor:** Also composed of punched laminations with rotor slots for rotor winding [TMO 17].

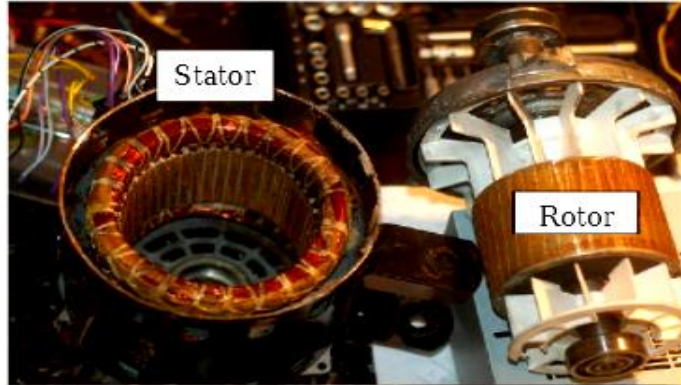


Figure IV.1: Induction Motor Parts.

IV. 3 Operating Principle of Induction Motors:

We need to give double excitation to make a DC motor to rotate. In the DC motor, we give one supply to the stator and another to the rotor through brush arrangement. But in induction motor, we give only one supply, so it is interesting to know how an induction motor works. It is simple, from the name itself we can understand that here, the induction process is involved. When we give the supply to the stator winding, a magnetic flux gets produced in the stator due to the flow of current in the coil. The rotor winding is so arranged that each coil becomes short-circuited [13].

IV. 4 Synchronous Speed and the Slip:

The difference between the stator (synchronous speed) and rotor speeds is called the slip. The synchronous speed ($N_{syc.}$) of the magnetic field is given by:

$$N_{syc} = \frac{20f}{p} \quad \text{In rpm} \quad (IV.1)$$

Where: f is the frequency of the supply, and P is the number of poles.

If N_r is the speed of the rotor (in rpm) then the difference between the synchronous speed and rotor speed is called the (slip) and is defined in per unit as

[TMO 17]:
$$S = \frac{N_{syc} - N_r}{N_{syc}} \quad \text{unit less (per unit)} \quad (IV.2)$$

- For induction motors $N_{syc} > N_r$ and the slip is always positive.
- At no-load the slip is nearly zero.

IV. 5 Advantages of Induction Motor:

- The most important advantage of an induction motor is that its construction is quite simple in nature. The working of the motor is independent of the environmental condition. This is because the induction motor is Robust and mechanically strong.
- A Squirrel cage induction motor does not contain Brushes, Slip rings and Commentators. Due to this reason, the cost of the motor is quite low. However, Slip Rings are used in Wound type induction motor to add external resistance to the rotor winding [12].

IV. 6 SVPWM Controlled ZSI Drive for Speed Control of three-Phase Induction Motor:

Proposed circuitry consists of a DC input from a PV cell; the block diagram of the proposed circuitry is shown in Figure (IV.2).

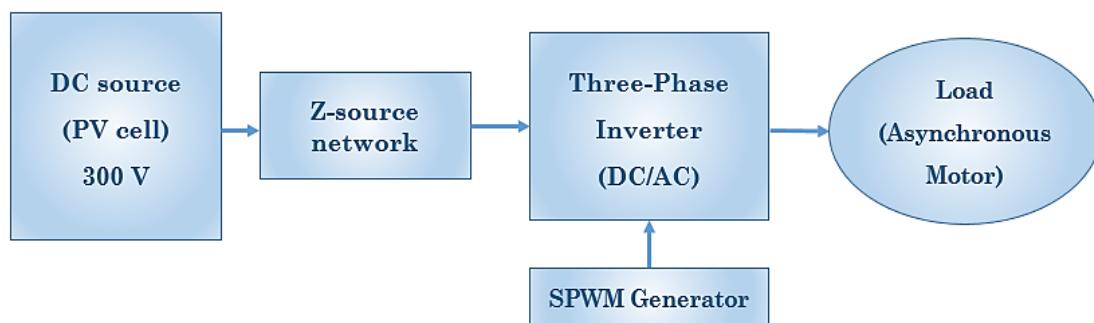


Figure IV.2: Project block diagram.

Output from PV Cell is DC power is fed to the Inverter as input. The inverter chosen here is a Z source inverter (ZSI). The reason of this work is to increase the induction motor speed using the z-source inverter Technique. We will explain this in the next section, which concerns simulations results.

IV. 7 Simulation Model:

IV.7.1 Simulink Model of MAS connected with three phase VS:

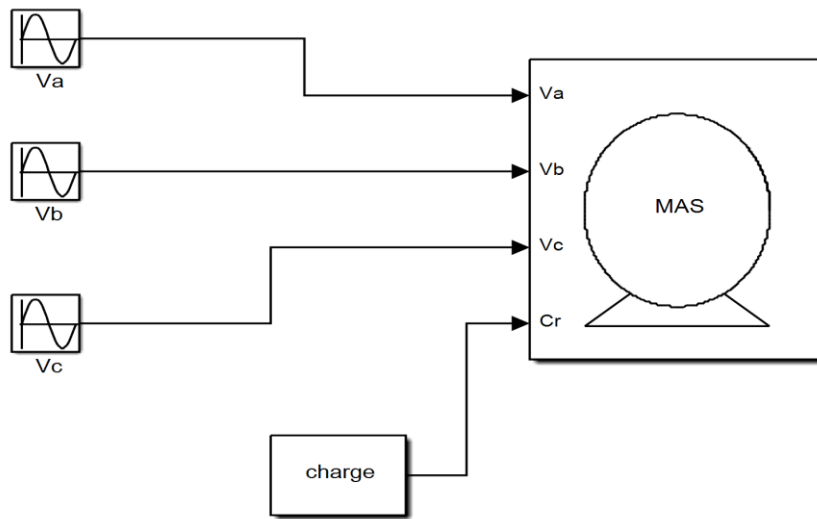


Figure IV.3: Model of the asynchronous machine connected with three phase voltage source.

See at [Annex D] the block diagram of the asynchronous machine.

IV.7.2 Simulink Model of MAS connected with three phase ZSI:

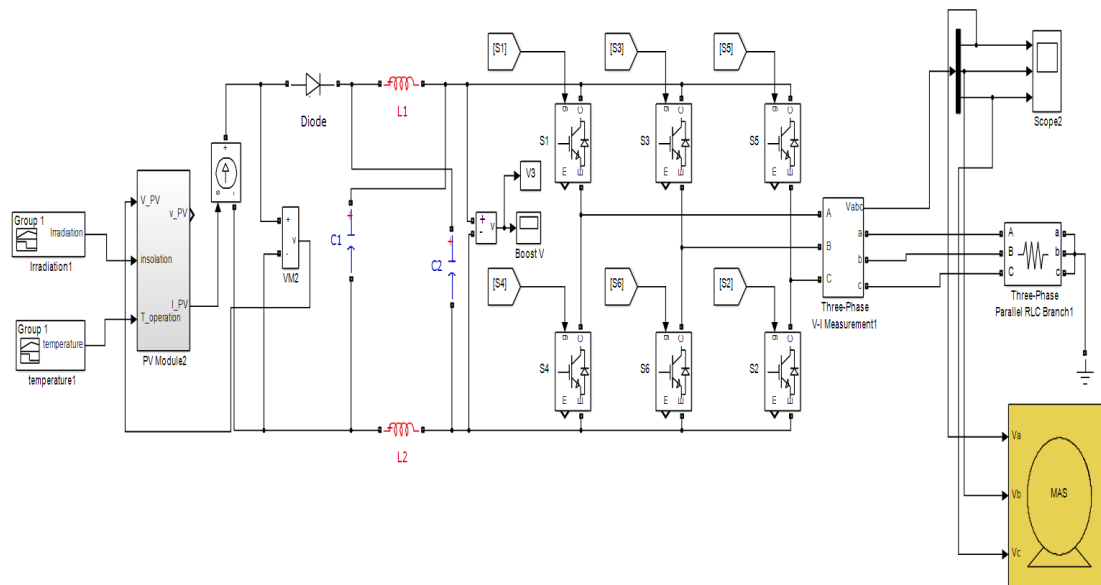


Figure IV.4: Model of the asynchronous machine connected with three phase ZSI controlled by SPWM.

IV. 8 Simulation Results:

IV.8.1 The asynchronous machine simulation result:

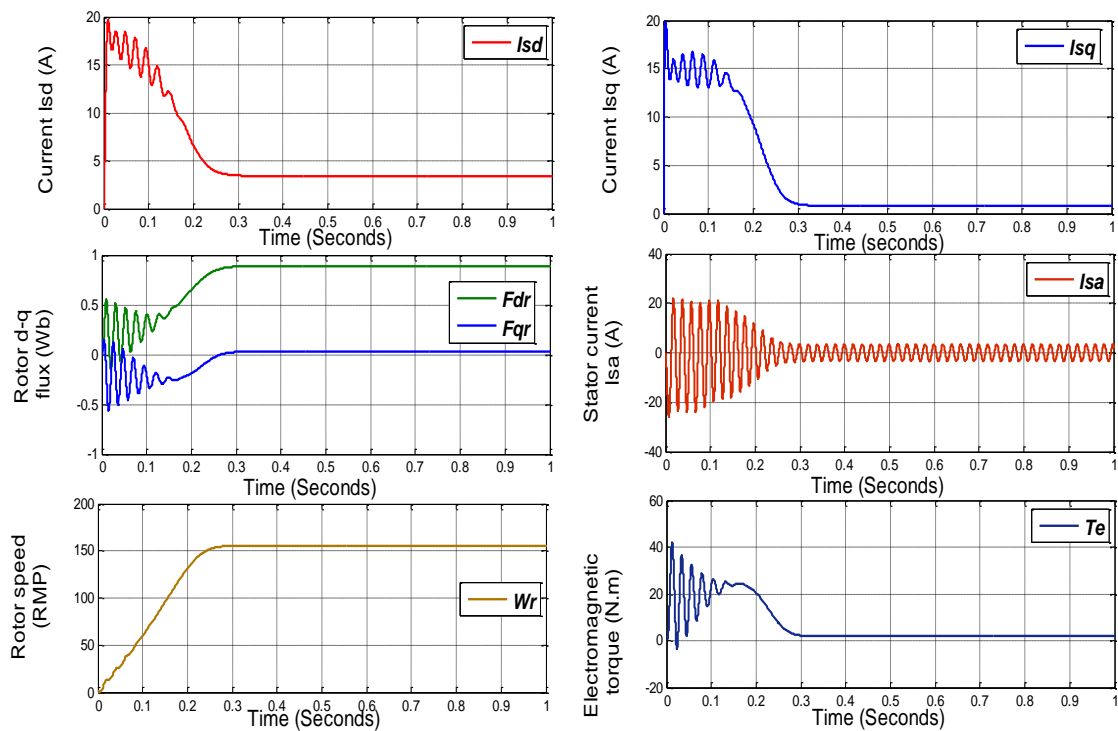


Figure IV.5: Output waveforms of parameter of IM powered by three phase voltage source.

Analyze and discuss:

- During starting, the electromagnetic torque is strongly oscillating and becomes approximately zero in steady state at the instant 0.3s; the starting torque reaches a value of 40N.m. When applying a load of 22N.m, the electromagnetic torque tends towards the value of the load torque.
- The starting current reaches 20A, exhibits considerable oscillations and then decreases to its value in the steady state.
- The rotor fluxes F_{rd} and F_{rq} are oscillatory during start-up then stabilize at their values in steady state at the instant 0.3 (s). When applying a load of 22 (N.m), the fluxes F_{rd} and F_{rq} increase.
- From the instant 0s to 0.3s the motor speed increases when applying a load. Then; in steady state the motor rotates at its synchronous speed (154 rad / sec).

IV.8.2 ZSI fed induction motor drives simulation result:

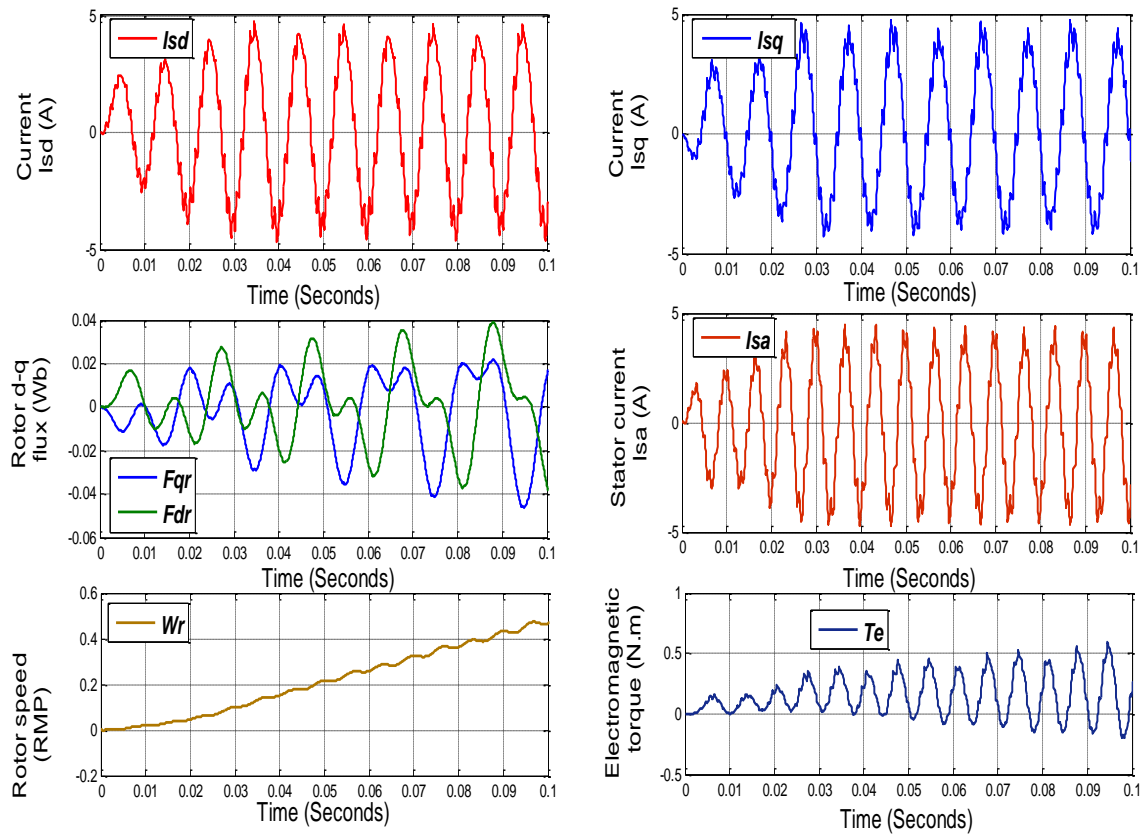


Figure IV.6: Output waveforms of parameter of IM powered by three phase ZSI.

🔧 Analyze and discuss:

- We have observed that the electromagnetic torque increases from the moment of starting. Then stabilize at their steady-state values
- The starting current exhibits oscillations and then increases to its value in the steady state.
- The rotor fluxes F_{rd} and F_{rq} are oscillatory during start-up then stabilize at their values in steady state.
- The synchronous speed is increasing.

IV. 9 Conclusion:

This chapter explores the ZSI controlled by SPWM with solar photovoltaic as source in drive application for enhancing the performance of induction motor. The proposed Z-source inverter was higher efficient, higher performance, cost effective, and uses fewer active components.

***GENERAL CONCLUSION AND
FUTURE WORKS***

General conclusion:

The work presented in this project falls within the framework of the development of power electronics in general and converters in particular, in order to improve systems for producing electrical energy from renewable sources. The objective of this project is to study Z-Source inverter and their different control strategies, with the aim of integrate it into a photovoltaic system.

We started with a current-state of a photovoltaic system through the different kinds of renewable energy, and gave a general overview of the recently introduced z-source converter, some topologies are given to show how advanced this type of converter is. We find that, PV system generation is probably the most efficient way to utilize solar energy. It has many attractive features like operation without moving parts, no emissions, high temperature, no noise, high modularity etc.

In the second chapter has modeled a photovoltaic generator and presented its main characteristics (P-V, I-V), then we introduce the MPPT command (P&O algorithm). Through the latest, we have observed that the PV generator has maximum power, and it is too sensitive to changes in irradiation and temperature.

The third chapter has presented the theoretical analysis and design of Z-source inverter. The Z-source inverter employs a unique impedance network to couple the three-phase inverter two levels main circuit of the power source, This research also finds out the differences between Z-source inverter and traditional inverters in essence, pointed out the superiority of Z-source inverter.

The use of the Z-Source network makes it possible to replace the DC-DC converter, which reduces the number of switching stages, as well as the number of switches. This means better efficiency, optimized volume and lower construction costs.

The control methods with the insertion of shoot-through states of Z-Source inverter have been studied. The proposed scheme under SPWM and SVPWM controls is simulated with the assistance of MATLAB/SIMULINK and the simulation results are obtained for constant value of modulation index.

Simulation results show that the sinusoidal load voltage and current can be achieved by the ZSI using filter with higher magnitude and frequency as

compared to the traditional inverter. It proves that output voltage matches with the design analysis. In addition, the output voltage has a linear relationship with modulation index.

In the last chapter, we used the induction motor to apply the simulation result of the z-source inverter, solar photovoltaic as source in drive application. The object is improving the performance of induction motor.

Future Works:

- ✚ In This Project the proposed topology is connected to solar based system in future it can likewise be tied to different other renewable energy sources like wind energy system.
- ✚ Some other MPPT algorithm can be tried and tested.
- ✚ The typology proposed in this project is three-phase Z-Source inverter has two levels, in the future it can also be used other topologies of ZSI like the quasi-Z-source inverter or the Trans-Z-source inverter are coupled with solar system or other renewable energy.

Bibliography

- [GSH 17] **Gorjian, Shiva.** "An Introduction to the Renewable Energy Resources." Unpublished, Unpublished, 2017, doi:10.13140/RG.2.2.27055.53928.
- [BYA 17] **Baddou, Yassine.** Solar Thermal Systems for Domestic Water Heating Applications in residential buildings: Efficiency and economic viability analysis of monitored plants. BS thesis. University of Polytechnic de Catalonia, 2017.
- [GCU 10] **García-Valverde, Rafael, Judith A. Cherni, and Antonio Urbina.** "Life cycle analysis of organic photovoltaic technologies." *Progress in Photovoltaics: Research and Applications* 18.7 (2010): 535-558.
- [JNJ 15] **Jean, Joel, et al.** "Pathways for solar photovoltaics." *Energy & Environmental Science* 8.4 (2015): 1200-1219.
- [DKS 15] **D.Kirubakaran, S. Kamalakkannan,** Comparative Analysis of Traditional Inverter and Z-Source Inverter for PV System, INDIAN JOURNAL OF APPLIED RESEARCH, 2015.
- [LDC 16] **Fara,Laurentiu, and Dan Craciunescu.** "Output analysis of stand-alone PV systems: modeling, simulation and control." *Energy Procedia* 112.October 2016 (2017): 595-605.
- [MSG 16] **P. Mohanty, K. Sharma, M. Gujar, M. Kolhe, and A. Azmi,** Solar Photovoltaic System Applications. Springer International Publishing, 2016. PV System Design for Off-Grid Applications, pp. 49–83.
- [BDP 14] **Bhattacharyya, Subhes C., and Debajit Palit, eds.** Mini-grids for rural electrification of developing countries: analysis and case studies from South Asia. Springer, 2014.
- [KSA 13] **Kalogirou, Soteris A.** Solar energy engineering: processes and systems. Academic Press, 2013.
- [SAK 10] **S. Thangaprakash and A. Krishnan,** "Implementation and critical investigation on modulation schemes of three phase impedance source inverters," *Iranian. J. Electric. Electron. Eng.*, Vol. 6, No. 2, pp. 84-92, 2010.
- [PFZ 03] **Peng F.Z.** Z-source inverter. *IEEE Transaction on Industrial Application*, 2003; 39(2):504–510.
- [AER 17] **Adle, Rahul, et al.** "Photovoltaic based series z-source inverter fed induction motor drive with improved shoot through technique." *Energy Procedia* 117 (2017): 329-335.
- [SHS 18] **Shrey Sharma,** Control and design of Quasi-Z-Source Inverter (qZSI) for grid connected Photovoltaic (PV) arrays, Master's thesis in Electric power engineering, University Of Technology Gothenburg, Sweden 2018.

- [EHA 16] **Ellabban, Omar, and Haitham Abu-Rub.** "Z-source inverter: Topology improvements review." *IEEE Industrial Electronics Magazine* 10.1 (2016): 6-24.
- [BKP 17] **Barla pavanil, Kanuri venkatesh, Pudisekhar and CH. Anandbabu,** "A Review on Z-Source Inverter Topologies", *international Journal of Pure and Applied Mathematics Volume 114 No. 8* 2017, 201-210.
- [SAV 17] **Saravanan, V., et al.** "Z Source Inverter Topologies-A Survey." *Bulletin of Electrical Engineering and Informatics* 6.1 (2017): 1-12.
- [AUS 13] **Ali, U. Shajith, et al.** "A novel carrier based pulse width modulation technique for quasi-z-source inverter with improved voltage gain." *2013 International Conference on Circuits, Power and Computing Technologies (ICCPCT)*. IEEE, 2013.
- [PNR 11] **Pandiarajan, Natarajan, and Ranganath Muthu.** "Mathematical modeling of photovoltaic module with Simulink." *2011 1st International Conference on Electrical Energy Systems*. IEEE, 2011.
- [KRS 18] **Kumar, Raj, and S. K. Singh.** "Solar photovoltaic modeling and simulation: As a renewable energy solution." *Energy Reports* 4 (2018): 701-712.
- [SAS 12] **Satpathy, Saurav.** *Photovoltaic power control using MPPT and Boost converter*. Diss. 2012.
- [KDJ 18] **KERDOUN, Djallel, et al.** *Contribution a l'étude d'une installation photovoltaïque avec stockage connectée au réseau électrique*. 2018. PhD Thesis. Mentouri Brothers University of Constantine.
- [KSB 14] **Kolsi, S, H. Samet, and M. Ben Amar.** "Design analysis of DC-DC converters connected to a photovoltaic generator and controlled by MPPT for optimal energy transfer throughout a clear day." *Journal of Power and Energy Engineering* 2014 (2014).
- [KVN 13] **Kannan, V. Kamatchi, and N. Rengarajan.** "Photovoltaic system interface with a DC-DC boost converter in D-STATCOM for power quality improvement." *Istanbul University-Journal of Electrical & Electronics Engineering* 13.1 (2013): 1597-1604.
- [EAO 10] **Elshaer, M., A. Mohamed, and O. Mohammed.** "Smart optimal control of DC-DC boost converter in PV systems." *2010 IEEE/PES Transmission and Distribution Conference and Exposition: Latin America (T&D-LA)*. IEEE, 2010.
- [BEF 16] **BENZINEB, Fairouz.** "ETUDE ET COMMANDE D'UN ONDULEUR Z-SOURCE: Application aux systèmes photovoltaïques." (2016).
- [ACM 13] **Aouchiche, N., MS Aït Cheikh, and A. Malek.** "Poursuite du point de puissance maximale d'un système photovoltaïque par les méthodes de l'incrémentation de conductance et la perturbation & observation." *Revue des Energies Renouvelables* 16.3 (2013): 485-498.

- [KVT 13] **Kotak, V. C., and PretiTyagi.** "DC to DC Converter in maximum power point tracker." *International Journal of Advanced Research in Electrical, Electronics and Instrumentation Engineering* 2.12 (2013): 6115-6125.
- [FBN 16] **Faiza, B. E. N. A. D. E. L.** *Etude Et Simulation D'une Commande MPPT Pour Système PV.* Diss. Universite de Mohamed Boudiaf M'sila Faculte de Technologie, 2016.
- [BPR 13] **Bhatnagar, Pallavee, and R. K. Nema.** "Maximum power point tracking control techniques: State-of-the-art in photovoltaic applications." *Renewable and Sustainable Energy Reviews* 23 (2013): 224-241.
- [LNS 12] **Suresh, L., GRS Naga Kumar, and M. V. Sudarsan.** "Modeling and simulation of Z-source inverter." *From the Selected Works of suresh L* (2012).
- [KJS 17] **Kouhanjani, Masoud Jokar, and Ali Reza Seifi.** "Comparison of VSC and Z-source converter: power system application approach." *Advances in Electrical and Electronic Engineering* 15.1 (2017): 12-20.
- [ZHF 06] **Zhang, Fan, et al.** "A new three-phase ac-ac Z-source converter." *Twenty-First Annual IEEE Applied Power Electronics Conference and Exposition, 2006. APEC'06. IEEE, 2006.*
- [RYO 17] **Riache Younes.** "Commande d'un onduleur Z-Source par la stratégie SVM modifiée à quatre court-circuits pour une application PV connectée au réseau." Master thesis in Electrical Engineering. National Polytechnic School (ENP), El Harrach, Algiers, Algeria, 2017.
- [MOL 17] **Mohamed Lamine MESSAOUD.** "Commande d'un onduleur Z-Source à stratégie SVM modifiée à six courts-circuits pour une application PV connecté au réseau." Master thesis in Electrical Engineering. National Polytechnic School (ENP), El Harrach, Algiers, Algeria, 2017.
- [LPC 04] **Loh, Poh Chiang, et al.** "Pulse-width modulation of Z-source inverters." *Conference Record of the 2004 IEEE Industry Applications Conference, 2004. 39th IAS Annual Meeting. Vol. 1. IEEE, 2004.*
- [HZH 14] **Huang, Zhe.** "SVPWM Switching Pattern for Z-source Inverter, Simulation and Application." (2014).
- [SUU 11] **Supatti, Uthane.** *Low cost z-source converter/inverter system for wind power generation.* Michigan State University. Electrical Engineering, 2011.
- [SZP 05] **Shen, Miaosen, and Fang Z. Peng.** "Operation modes and characteristics of the Z-source inverter with small inductance." *Fortieth IAS Annual Meeting. Conference Record of the 2005 Industry Applications Conference, 2005.. Vol. 2. IEEE, 2005.*
- [ZPH 12] **Zope, Pankaj Hiranman.** "Modeling and simulation of z source inverter design and control strategies." Thesis submitted for the degree of doctor of philosophy in electronics and telecommunication engineering, Faculty of engineering and technology Jodhpur National University, Jodhpur June (2012).

- [RKA 17] **Rajesh, Kammari.** "Design and Analysis for Various Controlling Methods of a Z-Source Inverter." International Journal of Electrical Engineering. ISSN 0974-2158 Volume 10, Number 2 (2017), pp. 271-288. M.Tech, G.Pulla Reddy Engineering College, Kurnool, India.
- [SHM 04] **Shen, Miaosen, et al.** "Maximum constant boost control of the Z-source inverter." Conference Record of the 2004 IEEE Industry Applications Conference, 2004. 39th IAS Annual Meeting. Vol. 1. IEEE, 2004.
- [RKH 09] **Rostami, H., and D. A. Khaburi.** "Voltage gain comparison of different control methods of the Z-source inverter." 2009 International Conference on Electrical and Electronics Engineering-ELECO 2009. IEEE, 2009.
- [PMZ 05] **Peng, Fang Zheng, Miaosen Shen, and Zhaoming Qian.** "Maximum boost control of the Z-source inverter." IEEE Transactions on power electronics 20.4 (2005): 833-838.
- [USK 11] **Ali, U. Shajith, and V. Kamaraj.** "Z-Source inverter with a new space vector PWM algorithm for high voltage gain." ARPN Journal of Engineering and Applied Sciences 6.6 (2011): 9-13.
- [KVI 10] **Kumar, K. Vinoth, et al.** "Simulation and comparison of SPWM and SVPWM control for three phase inverter." ARPN journal of engineering and applied sciences 5.7 (2010): 61-74.
- [TQV 07] **Tran, Quang-Vinh, et al.** "Algorithms for controlling both the DC boost and AC output voltage of Z-source inverter." IEEE Transactions on Industrial Electronics 54.5 (2007): 2745-2750.
- [TQV 09] **Tran, Quang-Vinh, et al.** "Minimization of voltage stress across switching devices in the Z-source inverter by capacitor voltage control." Journal of Power Electronics 9.3 (2009): 335-342.
- [SML 18] **Sharma, Mahima, and Mahendra Lalwani.** "Performance evaluation of three-phase induction motor drive fed from Z-source inverter." Int J Appl Eng Res 13.8 (2018): 6098-6109.
- [CRA 14] **Cicy Mary Mathew, Rajan P Thomas and Acy M Kottalil.** SVPWM Controlled ZSI Drive for Speed Control of 3 Phase Induction Motor using PID Controller. International Journal of Engineering Research & Technology (IJERT). ISSN: 2278-0181. Vol. 3 Issue 2, February - 2014.
- [MGK 20] **Manohar, G., and K. Chiranjeevi.** "Cascaded H-Bridge Inverter for Wind Driven Isolated Squirrel Cage Induction Generators." CVR Journal of Science and Technology 18.1 (2020): 81-87.
- [TMO 17] **Therib, Mohammed.** Three Phase Induction Motors. (2017).

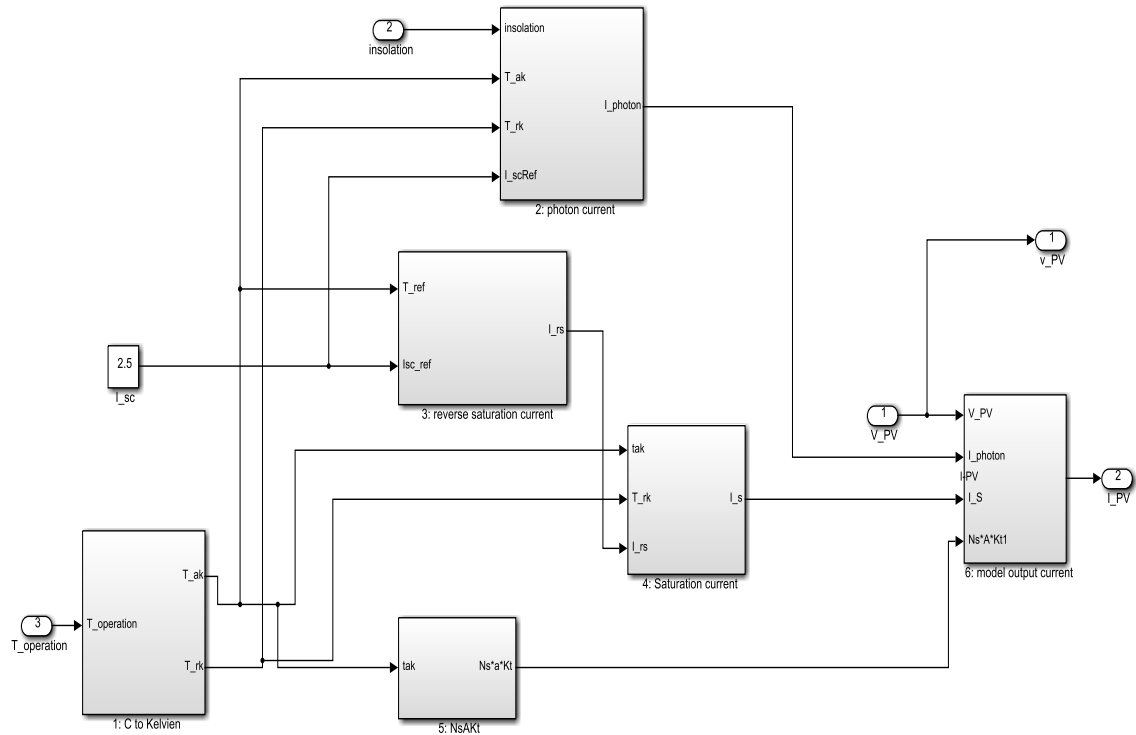
- **Web Sites:**

- [1] https://en.wikipedia.org/wiki/Solar_power#Mainstream_technologies, Accessed on Thursday 13th February, 2020 at 20:00.
- [2] <https://www.internationalrenewableenergyagency.org/>, Accessed on Friday 14th February, 2020 at 21:30.
- [3] http://www.irena-istra.hr/uploads/media/Photovoltaic_systems.pdf, Accessed on Sunday 08th March, 2020 at 11:00.
- [4] <https://www.ambientweather.com/solarradiation.html>, Accessed on Wednesday 4th March, 2020 at 13:38.
- [5] <http://www.pvresources.com/en/introduction/history.php>, Accessed on Wednesday 4th March, 2020 at 14:19.
- [6] <http://www.pvresources.com/en/solarcells/technologies.php>, Accessed on Wednesday 4th March, 2020 at 14:23.
- [7] <https://www.greenmatch.co.uk/blog/2015/09/types-of-solar-panels>, Accessed on Monday 9th March, 2020 at 15:16.
- [8] https://en.wikipedia.org/wiki/Amorphous_silicon, Accessed on Monday 9th March, 2020 at 15:09.
- [9] http://www.leonics.com/product/renewable/pv_module/pv_module_en.php, Accessed on Tuesday 3th March, 2020 at 20:46.
- [10] <http://www.pvresources.com/en/solarradiation/solarradiation.php>, Accessed on Saturday 15th February, 2020 at 16:00.
- [11] https://en.wikipedia.org/wiki/Solar_inverter, Accessed on Thursday 20th February, 2020 at 11:25.
- [12] https://www.academia.edu/39843923/Induction_Motor_Working_Principle_Type_and_Definition. Accessed on Thursday 10th September, 2020 at 13:15.
- [13] <https://www.electrical4u.com/induction-motor-types-of-induction-motor/>, Accessed on Thursday 10th September, 2020 at 12:48

ANNEX

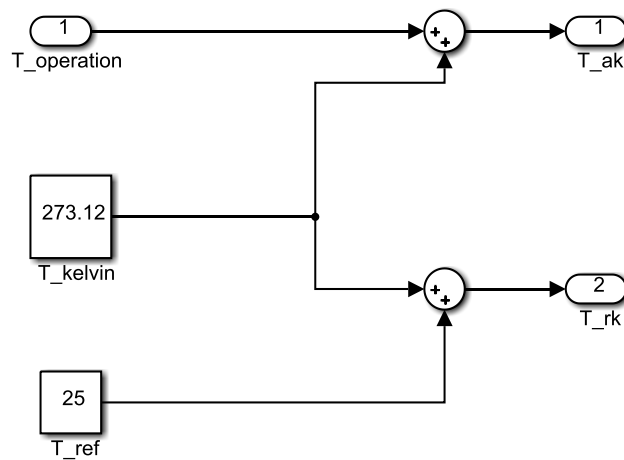
ANNEX A:

1. Step by step procedure for Simulink modeling of PV module:



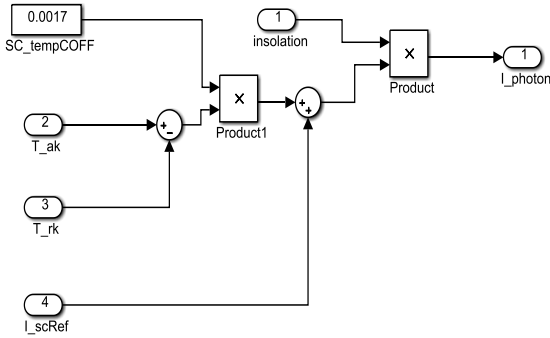
PV module (SOLKAR 36 W)

• **Step 1:**



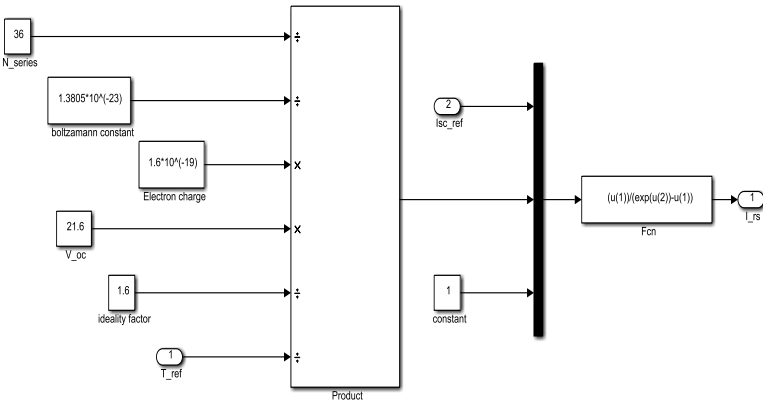
Circuit under subsystem 1

- Step 2:



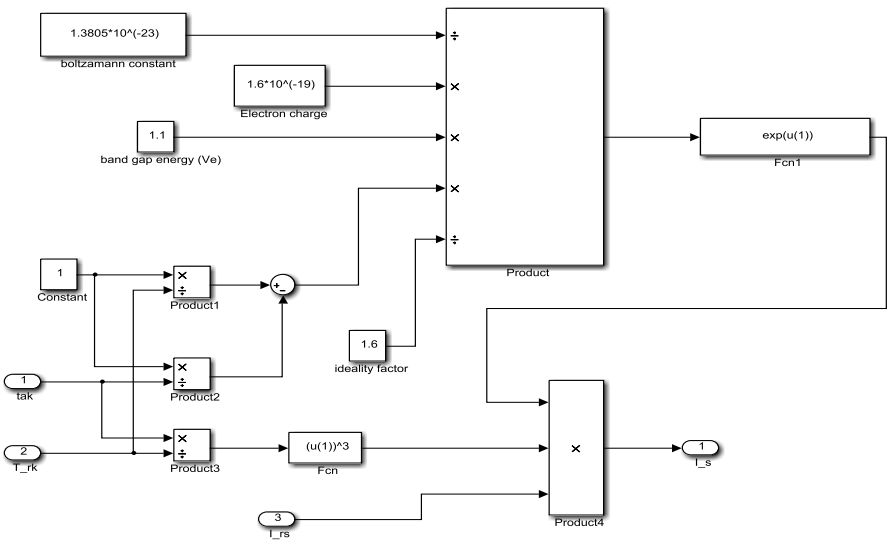
Circuit under subsystem 2

- Step 3:



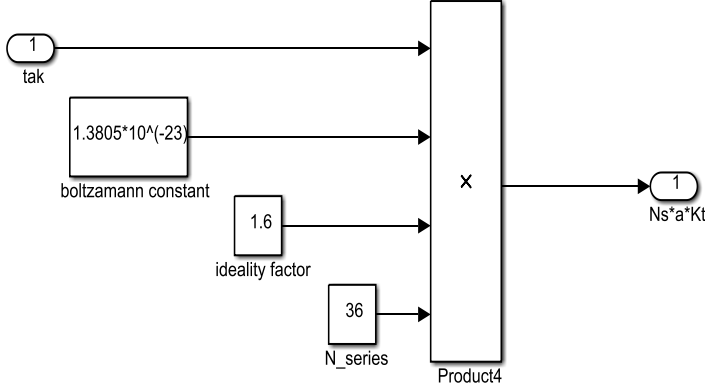
Circuit under subsystem 3

- Step 4:



Circuit under subsystem 4

- Step 5:



Circuit under subsystem 5

• Step 6:

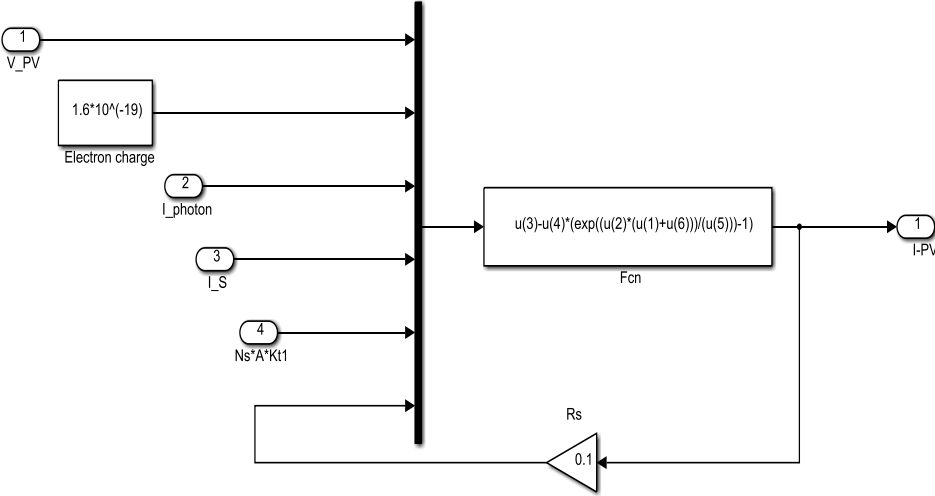


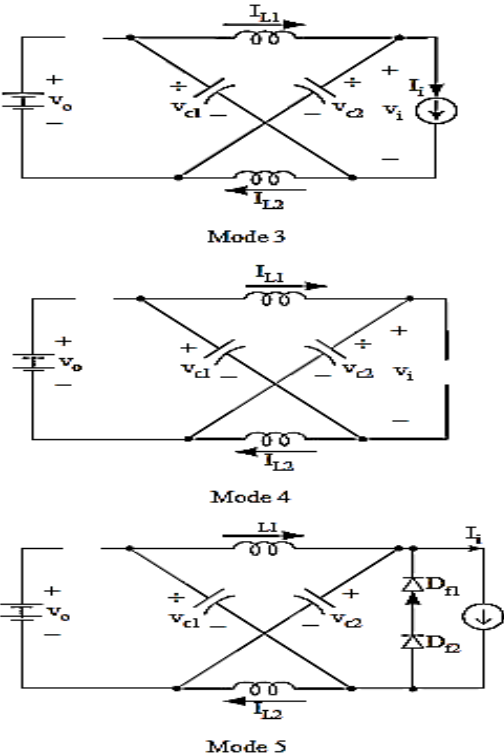
Figure6: Circuit under subsystem 6.

2. The boost converter specification [WSJ 14]:

Description	Value
Input voltage (V_{in})	16.6 V
the converter duty (D)	0.34
Output voltage (V_{out})	25 V
L_b	100 μ H
C_o	2400 μ F
Switching frequency (f)	5 KHz
Load (R)	7.36 Ohm

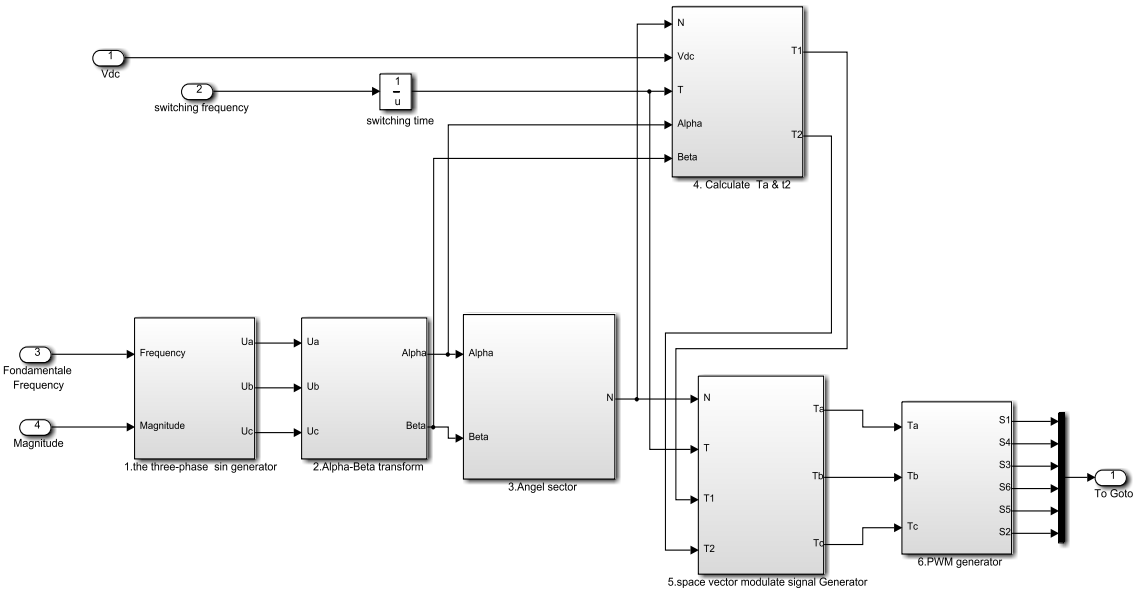
ANNEX .B:

- A news modes operating of ZSI:



ANNEX C:

- Simulink model of SVPWM signal generator:



ANNEX D:

1. Rated Data of the Tested Induction Motor (IM):

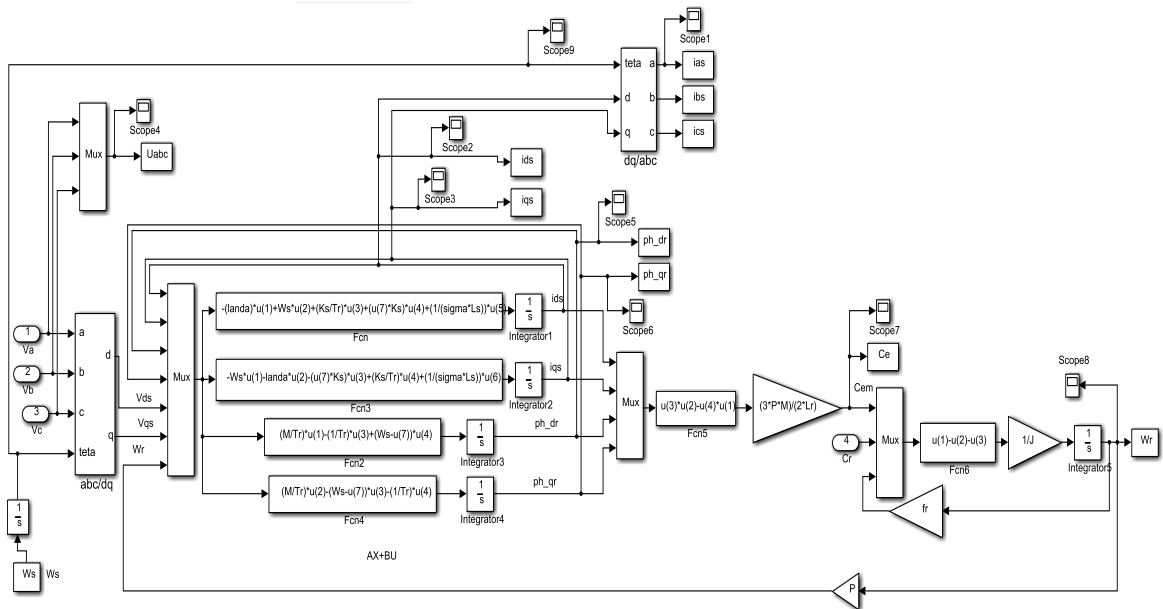
$L_r = 0.274$; $L_s = 0.274$; $R_s = 4.85$; $R_r = 3.81$; $M = 0.258$; $P = 2$; $J = 0.031$;

$f_r = 0.0114$; $W_s = 2 * \pi * 50$; $\sigma = 1 - (M^2 / (L_s * L_r))$; $T_r = L_r / R_r$;

$K_s = M / (\sigma * L_s * L_r)$; $V_{sn} = 10$; $V_{s0} = 2$; $W_{sn} = 4$; $W_{s0} = 0.2$;

$\lambda_{da} = R_s / (\sigma * L_s) + R_r * M^2 / (\sigma * L_s * L_r^2)$

2. Model of Induction Motor:



Simulink model of induction motor